August 2019

Obesity Suppresses Pigment Epithelium-Derived Factor and Alters Pro-Tumorigenic Signaling Pathways in Prostate Cancer

Nizar Ahmed Khamjan
University of Wisconsin-Milwaukee

OBESITY SUPPRESSES PIGMENT EPITHELIUM-DERIVED FACTOR AND ALTERS

PRO-TUMORIGENIC SIGNALING PATHWAYS IN PROSTATE CANCER

by

Nizar A. Khamjan

A Dissertation Submitted in

Partial Fulfillment of the

Requirements for the Degree of

Doctor of Philosophy

in Health Sciences

at

The University of Wisconsin-Milwaukee

August 2019

ABSTRACT

OBESITY SUPPRESSES PIGMENT EPITHELIUM-DERIVED FACTOR AND ALTERS PRO-TUMORIGENIC SIGNALING PATHWAYS IN PROSTATE CANCER

by
Nizar Khamjan

The University of Wisconsin-Milwaukee, 2019
Under the Supervision of Professor Jennifer A. Doll

Background: Pigment epithelium-derived factor (PEDF), a multifunctional protein, is a potent tumor suppressor and anti-angiogenic factor. PEDF has been identified as a novel regulator of lipid metabolism via binding and activating adipose triglyceride lipase, which stimulates lipolytic pathways. PEDF-deficient mice develop prostatic hyperplasia that progresses to cancer when these mice are fed a high fat diet (HFD). PEDF expression is decreased in prostate cancer (PCa) patient tissues. Conversely, PEDF treatment inhibits PCa growth in mouse models. Recently, our lab has demonstrated that excess oleic acid (OA) treatment, an *in vitro* obesity model, suppresses secreted PEDF expression in PCa cell lines (LNCaP, DU145, and PC-3) and suppresses cellular PEDF expression in androgen-independent PCa cell lines (DU145 and PC-3 cells). This is of interest because PCa patients who are obese are at a higher risk of aggressive disease and more likely to die from the disease. However, the molecular mechanisms through which excess OA down-regulates PEDF *in vitro* are unknown. For the *in vitro* studies, we first investigated one OA receptor, G protein-coupled receptor 40 (GPR40), and tested if OA-mediated PEDF suppression was

dependent on calcium (Ca^{2+}) and/or peroxisome proliferator-activated receptor gamma (PPARγ) signaling pathways. In addition, it is unknown if obese conditions suppress PEDF *in vivo* within PCa tissues or within PCa xenograft tumors. Thus, we hypothesize that excess lipids, in obesity and HFD microenvironments, alter lipid metabolism, which in turn, increases pro-tumorigenic activity and decreases PEDF expression in PCa. To study this hypothesis, we used an excess OA model *in vitro* and two *in vivo* PCa models.

Methods: We treated RWPE-1, LNCaP, DU145, PC-3, and TRAMPC2 with excess OA at 1 mM for 48 hours. Then, cells were counted, viability was assessed, and PEDF levels were quantified by enzyme-linked immunosorbent assay (ELISA). For *in vivo* studies, two obese models were used: (1) a xenograft model using the TRAMPC2 cell line injected in male WT mice and obese (ob/ob) mice and (2) male Pbsn-Cre^{+}-PTEN$^{fl/fl}$ mice fed either a control diet (CD) or a HFD. All mice were in a C57Bl/6J background. Blood samples, TRAMPC2 tumor xenograft tissue, mouse PCa tissues, liver, and adipose tissues were collected. PEDF levels and pro-tumorigenic pathway mediators were evaluated by ELISA and by Western blot, respectively.

Results: For the *in vitro* study, we found that OA did not interact with the GPR40 receptor and/or PPARγ to rescue secreted PEDF levels in LNCaP, DU145, and PC-3 cells. In Pbsn-Cre^{+}-PTEN$^{fl/fl}$ model, the prostate weight of HFD-fed mice was increased as compared to CD-fed mice (P-value <0.042). In the TRAMPC2 xenograft model, we

observed a significant increase in tumor volume and weight in TRAMPC2 tumors grown in ob/ob mice as compared to tumors grown in lean mice (P-value <0.018). Tumor PEDF levels were significantly decreased in TRAMPC2 xenograft tumors grown in ob/ob mice compared to TRAMPC2 xenograft tumors grown in WT mice (P-value <0.024). Lastly, in an effort to identify other signaling pathways altered in TRAMPC2 tumor tissues grown in ob/ob mice versus WT mice, we found a significant reduction in superoxide dismutase 2 (SOD2; P-value <0.018) and serine palmitoyltransferase (SPT; P-value <0.050). Interestingly, while previous studies showed that obesity increased circulating PEDF, here we did not find an increase in circulating PEDF levels in ob/ob mice with TRAMPC2 xenograft tumors as compared to WT mice. Moreover, circulating PEDF levels were actually significantly decreased in HFD-fed Pbsn-Cre[+]-PTEN^{fl/fl} mice compared to CD-fed Pbsn-Cre[+]-PTEN^{fl/fl} mice (P-value <0.001).

Conclusion: This is the first study to report that an obese microenvironment suppresses circulating PEDF and suppresses PEDF, SOD2, and SPT in mouse PCa tissues. Therefore, these data indicate that reduced PEDF, SOD2, or SPT levels could be mechanisms of obesity-driven PCa progression.

v

TABLE OF CONTENTS

LIST OF FIGURES

LIST OF TABLES

ACKNOWLEDGMENTS

First and foremost, I would like to express my special and deepest appreciation to my advisor, Dr. Jennifer A. Doll, who has been a tremendous mentor for me for 7 years. Dr. Doll provided me the invaluable opportunity to do research in her lab and provided unlimited guidance throughout this project. She has taught me critical thinking about methodology to conduct science and how to present the research work as clearly as possible. She provides me a strong and a solid foundation that will guide me to a successful career route. Again, I would like to sincerely thank her for encouraging my research and for all the useful comments, remarks, and engagement through the learning process of this PhD dissertation.

I would also like to express my gratitude to my committee members, Dr. Dean T. Nardelli, Janis T. Eells, Elizabeth S. Liedhegner, and Xuexia Wang for their support, comments, and instructions. I would especially like to thank my parents for their unending love, support, prayers, caring and sacrifices. I would like to express my special thanks to my wife, Reham, and my children, Majd and Fajir, for their love, support and patience during the past eight years. Last, but not least, I want to thank my current and former lab members and my friends for their support and encouragement to complete the research work directly or indirectly.

INTRODUCTION

Prostate cancer

The prostate is a 4 cm in width gland of the male reproductive system. The primary function of the prostate gland is to produce seminal fluid that helps to protect and activate the sperm. The prostate consists of three glandular regions: the peripheral zone, central zone, and transitional zone. A fourth, non-glandular region, is the anterior fibromuscular stroma [1]. The three most common diseases of the prostate are prostatitis, benign prostatic hyperplasia (BPH), and prostate cancer (PCa). PCa is a leading men's health concern because PCa is the most commonly diagnosed type of cancer and the second leading cause of cancer-related death in men in the United States [2]. In the US alone, it is estimated that about 174,650 men will be diagnosed with PCa, and more than 31,620 patients will die from the disease in 2019 [3]. Approximately 95% of PCa are adenocarcinomas: 70% of which is localized in the peripheral zone, 15-20% in the central zone, and 10-15% in the transitional zone [1], [4]. The early stages of PCa do not present with symptoms. However, in advanced stages of PCa, there are symptoms, including difficulty urinating, sudden urge to urinate, dysuria, and hematuria [5].

A variety of diagnostic tools and technologies are available to diagnose PCa. The prostate specific antigen (PSA) blood test and the digital rectal examination (DRE) are used as screening tools while transrectal ultrasound-guided biopsy (TRUS) is used as the diagnostic test for PCa. An elevated PSA level may indicate the presence of PCa;

however, the test is not specific, as other diseases of the prostate and obesity affect PSA levels [6]. In DRE, the prostate gland is physically examined to estimate the size of the prostate gland and to identify if hard, lumpy, or abnormal areas are present in the prostate; however, this physical exam does not provide an appropriate estimation for the size of the prostate gland in obese patients as they are likely to have an enlarged prostate [6]. A biopsy with histologic examination is necessary for a diagnosis of PCa. If a biopsy confirms the presence of PCa, grading and staging systems are used for histologic classification and reporting PCa. Other imaging techniques such as bone scan and positron emission tomography scan are used to determine if PCa has metastasized beyond the prostate for staging purposes.

The staging system is known as the TNM (tumor, node, and metastasis) system that is used in many cancers including PCa [7]. Each category, i.e. tumor, node, and metastasis, has subdivisions in each cancer type to allow precise staging of the cancer. T describes the size of PCa and also indicates if the tumor has invaded into the nearby seminal vesicle structure or other structures. N describes spread of PCa to regional lymph nodes while M refers to metastasis of PCa to other parts of the body [7].

The Gleason grading system uses a 1–5 scale according to the appearance of the glands and cells when stained with hematoxylin and eosin [8]. The most prominent pattern and the second most common pattern are added together to give a Gleason score of 2-10 [8]. A score that is 6 or over is considered PCa, and a score of 7 and

above indicates a clinically aggressive PCa [8]. If a diagnosis of PCa is confirmed, prognosis and treatment options are dependent on several factors such as the stage and grade of PCa [5]. Surgery, radiotherapy, hormone deprivation therapy, immunotherapy, and chemotherapy are all options for treating PCa [5]. Even though much progress has been made in the diagnosis and treatment of PCa, the etiology of PCa remains largely unknown, but there are several risk factors have been firmly established.

Both genetic and environmental factors contribute to PCa development [2]. Aging is one of the most significant risk factors, with most cases of PCa occurring in men over the age of 65 [2]. Approximately 80% of men, by the age of 80, will be diagnosed with PCa, while PCa is very rarely diagnosed in men under the age of 40 [9]. PCa occurs more commonly in men of African or Caribbean descent and less often in other races [10]. This might be related to genetic polymorphisms, or allele frequencies, between races. Another risk factor for PCa is a diet that is high in fats, red meat, and dairy products, which is characteristic of a Western diet [10]. Obesity is often a consequence of a Western / high fat diet (HFD), and most studies have shown an association between obesity and increased risk of progression and death from PCa [11], [12]. Clinically, normal weight, overweight, and obesity are determined by using body mass index (BMI) and waist/hip ratio systems [13]. BMI is the most widely used measure to define obese individuals. Its calculation is based on weight in kilograms divided by

square of height in meters (kg/m^2). A score of 20-24.9 kg/m^2 is normal weight; 25-29.9 kg/m^2 is overweight; and, $\geq$ 30 kg/m^2 is considered obese [13].

Vidal *et al.* examined the association between obesity and risk of low- and high-grade PCa among 6,427 men; 1,739 men (27%) were normal weight, 3,384 (53%) men were overweight, and 1,304 (20%) were obese [14]. They concluded that obesity was associated with low-grade PCa (OR, 0.79; P-value =0.01) and high-grade PCa (OR, 1.28; P-value =0.042) [14]. In a systematic review, a diet high in red meat, dietary fat, and milk intake increased the risk of PCa while high fruit and vegetable intakes were found to be preventive in PCa [15].

PCa, lipid metabolism, and obesity

Fatty acids (FA) are a type of lipid that is identified based on carbon chain length or the number and position of double bonds in the carbon chain [16]. Carbon length classification is divided as short-chain FA (< 6 carbons), medium-chain FA (6-12 carbons), long-chain FA (13-21 carbons), and very long chain FA ($\geq$ 22 carbons) [16]. Saturated FA (SFA) have no double bonds and are mainly found in animal fat sources such as butter, milk, meat, salmon, and eggs [16], [17]. Palmitic acid (PA) and stearic acid (SA) are the most common SFA found in the oils and fats of animals. Unsaturated FA that have only one double bond are called monounsaturated FA (MUFA), and FA that have multiple double bonds are called polyunsaturated FA (PUFA) [16].

Oleic acid (OA), which is an omega (ω)-9 FA, is the most common MUFA in the body and in human adipose tissues [18]. The omega system identifies the position of the double bond in MUFA [16]. The main sources of OA are vegetable oils such as olive, canola, and sunflower oils, but it is also found in beef, chicken, eggs, nuts, and seeds. ω-3 and ω-6 PUFA exist in high amount in nuts, olive, oil, diary, seeds, fish, oyster, and shrimp [19]. Examples of ω-3 PUFA are alpha-linoleic acid (ALA), eicosapentaenoic acid (EPA), and docosahexaenoic acid, while examples of ω-6 PUFA are linolenic acid (LA) and arachidonic acid. Data obtained from epidemiological studies on the risk of PCa associated with PUFA levels are inconsistent [20], [21].

In a prospective questionnaire study of 47,866 men, Leitzmann *et al*. evaluated dietary LA intake with respect to PCa risk. They found that dietary LA intake was unrelated to the risk of PCa [22]. In a case-control study of 89 PCa cases and 38 healthy controls from North Carolina, Godley *et al.* presented that increased LA, an ω-6 PUFA, isolated from erythrocyte membranes, are associated with a 5-fold increased risk of PCa compared to men with low levels of LA (OR 3.54; P-value <0.04) [23]. Newcomer *et al*. isolated ALA, an ω-3 PUFA from erythrocyte membranes from PCa patients (n= 67) and healthy controls (n= 156) from Washington State. They showed that men with the highest levels of ALA ω-3 PUFA, compared to the men with the lowest levels of ALA ω-3 PUFA, had a significantly increased risk of PCa (OR= 2.3; P-value =0.01) [24]. A recent published study examined associations between PCa grades and ω-3 FA levels in 157 men diagnosed with low-risk PCa. Moussa *et al.* found that EPA

5

(ω-3 FA) levels were elevated in prostate tissue, but not in red blood cells, and the EPA elevation was associated with high-grade PCa (OR= 0.25; 95% CI= 0.08–0.79; P-value =0.03) [25]. Yang *et al.* studied the relationship between PCa risk and the total levels of ω-3 FA in serum samples obtained from PCa (n= 19), BPH (n= 24), and healthy subjects (n= 21) [26]. They showed that total ω-3 PUFA serum levels were high in PCa and BPH patients as compared to the healthy subjects [26]. When Yang *et al.* assessed OA (MUFA), LA (PUFA), and PA (SFA) individually from the total levels of FA, they observed no significant differences between PA, OA, and LA levels in all subject groups [26].

In a nested case-control study conducted in men (n= 1061) from several European countries, Aardestrup *et al.* investigated the relationship between the levels of PA (SFA) extracted from plasma phospholipids and PCa development. They found that the highest quintile of PA is correlated with the presence of localized and low-grade PCa as well as a higher risk of high-grade PCa (OR 1.47; P-value =0.032) compared with the lowest quintile of PA [27]. Together, epidemiological data regarding FA and risk of PCa development are inconsistent. These divergences are common in epidemiological studies because types of epidemiological studies, study design, study size, analysis, and reporting are different between studies [28]. Although the stated epidemiological studies were focused on linking FA to the risk of PCa, several mouse studies have been performed to further explore the effects of excess lipids on PCa progression.

Excess lipids that occur with obesity are stored as lipid droplets in cells. Lipid droplets play crucial roles in protecting cancer cells through reduction of lipotoxic cell damage, maintenance of energy and redox homeostasis, and regulation of FA trafficking and distribution [29]. In addition, lipid droplets contribute to cancer cell survival via protection against endoplasmic reticulum stress, membrane homeostasis, and regulation of autophagy [29]. The effects of excess lipids and dietary FA on PCa progression have been investigated through epidemiological and clinical studies as well as in both *in vitro* and *in vivo* models of PCa.

Transgenic adenocarcinoma of the mouse prostate (TRAMP) and phosphatase and tensin homolog (PTEN)-deficient mouse mice are two mouse models of PCa that are widely used to study the molecular mechanisms of PCa progression [30]. Time to tumor initiation, time to tumor penetration, and pathology of PCa tissues vary between models [30]. TRAMP mice are generated by prostate-specific probasin (Pbsn) promoter driving a viral oncogene, SV40 large T antigen, to develop PCa. These mice are characterized by prostatic hyperplasia at 8-12 weeks, by mouse prostatic intraepithelial neoplasia (mPIN) at 18-24 weeks, and by adenocarcinoma at 28 weeks [30]. Another model is Pbsn-Cre+PTEN$^{fl/fl}$ mice. These mice develop PCa due to Cre recombinase activation under the prostate-specific Pbsn promoter [31]. These mice are well characterized and develop murine prostatic intraepithelial neoplasia (mPIN) by 6 weeks of age [31]. They progress from mPIN to invasive adenocarcinoma by 9 weeks of age,

and then to metastatic carcinoma by 12 weeks of age [31]. PTEN$^{+/-}$ mice are also used to study the feature of hyperplasia and mPIN, but these mice take about 40-65 weeks to develop adenocarcinoma [30].

Liu *et al*. examined whether HFD promoted PCa progression in PTEN$^{+/-}$ mice. Liu *et al*. fed PTEN$^{+/-}$ mice with a HFD deriving 45% kcal from fat or a control diet (CD) deriving 12% kcal from, beginning at 12 months of age for 3 and 6 months [32]. Liu *et al*. found that HFD augmented the progression of mPIN in PTEN$^{+/-}$ mice [32]. In addition, a HFD increased expression of phosphorylated Akt and mitogen-activated protein kinase (MAPK) proteins by 2-fold in the prostate of PTEN$^{+/-}$ mice, but not in PTEN$^{+/+}$ mice. Similarly, the mRNA levels of β-catenin, peroxisome proliferator-activated receptor (PPARγ), and sterol regulatory element binding proteins were elevated in HFD-fed PTEN$^{+/-}$ mice, but not in PTEN$^{+/+}$ mice [32]. Similar observations were reported in a study by Chen *et al* [33]. In this study, Pbsn-Cre^{+}PTEN$^{fl/fl}$ mice were fed either a HFD containing 60% kcal fat or a CD containing 17% kcal fat, starting at the age of 12 months for 3 months. A qualitative examination of the prostate tumors, isolated from HFD-fed PTEN$^{fl/fl}$ mice and stained with Oil Red O (ORO), displayed strong lipid accumulation [33].

Another study used TRAMP mice fed either a Western diet containing 21.2% fat and 0.2% cholesterol or a CD containing 4.5% fat and 0.002% cholesterol), starting at the age of 8 weeks for 20 weeks [34]. An increase in body weight and larger tumors

8

were observed in TRAMP mice fed a Western diet compared to TRAMP mice fed a CD [34]. A higher grade and poorly differentiated adenocarcinomas were found in TRAMP mice fed a Western diet as compared to a CD-fed mice [34]. In addition, the expression levels of cyclin D1, used as a marker of increased proliferation and evaluated by immunohistochemistry, were elevated in the ventral prostate of TRAMP mice fed a Western diet compared mice fed a CD [34].

Ribeiro *et al.* used three types of obese C57Bl/6J mice (n= 6/group): diet-induced obesity (DIO) mice; obese ob/ob mice, which are genetically deficient in leptin; and, db/db mice, which are genetically deficient in leptin receptor [35]. They also included WT mice on a standard laboratory diet. DIO mice were fed a HFD (45% kcal from fat), starting at 21 days of age. All three obese mice, as well as WT mice, were used to investigate the cellular growth of mouse prostate adenocarcinoma cell line (RM1), which is syngeneic to C57Bl/6J mice [35]. RM1 cells at 3.0 X 10^5 cells were subcutaneously inoculated, and tumor growth was monitored for 14 days [35]. The tumors from ob/ob mice (2.82 ± 0.46 g) and DIO mice (2.78 ± 0.19 g) were significantly heavier than tumors from wildtype (WT) mice (1.00 ± 0.24 g). However, the tumors from db/db mice were smaller than tumors from WT mice. Together, the above studies are consistent in demonstrating that obesity and/or a HFD accelerate PCa progression. However, while several studies have examined the association between obesity and aggressive PCa, little is known about molecular mechanisms that mediate obesity-driven PCa progression.

In a study of 125 obese Caucasian men, serum pigment epithelium-derived factor (PEDF) levels were significantly and positively correlated with BMI (r = 0.285; P-value =0.001) and with waist-to-hip ratio (r = 0.380; P-value <0.0001) [36]. Likewise, Jenkins *et al*. found that the serum PEDF concentrations were correlated with BMI (r = 0.28; p-value =0.046) in control (n= 54) and in Type 2 diabetes patients (n= 96) [37]. With weight loss, circulating PEDF decreased, and the reduction of circulating PEDF levels was significantly and positively associated with body weight loss decreased BMI (r = 0.788; P-value =0.0001), waist circumference (r = 0.681; p-value =0.0001), and hip circumference (r = 0.569; P-value =0.0001) [36].

To investigate this association, several mouse studies have been reported. Crowe *et al.* used C57Bl/6J mice that were fed either a HFD (60% kcal from fat) or a CD (4% kcal from fat) starting at eight-weeks old for 12 weeks [38]. The body weight of HFD-fed mice was 35.8 ± 1.2 while the body weight of a CD-fed mice was 28.9 ± 0.6. The plasma levels of PEDF were found to be significantly increased in HFD-fed mice (~ 15 ng/ml) as compared to mice fed a CD (~ 4.9 ng/ml) [38]. The plasma PEDF levels were positively correlated with increased body weight [38]. In addition, the PEDF mRNA and protein levels were elevated in adipose tissues from HFD-fed mice as compared to CD-fed mice [38]. Similar increases of PEDF mRNA and protein levels were observed in the adipose tissue of ob/ob mice compared to WT mice [38]. However, Moreno-Navarrete *et al.* showed that PEDF levels in adipose tissue did not alter circulating

PEDF levels, and subsequently, they found that the liver was the main source of circulating PEDF levels [39].

Overall, these studies support an association between the increased circulating PEDF and increased body weight. Although the elevated circulating PEDF is firmly established in obese individuals, it is unknown which PEDF isoform is elevated and if it has an anti-tumor activity. Also, the increased PEDF could be a compensatory mechanism in response to increased body weight in obesity since its expression is decreased with the body weight loss [36], [40]. No study has examined PEDF expression in obese patients with PCa since previous studies were mainly focused on understanding the molecular mechanisms by which obesity increases PEDF levels in patients with other metabolic diseases such as diabetes.

PCa, pigment epithelium-derived factor, and signaling pathways

PEDF is a 418 amino acid, 50 kDa, multifunctional glycoprotein that was originally identified in retinal-pigmented epithelium cells [41]. PEDF exists in both intracellular and extracellular compartments and has cell-type specific functions. The functional roles of PEDF includes acting as a potent anti-angiogenic factor, a tumor suppressor protein, and a neuroprotective agent [42]. PEDF belongs to the non-inhibitory (serpin) family composed of two distinct groups. One group has a region called the reactive center loop, and this region interacts with proteases, but the other group does not have this active region [41]. The first group contains the family of protease inhibitors and plays a crucial role in inflammation, blood coagulation, and

extracellular matrix reconstitution. However, the second group, which includes PEDF, functions in hormone transport, molecular chaperones, and tumor suppression [41].

Two isoforms of PEDF, named PEDF-1 and PEDF-2, have been identified, and it seems that each isoform has a specific function [43]. PEDF-2 has more a potent anti-tumor activity than PEDF-1 [43]. Also, they have different charge and molecular mass: PEDF-1 is 46,063 ± 13 Da and PEDF-2 is 47,176 ± 87 Da [43]. There are also two synthetic peptides of PEDF that are a 34mer-residue fragment (amino acids 44-77) and a 44mer-residue fragment (amino acids 78-121) [44], [45]. The 34mer PEDF peptide plays a significant role in anti-cancer activities, including suppressing both tumorigenic and angiogenic activities. The 44mer PEDF peptide is responsible for the neurotrophic effects [44], [45]. In addition to the above PEDF functions, PEDF has been recently identified as a novel regulator of lipid metabolism through binding and activating adipose triglyceride lipase (ATGL) [46], [47]. This activity appears to be linked to the 44mer PEDF peptide since a study demonstrated that 44mer PEDF peptide treatment decreased triglyceride (TG) accumulation via ATGL activation in cardiomyocytes [48].

In tissue specimens from PCa patients, there is a decrease in PEDF expression that is correlated with metastasis and poor prognosis [49], [50]. Bryne *et al.* used lipid depleted serum samples from PCa patients (n= 12) to perform proteomic analysis using 2-dimensional difference gel electrophoresis to identify potential biomarkers in PCa [51]. They found a significant decrease in serum PEDF levels with higher grades of PCa (P-

value =0.012) [51]. However, Ide *et al.* evaluated serum PEDF levels using an enzyme-linked immunosorbent assay (ELISA) and found a statistically significant increase in PEDF levels in PCa patients (n= 100) compared to normal subjects (n= 100) [52]. Additionally, increased plasma PEDF levels in PCa patients were positively correlated with increasing Gleason score (P-value =0.014) [52]. In addition, Ide *et al.* found a statistically significant positive association between BMI and serum PEDF in healthy subjects (P-value =0.03), but not in PCa patients. These inconsistent findings in serum PEDF may be due to sample preparation and assays used to evaluate PEDF levels.

Doll *et al*. demonstrated that PEDF knockout (KO) mice developed mPIN and had increased prostate stromal microvessel density as compared to WT mice [49]. Recombinant PEDF (rPEDF) treatment of PC-3 tumor xenografts in male nude mice decreased stromal vasculature and induced apoptosis [49]. Consistent with this, Guan *et al*. found that treatment with an adenoviral vector-expressed PEDF decreased PC-3 xenograft tumor growth with decreased microvessel density as compared to adenoviral-lacZ construct or phosphate buffer saline treatment [53]. In PEDF-KO mice placed on a HFD for 8 weeks, the mPIN progressed to cancer (Doll *et al.* unpublished data). In addition, the PEDF-KO mice have increased lipid accumulation as demonstrated by increased ATGL staining (Doll *et al.* unpublished data). Collectively, these data indicate that PEDF functions as an anti-tumor protein and in the regulation of cellular lipid levels in PCa.

To understand how obesity affects PEDF levels in PCa cells, our lab used excess OA treatment to simulate obesity in PCa cell lines *in vitro*. OA treatment increased lipid accumulation in DU145 and PC-3 cells in a dose-dependent manner (Doll *et al.* unpublished data). Our lab's previous studies showed that the levels of secreted PEDF were reduced in all PCa cell lines, LNCaP, PC-3, and DU145, and in a normal prostate epithelial cell line, RWPE-1 treated with 1 mM OA, (Doll *et al*. unpublished data). Additionally, 1 mM OA treatment further suppressed intracellular PEDF levels in DU145 and PC-3 cells while no effects on intracellular levels of PEDF were observed in RWPE-1 and LNCaP cells (Doll *et al*. unpublished observation). Conversely, rPEDF treatment (10 and 50 nM) reduced intracellular TG levels in basal and in OA-treated conditions, with a concomitant increase in lipolysis (TG breakdown) in PC-3 cells (Doll *et al.* unpublished data). Likewise, PEDF's function in TG lipolysis has also been demonstrated in human cervical adenocarcinoma (HeLa) cells and hepatocytes [46], [54]. In HeLa cells transfected with a PEDF expression vector, in the presence of 0.4 mM OA, PEDF expression increased TG lipolysis [54]. PEDF has been shown to activate ATGL resulting to increased TG breakdown in hepatocytes [46]. Taken together, these data support a role for PEDF in regulating lipid metabolism.

Currently, it is not known how excess OA suppresses PEDF in PCa cells. There are several candidate pathways for this effect, including activation of the G protein-coupled receptor 40 (GPR40) and activation of peroxisome proliferator-activated receptor gamma (PPARγ) as well as Wnt/ β-catenin signaling. GPR40, also known as

14

free fatty acid receptor 1 (FFAR1), is found to be expressed at the mRNA level in both DU145 and PC-3 cells [55], thus making it a potential receptor for OA-mediated activity. Several studies report that medium- and long-chain free FA, including OA, are a ligand for GPR40 [56]–[58].

GPR40 is known to signal through several pathways, including intracellular Ca^{2+} signaling. Alterations in intracellular Ca^{2+} signaling levels have been shown in association with changes in PEDF levels in retinal and neuronal cells [59], [60]. In ARPE19 cells, a human retinal pigment epithelial cell line, thapsigargin (1 μM) increased cytoplasmic Ca^{2+} levels and reduced PEDF mRNA levels [59]. Another study showed that rPEDF at 1.15 nM increased the intracellular levels of Ca^{2+} levels in granule cells [60]. However, in isoproterenol-induced hypoxia, cardiomyocytes treated with rPEDF at 10 nM reduced intracellular Ca^{2+} levels [61]. Although the stated studies show an association between PEDF expression and intracellular Ca^{2+} levels, their regulation in PCa is still not well understood.

Interaction of GPR40 with OA has been demonstrated to stimulate intracellular Ca^{2+} in islet β-cells and muscle cells [56]–[58]. In islet β-cells, OA treatments at 1, 3, 5, and 10 μM increased Ca^{2+} levels in the presence of 11.2 mM glucose; however, inhibition of GPR40 by siRNA transfection impaired OA-induced Ca^{2+} levels in islet β-cells [57]. More recently, and consistent with this, OA treatment at 10 μM increased intracellular Ca^{2+} in human airway smooth muscle (HASM) cells while GPR40-

15

knockdown in HASM cells showed a decrease in Ca^{2+} in the presence of 10 μM OA

[62]. Similarly, OA treatments in concentration ranges 100-500 μM elevated cellular

Ca^{2+} levels via GPR40 in bovine neutrophils [63]. These studies reveal that activation of

GPR40 increases intracellular Ca^{2+} levels in some cell types. However, it still unknown if

OA interacting with GPR40-increased Ca^{2+} leading to PEDF suppression in PCa cells.

Therefore, we investigated if GPR40-induced intracellular Ca^{2+} activation is required for

PA-induced PEDF suppression in PCa.

Another possible molecular mechanism for OA-mediated effect is through PPARγ

activation. PPARγ is known as a master transcription factor controlling lipogenesis [64].

The expression levels of PPARγ were investigated in PCa clinical samples using IHC

staining, and PPARγ protein was detected in the nucleus and cytoplasm of PCa cells

and PIN, but no detection was observed in normal prostate tissue samples [65], [66]. In

an *in vitro* study, PPARγ expression was identified in LNCaP, DU145, and PC-3 cells

although the activation of PPARγ, using troglitazone or rosiglitazone at 5-10 μM, was

found to induce growth inhibition in these cells [67]. Interestingly, several studies

reported that the activity of PPARγ was affected by both OA and PEDF in other cell

types [68], [69], but their associated activity in PCa cells is still unknown. In 3T3-L1

adipocytes, OA treatments at 25, 50, and 100 μM increased PPARγ activity [70]. Ricchi

et al. found a similar observation in the effects of OA treatments at 0.66 mM and 1.32

mM on elevated PPARγ mRNA expression in hepatocellular carcinoma cell line

(HepG2) [71]. These two studies indicate that OA activates PPARγ in some cell types.

Data obtained from the effects of PEDF treatment on PPARγ activity were mixed [72], [73]. Wang *et al.* exhibited that in differentiating 3T3-L1 cells, 10 and 100 nM rPEDF treatment inhibited PPARγ [72]. However, Hirsch *et al.* found that exogenous rPEDF treatments at the dosages of 10, 50, and 100 nM increased the expression of PPARγ in DU145 and PC-3 [61]. These studies suggest an association between PEDF and PPARγ activity, but these activities are dependent on cell types. Herein, we investigated the contribution of PPARγ activity on OA-mediated PEDF suppression in PCa cells.

Wnt/β-catenin signaling (herein "Wnt signaling") has been found to be increased in advanced PCa [74] and to play a role in lipid regulation [75]. Additionally, PEDF has been recently identified as an antagonist for Wnt signaling [76], [77]. High levels of Wnt-1 and β-catenin were detected in LNCaP, DU145, and PC-3 while low levels were observed in normal human prostate epithelial cells (PrEC) using immunocytochemical analysis [74]. In PCa tissues, increased expression levels of Wnt-1 and β-catenin were found to be associated with advanced and metastatic PCa, whereas their expression was not detectable in normal prostate tissues [74]. Increased activity of β-catenin, as measured by immunostaining for β-catenin, was associated with PCa progression and invasive phenotype [78]. Low-density lipoprotein-related protein 6 (LRP6) and frizzled-1 are a co-receptor and receptor for Wnt signaling, respectively. Their interaction stimulates phosphorylation of LRP6 which in turn releases β-catenin into cytoplasm [79].

mRNA expression levels of LRP6 and Wnt ligand were upregulated in metastatic PCa patient tissues compared to the primary tumor, and the expression levels were associated with increased risk of recurrent PCa (hazard ratio= 6.955; P-value =0.0038) [78].

Several studies showed that using silibinin and salinomycin, a chemical inhibitor of LRP6, decreased DU145 and PC-3 cell proliferation through downregulation of Wnt signaling [80], [81]. Elevated activity of Wnt signaling promotes lipid accumulation in the liver of HFD-fed mice (60% kcal from fat) compared to mice fed a low-fat diet (10.5% kcal from fat) [82]. Consistent with Wnt signaling-induced lipid accumulation, Wnt3a treatment, which is a Wnt signaling activator ligand, increased the size and number of lipid droplet (LD) formation in HeLa (cervical cancer), A431 (epidermoid carcinoma) cells, and normal HepaRG hepatocytes. However, inhibition of Wnt signaling, using dickkopf-related protein-1 (DKK-1) binding to Wnt co-receptor, prevented Wnt3a-induced LD in HeLa cells [83]. In addition, HeLa cells that were treated with Wnt3a ligand in the presence of OA at 100 μg/ml showed an increase in the size and number of LD compared to the Wnt3a treatment alone [83]. These results indicate that the activation of Wnt pathways plays a significant role in LD formation. Data also determine that Wnt signaling functions in lipid metabolism.

Interestingly, Park *et al.* and Protiva *et al.* have found that PEDF acts as an antagonist for Wnt signaling [76], [77]. Using *in vitro* and *in vivo* models, they have

shown that PEDF binds to LRP6, Wnt co-receptor, leading to inhibition of Wnt signaling

in the liver and retina [76], [77]. β-catenin levels were elevated in oxygen-induced

retinopathy and very low-density lipoprotein receptor-KO mice; however, when these

mice were intravitreally administered with rPEDF, β-catenin levels were decreased [76].

Park *et al.* displayed that after 2 h of treatment, rPEDF at 40 and 80 nM plus Wnt3a

agonist ligand reduced p-LRP6, total LRP6, and β-catenin in ARPE-19, a human retinal

pigment epithelial cells [76]. Protiva *et al.* support this finding in the liver by showing that

the activity of Wnt signaling and pLRP6 were increased in the liver of PEDF-KO mice

compared to WT mice; however, PEDF administration (25 μg/kg) reduced p-LRP6, but

not total LRP6 in PEDF-KO [77]. Additional *in vitro* studies supporting this observation

demonstrated that human hepatocellular carcinoma cell lines (HepG2 and Huh-7)

showed an increase in the activity of p-LRP6-associated with an increase in the activity

of β-catenin when these cells were transfected with siRNA PEDF [77].

Collectively, these studies demonstrate that PEDF binds to LRP6, Wnt co-

receptor, resulting in inhibition of Wnt signaling in *in vitro* and *in vivo* models. The

relevance of PEDF interacting with LRP6-mediated Wnt signaling pathways in lipid

metabolism and PCa progression has yet to be revealed. Thus, our studies were

designed to investigate the association between PEDF and Wnt signaling in PCa.

Summary

Previous data indicated that excess OA treatment suppressed PEDF expression

while PEDF treatment stimulated lipolytic activity in PCa cells. However, the effects of

excess lipids on PEDF expression in obese and HFD microenvironments *in vivo* are still unclear in PCa. Additionally, the molecular mechanisms through which PEDF is down-regulated by excess OA *in vitro* are currently unknown in PCa. Thus, we investigated an OA receptor, GPR40, to determine its involvement in OA-mediated PEDF suppression in PCa. We examined two potential intracellular signaling pathways, Ca^{2+} and PPARγ, that could contribute to suppressing PEDF in OA-overloaded PCa cells. As stated above, all of these molecular candidates are expressed in PCa, but the functional effects and their interactions, in the context of obesity-induced PEDF suppression, remain unclear. Therefore, this study was aimed to investigate the hypothesis that ***excess lipids, in obesity and HFD microenvironments, alter lipid metabolism, which in turn, increases pro-tumorigenic activity and decreases PEDF expression in PCa****.* We used *in vitro, ex vivo,* and *in vivo* models of obesity to explore how PEDF responds to excess lipids (**Figure 1**). Thus, our project had the potential to identify PEDF suppression as a key mediator of excess lipid-mediated PCa progression which could be targeted as an alternative strategy for therapeutic development in obese PCa patients.

Hypothesis and specific aims

The central hypothesis of this study was that *excess lipids, in obesity and HFD*

microenvironments, alter lipid metabolism, which in turn, increases pro-tumorigenic

activity and decreases PEDF expression in PCa. To test this hypothesis, the following

specific aims were proposed:
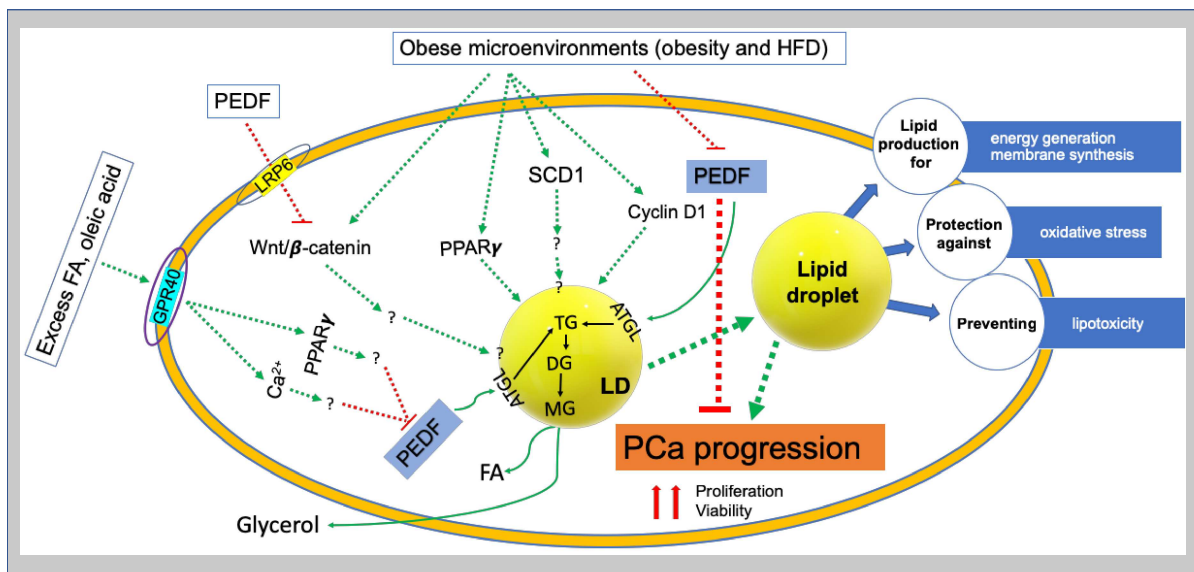
Figure 1. Proposed signaling pathways that are stimulated by an obese micromovement leading to accelerated PCa progression. The functions of lipid droplet were adopted from Petan *et al.* review article [29].

Specific Aim 1: Elucidate the molecular signaling pathways through which

excess OA, and other FA, suppress PEDF expression *in vitro*. <u>Working hypothesis:</u>

Excess OA activates GPR40-induced Ca^{2+} signaling and/or PPARγ signaling to

decrease PEDF expression in normal prostate and PCa cells.

Specific Aim 2: Determine if excess lipids, in obesity and HFD microenvironment, alter lipid metabolism by: (a) increased cyclin D1, (b) increased SCD1, and (c) decreased PEDF. *Working hypothesis: Pbsn-Cre$^+$PTEN$^{fl/fl}$ mice on HFD and ob/ob mice with TRAMPC2 xenografts have increased intracellular lipid levels-promoted lipid accumulation in PCa tissues, which in turn, accelerate PCa progression and reduced PEDF levels.*

Specific Aim 3: Elucidate if obesity and/or HFD increase the expression of PPARγ and Wnt signal pathways. *Working hypothesis: Pbsn-Cre$^+$PTEN$^{fl/fl}$ mice on HFD and ob/ob mice with TRAMPC2 xenografts have increased the expression of PPARγ and Wnt signaling pathways.*

MATERIALS AND METHODS

Cell culture

All cell lines were purchased from American type culture collection (ATCC, Manassas, VA). RWPE-1 cells were derived from an adult human prostatic epithelial cell line that was immortalized by transfection with human papillomavirus 18 [84]. LNCaP is a cell line derived from a supraclavicular lymph node metastasis of human prostatic carcinoma [85]. PC-3 was established from a human prostatic adenocarcinoma metastasis to bone [86], and DU145 is a cell line derived from a human prostate adenocarcinoma metastasis to the brain [87]. TRAMPC2 cells are a mouse PCa cell line derived from the TRAMP PCa model in a C57Bl/6J background [88]. The LNCaP, PC-3, DU145, and TRAMPC2 cell lines were maintained in Roswell Park Memorial Institute (RPMI) media (VWR, cat #. 10-040-cv) with 10% fetal bovine serum (FBS, Fisher, cat. # 26140079) and 1% penicillin/streptomycin (P/S, VWR, cat. # 30-002-CI). RWPE-1 cells were grown in Keratinocyte complete media (Fisher, cat. # 17005042). All cells were incubated at 37°C in 5% CO_2 for propagation.

Fatty acid preparation

FA (sodium oleate, sodium palmitate, or linoleic acid sodium salt) were dissolved in 100% methanol (Sigma-Aldrich, cat. # O7501, P9767, and L8134, respectively). PA only was heated at 55°C for 10 min to stimulate the solubility and to get a clear colorless solution. Then, FA solution was sterilized using a 0.22 µm syringe filter unit (Sigma-

Aldrich, cat. # SLGV033RS). After filtration, 5 mM of FA was prepared in 7.5% FA-free

BSA (Sigma-Aldrich, cat. # A8806). To stimulate FA/BSA conjugate, the mixture was

then incubated at 37°C for 1 h with shaking. FA assay kit (Abcam, cat. # ab185433) was

used to validate the final concentration of FA/BSA conjugate. However, we were not

able to verify the concentration of FA/BSA conjugate because the mixture of FA/BSA

interfered with FA assay reagents.

Cell treatment

RWPE-1, DU145, PC-3, and TRAMPC2 cells were plated at 20,000 cell/cm^2, but

due to their slow growth rate, LNCaP cells were plated at 40,000 cell/cm^2 in a 10-cm

tissue culture dish. The cells were then incubated at 37°C in 5% CO_2 for 18-24 h to

ensure cell attachment. After the incubation, media were aspirated, and the cells were

washed with 1x phosphate buffer saline without calcium or magnesium (PBS, Fisher,

cat. # MT21-031-CV). PBS was aspirated, basal media with only P/S was then added (5

ml/10 cm dish), and the cells were incubated for 4 h. After the 4 h incubation, basal

media was aspirated, and cells were treated with various agents. For FA type

experiments, OA/BSA, PA/BSA, or LA/BSA conjugate at 0.25, 0.5, and 1 mM

concentrations were prepared in basal media with P/S, added to the cells, and

incubated for 48 h. For the cell signaling experiments, the cells were treated with 1 mM

liquid OA plus or minus 10 μM GPR40 antagonist (GW1100; cat. # 10008908) [89], 10

μM Ca^{2+} chelator (BAPTA-AM; cat. # 15551) [90], or 10 μM PPARγ antagonist

(GW9662; cat. # 70785) [91]. GPR40 antagonist (GW1100), Ca^{2+} chelator (BAPTA-AM),

and PPARγ antagonist (GW9662) were purchased from Cayman chemical. GW9662

was dissolved in methanol while GW1100 and BAPTA-AM were dissolved in dimethyl

sulfoxide (DMSO). The cells were treated with 1 mM OA plus or minus each inhibitor of

interest or vehicle, and incubated for 48 h. After the incubation, cell samples were

collected as described below. The untreated group served as a control group for the

experiment. The vehicle (100% DMSO or 100% methanol) was included as an

additional control at an equivalent concentration to the inhibitor treatment group.

Conditioned media collection and concentration

After the 48 h incubation of the cells with treatment, conditioned media (CM)

were transferred from 10 cm dishes to 15 ml conical tubes, and 1X protease inhibitor

cocktail (PIC, Sigma-Aldrich, cat. # P8340) and phenylmethylsulfonyl fluoride (PMSF, 1

μM, Sigma-Aldrich, cat. # 93482) were added to a final dilution of 1:100. The collected

CM were centrifuged at 1000 x g for 10 min to precipitate cellular debris. Then, the

centrifuged CM were transferred to a clean 15 ml conical tube. Next, the CM were

filtered using a Millipore ultra-15 centrifugal filter device with a 3 kDa cutoff to

concentrate the protein (MilliporeSigma, cat. # UFC900324). The membrane of the

filtration device was pre-wet with 5 ml of sterile PBS and centrifuged at 4000 x g at 4°C

for 5 min. Then, 5 ml of CM and 5 ml of PBS were added to the membrane and

centrifuged at 4000 x g for 1-4 h. The final concentration of CM was approximately 10-

fold (500 μl). The concentrated CM was transferred to a 1.5 ml sterile siliconized microfuge tube and stored at -80°C until use.

Proliferation and viability assay

After the 48 h FA treatment, the proliferation and viability of the cells were quantified. Briefly, the cells were washed one time with PBS, and 1 ml of trypsin (Fisher, cat. # MT25053CI) was added to detach cells. Then, 50 μl aliquot of the trypsin/cell solution was taken and mixed with 50 μl of a 0.4% trypan blue exclusion dye. After a 5 min incubation, 15 μl of cell suspension was loaded onto a hemocytometer. The live cell number (unstained cells) and dead cell number (blue cells) were counted. The cell viability was calculated as a percentage by the formula: viability = (live cell number/total cell number) x 100%. Proliferation data were normalized to the untreated group.

MTT proliferation assay

PCa cells were plated at 40,000 cell/cm^2 in 96-well flat bottom and incubated overnight to allow attachment. Then, cells were washed with PBS and incubate in basal media media for 4 h. After 4 h, basal media were aspirated, experimental and vehicle treatments were added. The cells with treatment media were incubated for 48 h. Next, 100 μ of basal media plus 10 μl of 12 mM MTT (3-(4,5-dimethylthiazol-2-yl)-2,5-diphenyltetrazolium bromide) stock solution were added to each well and then

incubated at 37°C for 4 h. Then, 85 µl of medium was aspirated, and 50 µl of DMSO was added and mix. The plate was again incubated at 37°C for 10 min, absorbance was read at 540 nm.

Cell lysate (CL) collection

The collected cells were pelleted by centrifugation at 1000 x g for 8 min, and the supernatant was then discarded. Next, 350 µl of 1X cell lysis buffer (Sigma cat. # 9803S), which contained 1X PIC and 1 µM PMSF, was added. After that, the cells were incubated on ice for 5 min. The cell mixture was transferred to a microfuge tube and was vortexed for 30 sec. The sample was centrifuged at 14000 x g at 4°C for 10 min. Finally, the CL was transferred to a siliconized microfuge tube and stored at -80°C until used.

Protein quantification

Total protein in CL and CM samples was quantified using a standard Coomassie dye-binding assay (Thermo Fisher cat. # 1856209). Briefly, for CL, 1-5 µl of cell lysate was added to 490 µl of Coomassie reagent, and 1XPBS was added to bring the final volumes to 500 µl. For CM sample analysis, 490 µl of Coomassie reagent was transferred into centrifuge tubes, and 5 or 10 µl of CM was added. If 5 µl of CM was used, then 5 µl of PBS was added. The standards were prepared with prediluted bovine

serum albumin standards (Fisher, cat. # 23208). Then, 225 μl of samples and standards were transferred to wells into a 96-well plate in duplicate. The absorbance at 595 nm was measured in each well on a plate reader (Bio-Tek, KC4). The KC4 program generated a standard curve and calculated the mean concentrations of each sample.

Human PEDF quantification

A human enzyme-linked immunosorbent assay (ELISA) was used per the manufacturer's instructions (Bioexpress, Frederick MD, PEDF ELISA kit cat. # PED613-Human) to quantify PEDF levels in CM and CL samples. Briefly, 20 μg of total CL or CM protein was added to the wells in a pre-coated anti-PEDF antibody 96-well plate, in duplicate. The standards were prepared and added. The microtiter plate was covered and incubated at 37°C for 1 h. The mixture was aspirated from each well and washed 5 times with wash buffer to remove unbound antigen. PEDF primary antibody was added to the wells, and the microtiter plate was recovered and re-incubated at 37°C for 1 h. The plate was washed again 5 times to remove the unbound antibodies. Streptavidin peroxidase substrate was added to the wells and incubated at RT for 20 min. After the incubation, sulfuric acid stop solution was added to stop the reaction. The absorbance at 595 nm was measured in each well on a plate reader (Bio-Tek, KC4). The concentrations of PEDF were calculated based on the standard curve, and values were normalized to total protein.

Mouse strains and diets

All experimental procedures were approved by the Institutional Animal Care and Use Committee of University of Wisconsin-Milwaukee (UWM). All mice were housed in a specific pathogen-free condition in the animal facility at UWM. Mice were kept in a temperature-controlled room on 12 hours of light with 12 hours of dark cycle.

For a PCa tumor xenograft study, male C57Bl/6J WT and ob/ob mice (C57Bl/6J background) were purchased from The Jackson laboratory. WT and ob/ob mice were fed a standard chow diet (Teklad 7912), *ad libitum*. Ob/ob mice were used to mimic human obesity as they are genetically deficient in leptin, a satiety hormone, and thus overeat and become obese [92]. Mouse PCa TRAMPC2 cells, syngeneic to C57BL/6J mice, were used in this tumor xenograft study. For the HFD study, we used male Pbsn-Cre$^+$-PTEN$^{fl/fl}$ (C57Bl/6J background) mice, which develop PCa due to prostate-specific knockout of the PTEN tumor suppressor gene.

DNA preparation

For the generation of Pbsn-Cre$^+$-PTEN$^{fl/fl}$ mice for the HFD study, we crossed Pbsn-Cre$^+$ mice with PTEN$^{fl/fl}$ mice. These mice were bred and genotyped from a colony maintained in the Doll lab. Mouse tail tissue was obtained using a razor blade at 21 days of age. For DNA extraction, we used Puregene DNA Purification Kit (Qiagen cat. # 158267). Briefly, cell lysis solution was chilled on ice, and lysis cocktail was prepared by

combining 150 μl of ice-cold cell lysis solution and 0.75 μl of proteinase K solution. After

preparation of lysis cocktail, 150 μl was added to each tube containing a mouse tail

tissue and incubated at 55°C overnight (at least 16 h) with shaking. Next, samples were

cooled to RT, and 50 μl of protein precipitation solution was added. The mixture was

vortexed at high speed for 20 seconds to mix. Then, samples were centrifuged at

16,000 x g for 6 min.

After centrifugation, the supernatant, containing the DNA, was transferred into a

clean 1.5 ml microfuge tube containing 150 μl of 100% isopropanol. The samples were

gently mixed by inverting the tube and were then centrifuged at 16,000 x g for 10 min.

The supernatant was poured off, and the tube was drained using clean absorbent

paper. Next, 150 μl of 70% ethanol was added to each tube, and the tubes were gently

mixed by inverting them. Again, the samples were centrifuged at 16,000 x g for 10 min.

Then, the 70% ethanol was poured off, and the tube was again drained using clean

absorbent paper. The samples were allowed to air dry for 15 min. After that, 100 μl DNA

hydration solution was added to each tube. The samples were incubated at RT

overnight. DNA samples were stored at 4°C until use.

Pbsn-Cre and PTEN^{fl/fl} allele genotyping

The presence of the Pbsn-Cre transgene and PTEN^{fl/fl} gene allele was validated

using polymerase chain reaction (PCR). All primers were purchased from Invitrogen

(Carlsbad, CA) and reconstituted at 100 μM using sterile Tris-EDTA buffer. The primers

for Pbsn-Cre and PTEN$^{fl/fl}$ PCR reaction are shown in **Table 1**. We used the MJ

Research PTC100 thermal cycler (Watertown. MA). PCR cocktail was prepared for

each reaction (**Table 2** and **Table 3**). Next, 24 μl of PCR cocktail of Pbsn-Cre was

added to each tube, and 1 μl of tail DNA was added. The Pbsn-Cre PCR program is

shown in **Table 4**. For the PTEN reaction, and 23 μl of PCR cocktail was added to each

tube, 2 μl of tail DNA was added to appropriate tube. The PTEN PCR program is

presented in **Table 5**.

Table 1. Primer sequences for PCR	
P021 (Pb-Cre-F)	5'- CTG AAG AAT GGG ACA GGC ATT G -3'
C031 (Pb-Cre-R)	5'- CAT CAC TCG TTG CAT CGA CC -3'
OIMR9554 (PTEN-F)	5'- CAA GCA CTC TGC GAA CTG AG -3'
OIMR9555 (PTEN-R)	5'- AAG TTT TTG AAG GCA AGA TGC -3'

Table 2. Pbsn-Cre genotyping PCR reaction	
Component:	PB-Cre (in ml) for one reaction
mQH$_2$O	18.25
10x PCR buffer	2.5
50 mM MgCl$_2$	1
10 mM dNTP mix	0.5
20 µM primer - C031	0.625
20 µM primer - P021	0.625
5 U/µl JumpStart Taq	0.5
TOTAL	**24 ml**

Table 3. PTEN$^{fl/fl}$ genotyping PCR reaction	
Component:	PTEN (in ml) for one reaction
Water	9.3
Midsci Master Mix*	12.5
20 µM primer – OIMR0554	0.6
20 µM primer – OIMR0555	0.6
TOTAL	**23 ml**
* Bullseye Taq Plus Master Mix with red dye was purchased from MidSci (cat #. Betaqr-r).	

Table 4. Pbsn-Cre PCR program using MJ Research PTC100 thermal cycler			
Step	PCR process	Temperature (°C)	Time
1	Initial denature	94	3 min
2	Denature	94	30 sec
3	Annealing	60	30 sec
4	Elongation	72	30 sec
5	Repeat step 2-4, 34 more times (35 cycles total)		
6	Elongation	72	3 min
7	Hold, 10°C, indefinitely		

Table 5. PTEN PCR program using MJ Research PTC100 thermal cycler			
Step	PCR process	Temperature (°C)	Time
1	Initial denature	94	3 min
2	Denature	94	30 sec
3	Annealing	60	1 min
4	Elongation	72	1 min
5	Repeat step 2-4, 34 more times (35 cycles total)		
6	Elongation	72	2 min
7	Hold, 10°C, indefinitely		

TRAMPC2 xenograft study

Ob/ob (n= 40) and WT (n= 40) mice were ear-tagged for unique identification. At 3.5 months of age, the mice were anesthetized using 1-3% Isoflurane inhalation in a desiccator jar, and 5×10^6 TRAMPC2 cells were subcutaneously injected into the right flank of WT and ob/ob mice. The mice were monitored for tumor growth. Once palpable tumors were present, the tumors were measured weekly (longest length and perpendicular diameter recorded). Tumor volume was then calculated using the following formula: volume = [(length x width^2) x 0.52] [93]. Once the largest tumors reached 20 mm in diameter, all mice injected with TRAMPC2 xenografts were euthanized. Tumor tissues were harvested at approximately 6 months of age. Due to variability in tumor take rate and time to tumor initiation, only a subset of WT mouse tumor (n= 10) and ob/ob mouse tumor (n= 20) was used in the TRAMPC2 xenograft study. This subset was chosen based on the same tumor initiation time frame.

Pbsn-Cre$^+$-PTEN$^{fl/fl}$ HFD study

Pbsn-Cre$^+$-PTEN$^{fl/fl}$ mice were ear-tagged at weaning (21 days of age) for unique identification, and a piece of tail tissue was obtained as described above to confirm genotype. The mice were fed either a HFD (Harlan Teklad diet TD.06414, 60% kcal from fat; n= 18) or CD (**Table 6**; Harlan Teklad diet TD.08810; 16.8% kcal from fat; n= 18) starting at 2 months of age and were sustained for 4 months. Three to four mice were housed per cage. Food intake was measured weekly, and mouse weights were

also recorded weekly. At 6 months of age, serum was collected, and subcutaneous adipose tissue, epididymal fat pad, liver, and prostate lobes were harvested.

Table 6. Nutrient and energy information of the control diet and high-fat diet		
Diet ⟍ Component	CD (% kcal)	HFD (% kcal)
Protein	22.3	18.3
Carbohydrate	60.9	21.4
Fat	16.8	60.3

Blood collection and serum preparation

Blood samples were collected from both *in vivo* PCa models at harvest using an ocular sinus (retro-orbital) technique. Briefly, mice were placed in a desiccator jar containing 1-3% Isoflurane within a fume hood. When the mice were anaesthetized, blood samples were collected by inserting a pasteur pipette into the medial canthus of the eye and was gently moved into the sinus. When sufficient blood was obtained, the pasteur pipette was removed. A guaze pad was gently pressured to the mouse eye to facilitate hemostasis. The collected blood was dispensed into 1.5 ml microfuge tubes and kept at RT for at least 30 min to allow clot to form. Next, the clotted blood was centrifuged at 860 x g at RT for 10 min to remove cellular components. The serum was transferred into a 1.5 ml siliconized tube and was stored at -80°C until use.

<u>Tissue harvest</u>

To harvest mouse tissues, following blood collection, mice were returned to 1-3% Isoflurane to euthanize them by anesthesia overdose, followed by a cervical dislocation to ensure death. For TRAMPC2 xenograft study, tumor tissues were harvested and weighed. For Pbsn-Cre$^+$-PTEN$^{fl/fl}$ mice HFD study, subcutaneous adipose tissue, epididymal fat pad, liver, and prostate lobes were harvested. Both the prostate and epididymal fat pads were weighed. All collected tissues were flash frozen in liquid nitrogen and stored at -80°C until processing.

<u>Tissue homogenization</u>

A portion of TRAMPC2 tumor tissues was weighed and placed in a 1.5 ml microfuge tube on ice. For the Pbsn-Cre$^+$PTEN$^{fl/fl}$ model, all prostate lobes (ventral, dorsolateral, and interior) and periprostatic fat tissues were weighed. To homogenize the tissues, we used a tissue extraction reagent I (TER) (Invitrogen, Carlsbad, CA Cat # FNN0071). The volume of TER was calculated based on the total tissue weight (1 ml of TER per 0.1 g of tumor tissue) with 1X PIC, PMSF, and PhosSTOP (Sigma-Aldrich, cat. # 4906845001). The estimated volume of prepared TER solution was added to tumor tissues. Then, tumor tissues were homogenized using a motorized disposable pestle while kept on ice. After homogenization, samples were centrifuged at 10,000 RPM for 5 min. The supernatant was transferred into a 1.5 ml siliconized tube and kept on ice. Total protein content was quantified using a Coomassie dye-binding protein assay as

described under the protein quantification section using 10 µl tissue homogenate and 490 µl of Coomassie reagent.

Western blot assay

Western blot analysis was performed on the homogenized TRAMPC2 tumor tissue and on the PCa cell line CL samples. Primary antibodies, purchased from Cell Signaling Technology (CST; Danvers, MA and Abcam), were cyclin D1 (cat. # 2922), PPARγ (cat. #2430), pβ-catenin Thr41/Ser45 (cat. # 9565), β-catenin (cat. # 9562), E-cadherin (cat. # 3195), LRP6 (cat. # 3395), pLRP6 ser1490 (cat. # 2568), JNK (cat. # 3708), pJNK Thr183/Tyr185 (cat. # 4668), pERK1/2 Thr202/Tyr204 (cat. # 4377), AMPKα (cat. # 2532), pAMPKα Thr172 (cat. # 2535), and SOD2 (cat. # 13194). For a loading control, pan-actin (cat. # 8456) or GAPDH (cat. # 3683) was used. Serine palmitoyltransferase (SPT) was purchased from Abcam (cat. # ab23696). Secondary antibody conjugated to horseradish peroxidase (HRP) was purchased from CST (cat. # 7074).

Thirty µg of CL protein was separated by SDS-polyacrylamide gel electrophoresis [SDS-PAGE; 4-20% precast acrylamide gel (BIO-RAD, Hercules, CA)]. For a size standard, we used a pre-stained protein marker (MIDSCI, Valley Park, MO cat. # BEPAR or FPL1). Electroblotting was used to transfer the separated proteins from the gel to a polyvinylidene difluoride membrane (PVDF; GenHunter, Nashville, TN cat. #

88518). The PVDF membrane was blocked with either 5% non-fat dry milk or 5% BSA (Thermo Scientific cat. # BP1600-100). After hybridization with primary antibody, the appropriate secondary antibody, conjugated to HRP, was added. The proteins of interest were then detected using a chemiluminescent detection system (Thermo Scientific; cat #. 34095 or 34580) through enzymatic reaction with HRP. The blot was then exposed to X-ray film to obtain an autoradiogram for a permanent record. Densitometry (ImageJ, NIH) was performed on the resulting bands of the correct molecular weight for semi-quantitative analysis.

Mouse PEDF quantification

The concentration of mouse PEDF protein was measured using a Mouse PEDF ELISA following the manufacturer's protocol (MyBioSource, San Diego, CA cat. # MBS2887741). All reagents were brought to the RT and were prepared per the manufacturer's instructions. Standard reagent was reconstituted in 1 ml of sample diluent and was placed on an orbital rotator to ensure complete dissolution. Serial dilutions of standards were prepared. For TRAMPC2 tumor tissues, 0.05 μg of total protein/well was prepared in sample diluent before the samples were loaded into wells in duplicate in 96-well plate. Mouse serum samples were diluted at 1:20 in sample diluent before they were loaded into the ELISA plate in duplicate.

Next, 100 µl of standards and samples were loaded into wells in duplicate. Then, the plate was covered and incubated at 37°C for 2 h. After 2 h of incubation, standards and sample liquids were aspirated from each well. Then, 100 µl of Detection Solution A was added to each well. The plate was sealed and incubated at 37°C for 1 h. After incubation, the detection solution A was aspirated, and the plate was washed with 1X wash buffer that left in wells for 1-2 min. The wash buffer was aspirated, and the wash was repeated for a total of three washes. After washing, 100 µl of Detection Solution B was added to each well. The plate was sealed and incubated for 1 h. The plate was washed again for a total of 5 times. Next, 90 µl of substrate solution was added to all wells, and the plate was covered and incubated 37°C for 10-20 min. 50 µl of stop solution was added to each well. The plate was read at 450 nm using the Synergy HT plate reader (Biotek, Winooski, VT). The unknown PEDF levels of each sample were calculated from the standard curve.

Serum mouse leptin quantification

The serum concentration of leptin was measured using Mouse/Rat Leptin Quantikine ELISA Kit per the manufacturer's protocol (R&D system, Minneapolis, MN cat. # MOB00). Serum of CD-fed Pbsn-Cre[+]PTEN^{fl/fl} mice was diluted 20-fold into calibrator diluent RD5-3 while serum of HFD-fed Pbsn-Cre[+]PTEN^{fl/fl} mice was diluted 100-fold into calibrator diluent RD5-3. The Mouse/Rat leptin standard was reconstituted with 2 ml of calibrator Diluent RD5-3. Then, 50 µl of assay diluent RD1W was added to

each well followed by adding 50 μl of standard, control, and samples. Next, the plate was gently mixed by tapping the plate frame for 1 min, then covered with an adhesive strip, and incubated at RT for 2 h. After incubation, the plate was washed with 1X wash buffer for five times, and 100 μl of Mouse/Rat leptin conjugate was added to each well. Then, the plate was covered with an adhesive strip and incubated at RT for 2 h. After that, the plate was washed with 1X wash buffer for 5 times, and next, 100 μl of substrate solution was added to all wells. Then, the plate was protected from the light and incubated at RT for 30 min. Then, 100 μl of stop solution was added to each well, and absorbance was determined at 450 nm using the Synergy HT plate reader (Biotek, Winooski, VT). The unknown concentration of leptin was calculated from the generated standard curve.

Statistical analysis

All *in vitro* experiments were repeated at least twice with similar results. Student's t-test was used to determine changes on cell proliferation (total cell number, live cell number, and viability), and PEDF levels between groups. If a data set included values that were above or below the detection limit of the assay, a Mann–Whitney U test was used. One-way ANOVA was performed to determine significant differences in dose-response experiments. If a significant difference in group means was revealed by one-way ANOVA, Post-hoc Bonferroni procedure was used for pairwise comparison. Statistical significance was set at $p < 0.05$, and data from the *in vitro* study were

presented as the mean ± standard deviation of the mean (SD) while data from the *in vivo* study were presented as the mean ± standard error of the mean (SEM).

RESULTS

INVESTGATION OF SIGNALING PATHWAYS MEDIATING FATTY ACID-INDUCED

PEDF SUPPRESSION IN PCA CELLS *IN VITRO*

The effects of FA on the proliferation and viability of normal prostatic epithelial

cells and PCa cells

In previous studies, a stimulatory growth response to excess OA was observed in

two androgen-independent PCa cells, PC-3 and DU145; however, normal prostatic

epithelial cells, RWPE-1, and androgen-dependent PCa cells, LNCaP, did not show this

stimulatory growth response to excess OA (Doll *et al.* unpublished data). Particularly,

OA at the dosage of 0.1-1.5 mM stimulated the proliferation of PC-3 and DU145 cells

after 48 h of incubation in a concentration-dependent manner compared to untreated

group (Doll *et al.* unpublished data). As published studies showed that OA treatments

interact with GPR40 receptor leading to activated cytoplasmic Ca^{2+} and/or PPARγ [57],

[94], we wanted to investigate whether these molecules are necessary for OA to exert

its pro-proliferative effects on PCa cells (**Figure 1**). In this study, the cells were treated

with 1 mM OA, ready to use from Sigma-Aldrich, in the presence or absence of GPR40

inhibitor (GW110), Ca^{2+} chelator (BAPTA AM), or PPARγ inhibitor (GW9662) at 10 μM.

OA treatment at 1 mM was used to simulate obesity *in vitro* (Doll *et al*. unpublished

42

study)*.* Then, proliferation and viability were assessed using a direct cell count with trypan blue exclusion dye, respectively.

Consistent with previous studies, total live numbers of LNCaP cells were not changed with OA plus or minus the GPR40 inhibitor, GW1100, treatment at 10 μM (**Figure 2A**). Likewise, these treatments did not change viability in LNCaP cells (**Figure 2B**). OA alone or with GW1100 inhibitor did not change DU145 cell proliferation and viability (**Figure 3A** and **3B**). This observation is inconsistent with our lab previous data as proliferation was shown to increase with 1 mM OA. Proliferation and viability of RWPE-1 and PC-3 cells were also tested with OA alone or with the GPR40 inhibitor. However, the proliferation data were not presented since large variances within experiments was found. The current data suggest that OA treatment alone or with GPR40 inhibitor did not affect LNCaP and DU145 cells.
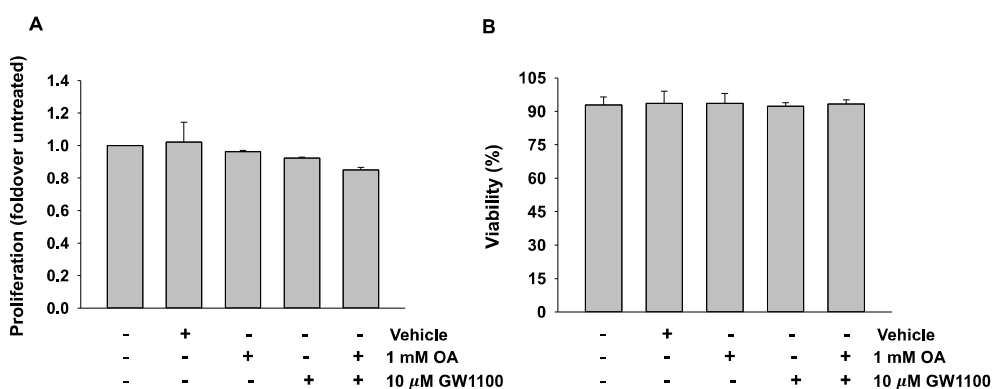
Figure 2. Proliferation and viability were not affected in LNCaP cells treated with 1 mM oleic acid (OA) +/- GPR40 inhibitor. LNCaP cells were seeded at 40,000 cells/cm^2 in tissue culture dishes. The cells were incubated overnight and were then treated with 1 mM OA +/- 10 μM GW110 or vehicle (DMSO; 5.2 μl). After 48 h of incubation, cells were collected, and proliferation (**A**) and viability (**B**) were assessed by hemocytometer with trypan blue dye. No significant changes were observed among groups compared to untreated group. Proliferation data are presented as fold over the untreated control group. Both data sets are presented as the mean ± SD. The experiment was repeated at least twice with similar results.

Figure 3. Proliferation and viability levels are not changed in DU145 cells treated with 1 mM oleic acid (OA) +/- GPR40 inhibitor. DU145 cells were seeded at 20,000 cells/cm^2 in tissue culture dishes. The cells were incubated overnight and were then treated with 1 mM OA +/- 10 μM GW110 or vehicle (DMSO; 5.2 μl). After 48 h of incubation, cells were collected, and proliferation (**A**) and viability (**B**) were assessed by hemocytometer with trypan blue dye. No significant changes were observed among groups compared to untreated group. Proliferation data are presented as fold over the untreated control group. Both data sets are presented as the mean ± SD. The experiment was repeated at least twice with similar results.

We next examined if Ca^{2+} was necessary for excess OA to produce its pro-proliferative effects on PCa cell growth. PC-3 cells were treated with 1 mM OA plus or minus 10 μM Ca^{2+} chelator (BAPTA AM). OA alone or in the presence of BAPTA AM treatment did not change the proliferation of PC-3 cells (**Figure 4A**). With regards to cell viability, no significant difference was observed between groups in PC-3 cells (**Figure 4B**). We also examined RWPE-1 cells treated with OA plus or minus the BAPTA AM chelator, but no consistency within experiments was observed (data not shown).
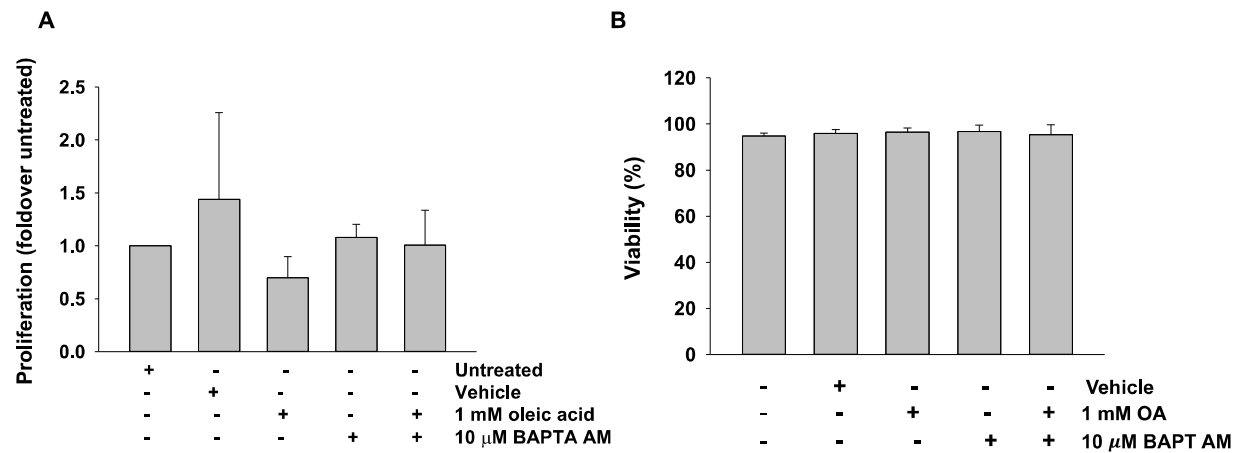
Figure 4. PC-3 cell proliferation is not changed with 1 mM oleic acid (OA) treatment +/- Ca^{2+} chelator. PC-3 cells were seeded at 20,000 cells/cm^2 in tissue culture dishes. The cells were incubated overnight and were then treated with 1 mM OA +/- 10 μM BAPT AM or vehicle (DMSO; 1.9 μl). After 48 h of incubation, cells were collected, and proliferation (**A**) and viability (**B**) were assessed by hemocytometer with trypan blue dye. No significant changes were observed among groups compared to untreated group. Proliferation data are presented as fold over the untreated control group. Both data sets are presented as the mean ± SD. The experiment was repeated at least twice with similar results.
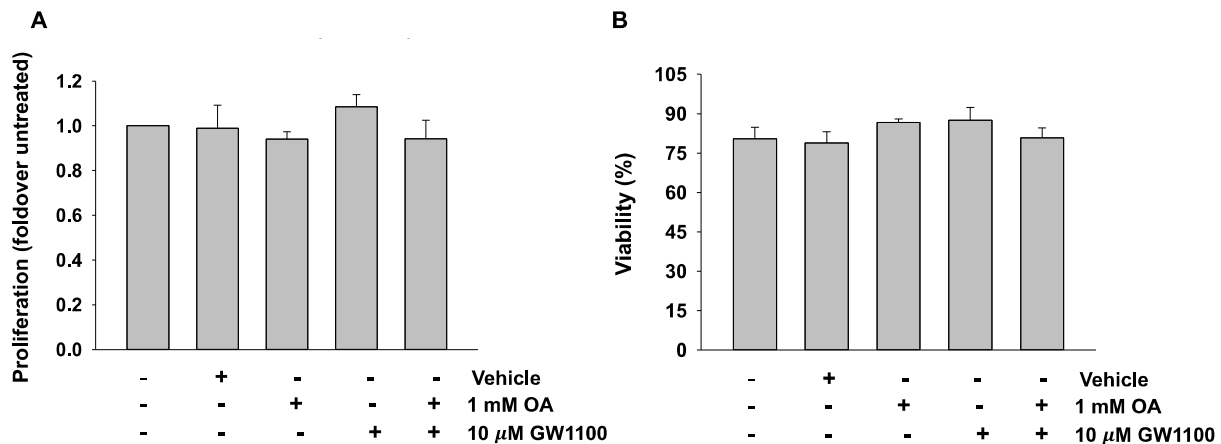
In additional to GPR40 and Ca^{2+} inhibitors, a PPARγ inhibitor was studied to test whether PPARγ activity was necessary for excess OA-signaling effects on DU145 and PC-3 cell proliferation and viability. RWPE-1 and DU145 cells displayed no effects on cell growth and viability when the cells were treated with OA alone or in the presence of GW9662 inhibitor (**Figure 5** and **Figure 6**).
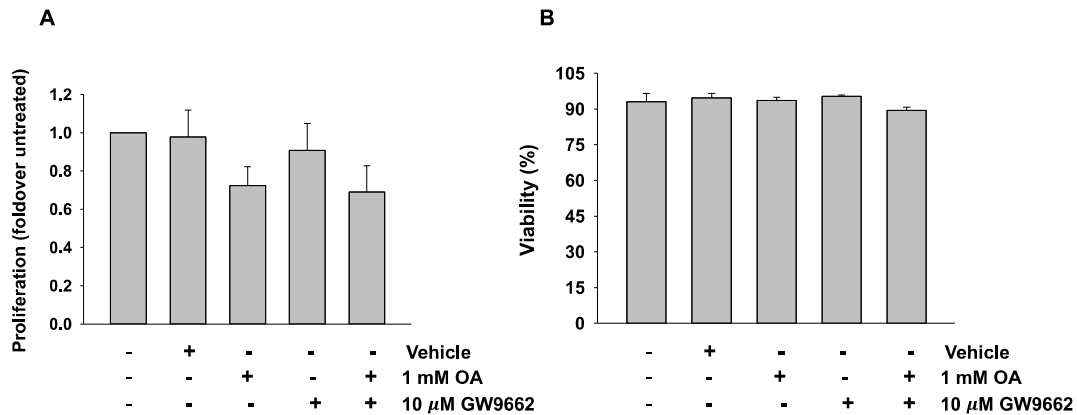
Figure 5. Oleic acid (OA) +/- PPARγ inhibitors do not change RWPE-1 cell proliferation. RWPE-1 cells were seeded at 20,000 cells/cm^2 in tissue culture dishes. The cells were incubated overnight and were then treated with 1 mM OA +/- 10 μM GW9662 or vehicle (ethanol; 6.9 μl). After 48 h of incubation, cells were collected, and proliferation (**A**) and viability (**B**) were assessed by hemocytometer with trypan blue dye. No significant changes were observed among groups compared to untreated group. Proliferation data are presented as fold over the untreated control group. Both data sets are presented as the mean ± SD. The experiment was repeated at least twice with similar results.

Figure 6. Proliferation and viability are not changed in DU145 cells treated with 1 mM oleic acid (OA) +/- PPARγ inhibitor. DU145 cells were seeded at 20,000 cells/cm^2 in tissue culture dishes. The cells were incubated overnight and were then treated with 1 mM OA +/- 10 μM GW9662 or vehicle (ethanol; 6.9 μl). After 48 h of incubation, cells were collected, and proliferation (**A**) and viability (**B**) were assessed by hemocytometer with trypan blue dye. No significant changes were observed among groups compared to untreated group. Proliferation data are presented as fold over the untreated control group. Both data sets are presented as the mean ± SD. The experiment was repeated at least twice with similar results.

46

Nonetheless, LNCaP cells exhibited a significant decrease in proliferation when the cells were treated with OA alone, but not with PPARγ inhibitor, as compared to untreated group (P-value =0.002; **Figure 7A**). No changes were observed in LNCaP cell viability with OA in the presence or absence of PPARγ inhibitor (**Figure 7B**). A significant decrease was found in the proliferation of PC-3 cells treated with OA alone or in the presence of GW9662 (P-value <0.001; **Figure 8A**) whereas no changes were observed in the viability of PC-3 (**Figure 8B**). Of note, the observed proliferation data regarding LNCaP and PC-3 cells treated with OA alone are contrasted with what we have found in the first experiments. TRAMPC2 cells have not been previously tested with OA treatment alone or in the presence of PPARγ chemical inhibitors. We found that OA alone treatment significantly decreased TRAMPC2 cell proliferation compared to untreated group (P-value =0.043; **Figure 9A**). However, no changes were found in viability of TRAMPC2 cells treated with the PPARγ chemical inhibitor alone or plus OA (**Figure 9B**).
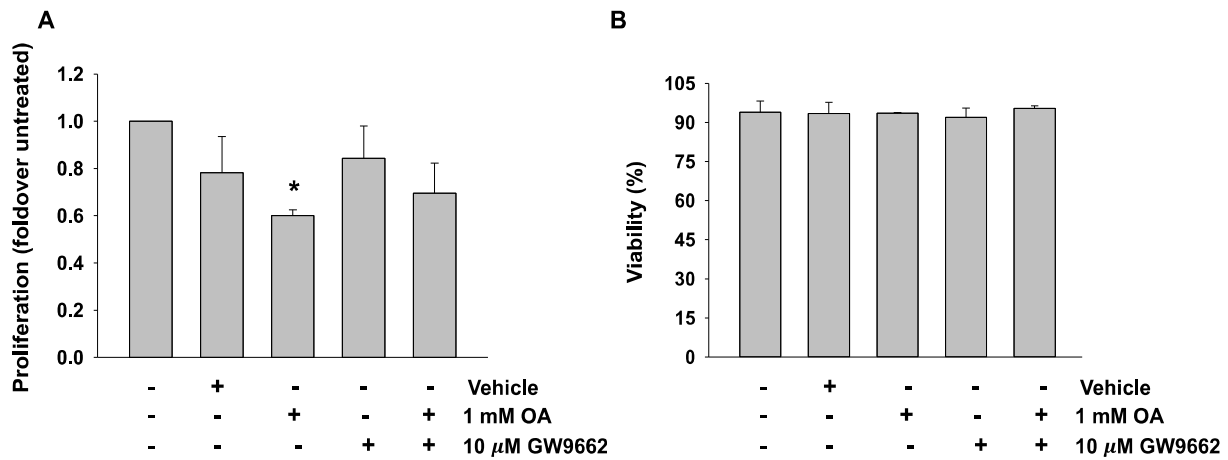
Figure 7. Oleic acid (OA) treatment decreases LNCaP cell proliferation. LNCaP cells were seeded at 40,000 cells/cm^2 in tissue culture dishes. The cells were incubated overnight and then were treated with 1 mM OA +/- 10 μM GW9662 or vehicle (ethanol; 6.9 μl). After 48 h of incubation, cells were collected, and proliferation (**A**) and viability (**B**) were assessed by hemocytometer with trypan blue dye. *P-value =0.002 compared to untreated group. PPAR*γ* inhibitor treatment had no effects. Proliferation data are presented as fold over the untreated control group. Both data sets are presented as the mean ± SD. The experiment was repeated at least twice with similar results.
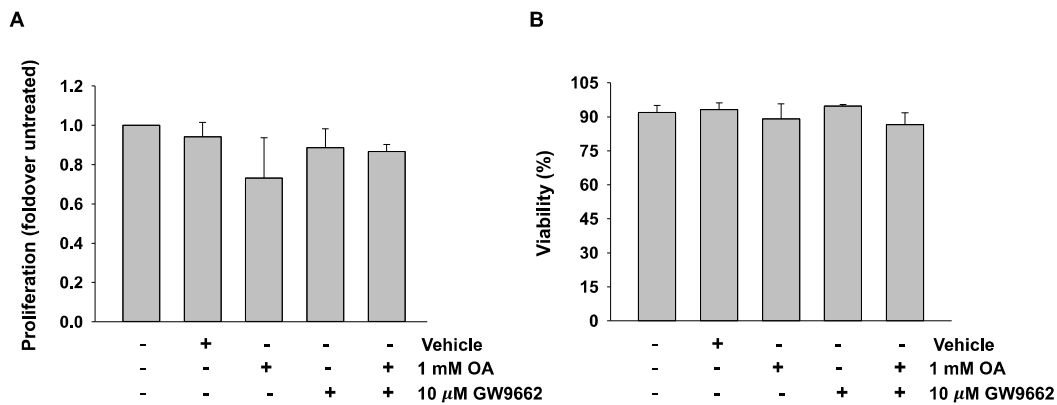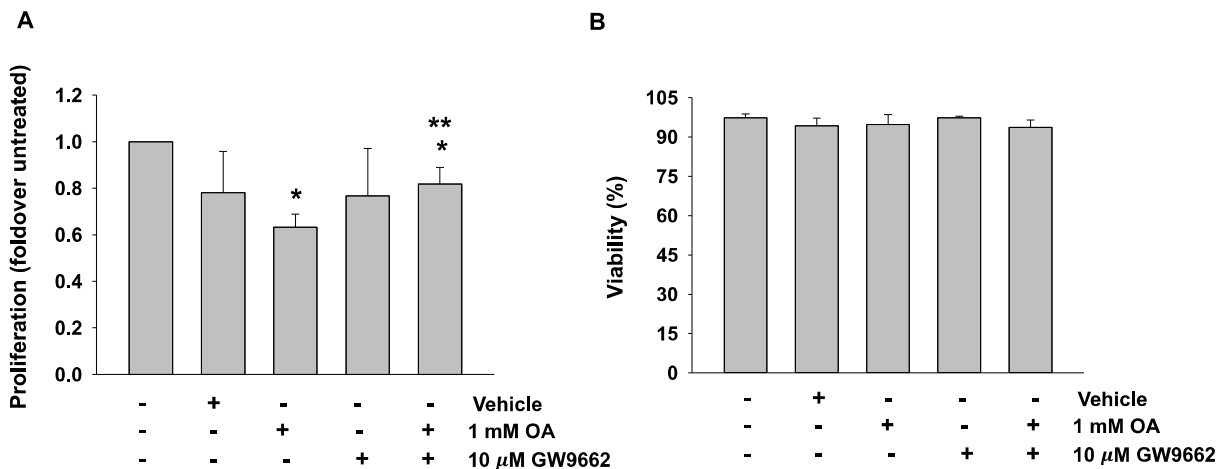

Figure 8. Proliferation of PC-3 cells treated with 1 mM oleic acid (OA) alone or with PPAR*γ* inhibitor was decreased. PC-3 cells were seeded at 20,000 cells/cm^2 in tissue culture dishes. The cells were incubated overnight and were then treated with 1 mM OA +/- 10 μM GW9662 or vehicle (ethanol; 6.9 μl). After 48 h of incubation, cells were collected, and proliferation (**A**) and viability (**B**) were assessed by hemocytometer with trypan blue dye. *P-value <0.001 compared to untreated; **P-value =0.025 compared to 1 mM OA. Proliferation data are presented as fold over the untreated control group. Both data sets are presented as the mean ± SD. The experiment was repeated at least twice with similar results.

48
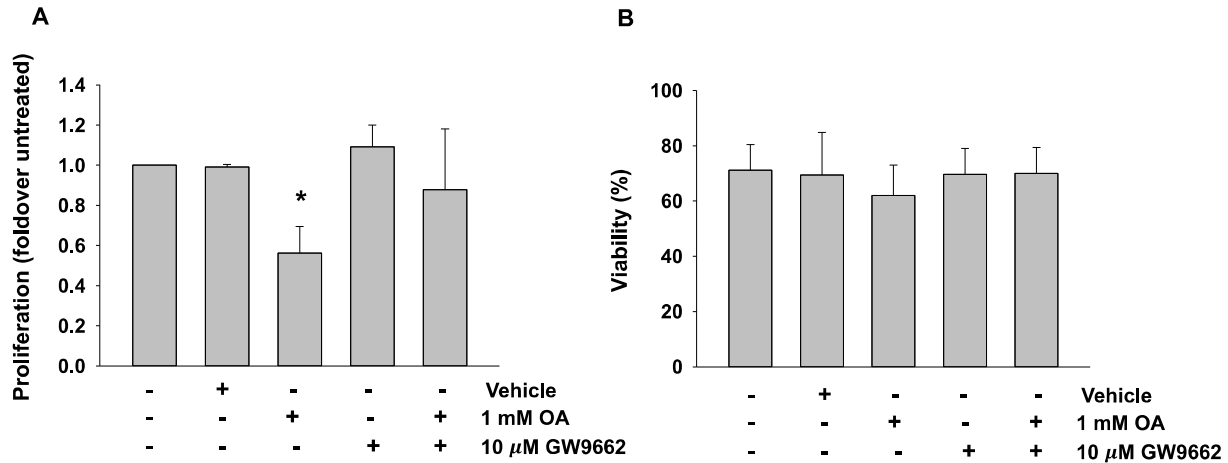
Figure 9. Proliferation of TRAMPC2 cells is decreased with 1 mM oleic acid (OA) alone. TRAMPC2 cells were seeded at 20,000 cells/cm^2 in tissue culture dishes. The cells were incubated overnight and were then treated with 1 mM OA +/- 10 μM GW9662 or vehicle (ethanol; 6.9 μl). After 48 h of incubation, cells were collected, and proliferation (**A**) and viability (**B**) were assessed by hemocytometer with trypan blue dye. *P-value =0.043 compared to untreated group). Proliferation data are presented as fold over the untreated control group. Both data sets are presented as the mean ± SD. The experiment was repeated at least twice with similar results.

Since our data suggested that OA treatment exerted inconsistent growth results in LNCaP and PC-3 cells, we expanded our work to test other FA, linoleic acid (LA) or palmitic acid (PA), in excess for their effects on PCa proliferation and viability. PC-3 cells were treated with LA/BSA (ω-6 PUFAs) or PA/BSA (SFA) conjugate, which were prepared in our lab as liquid versions were not commercially available. We included liquid OA, ready to use from Sigma-Aldrich, or OA/BSA, conjugated in our lab, as a control. LA/BSA treatment had no effects on the proliferation or viability of PC-3 cells (**Figure 10A** and **10B**). However, a significant reduction was found in PC-3 cell proliferation treated with PA/BSA conjugate (P-value <0.001; **Figure 11A**); whereas, no

changes were observed in viability of PC-3 cells treated with PA/BSA conjugate (**Figure 11B**). This observation was inconsistent with OA obtained from Sigma-Aldrich. These results indicate that PA/BSA has inhibitory effects on PC-3 cells. We also examined the effects of OA/BSA, prepared in our lab, on TRAMPC2 cells. We found that OA/BSA conjugate significantly decreased TRAMPC2 cell proliferation compared to untreated group (P-value <0.001; **Figure 12A**); however, the viability and metabolic activity of TRAMPC2 cells were not changed in the presence of OA/BSA conjugate (**Figure 12B** and **12C**).
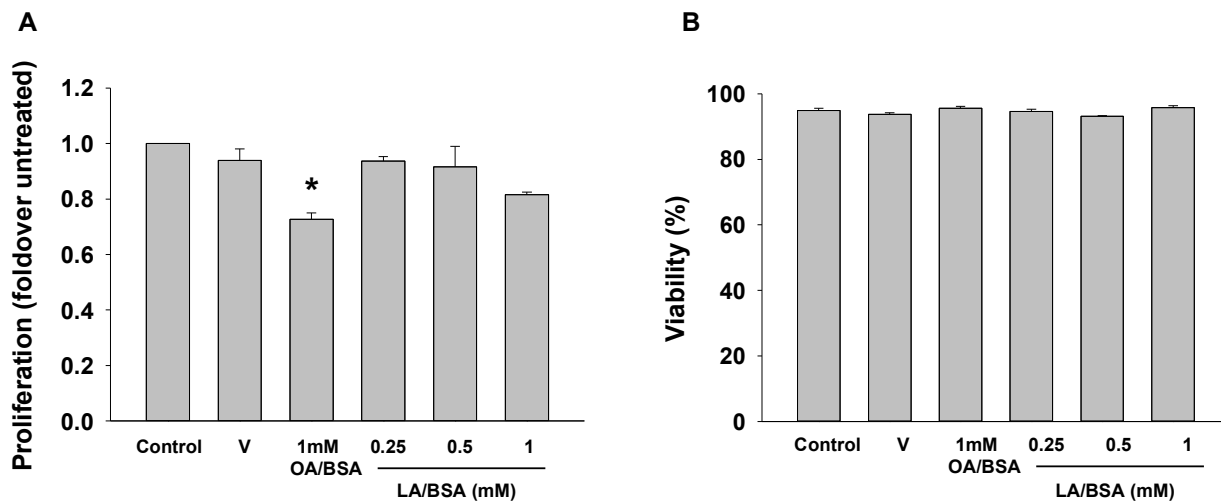
Figure 10. Linoleic acid (LA)-conjugated BSA treatment does not affect the proliferation and viability of PC-3 cells. PC-3 cells were seeded at 20,000 cells/cm^2 in tissue culture dishes. The cells were incubated overnight and were then treated with LA/BSA conjugation in a dose-response curve or vehicle (1mM OA/BSA). After 48 h of incubation, cells were collected. Proliferation (**A**) and viability (**B**) were assessed by hemocytometer with trypan blue dye. No statistically significant changes were observed with LA/BSA treatment. Proliferation data are presented as fold over the untreated control group. Both data sets are presented as the mean ± SD. The experiment was repeated at least twice with similar results. V, vehicle (methanol + BSA); and LA/BSA, linoleic acid/bovine-serum albumin conjugation.
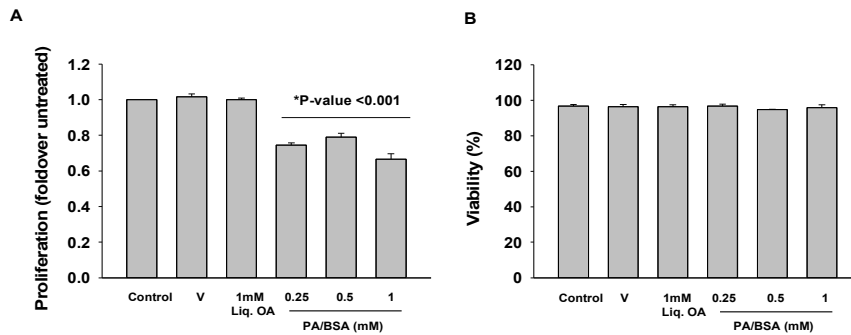
Figure 11. Palmitic acid (PA)-conjugated BSA decrease the proliferation of PC-3 cells. PC-3 cells were seeded at 20,000 cells/cm^2 in tissue culture dishes. The cells were incubated overnight and were then treated with PA/BSA conjugation in a dose-response curve or vehicle (1 mM liq. OA). After 24 h of incubation, cells were collected. Proliferation (**A**) and viability (**B**) were assessed by hemocytometer with trypan blue dye. *P-value <0.001 compared to untreated group. Proliferation data are presented as fold over the untreated control group. Both data sets are presented as the mean ± SD. The experiment was repeated at least twice with similar results. V, vehicle (methanol + BSA); Liq. OA, liquid oleic acid; and PA/BSA, palmitic acid/bovine-serum albumin conjugation.
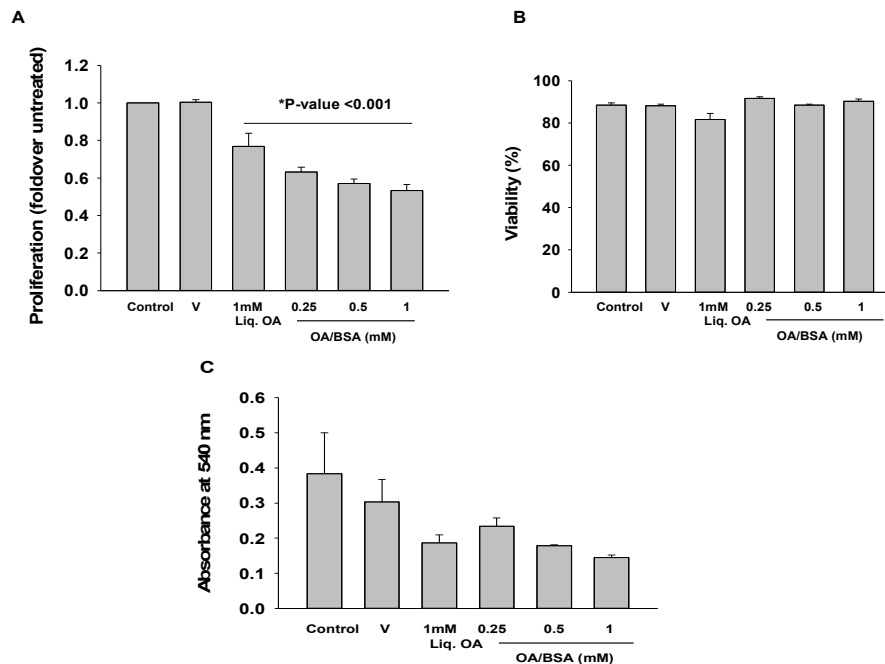
Figure 12. Oleic acid (OA)-conjugated BSA decreases the proliferation of TRAMPC2 cells. TRAMPC2 cells were seeded at 20,000 cells/cm^2 in tissue culture dishes and a 96-well plate. The cells were incubated overnight and were then treated with OA/BSA conjugation in a dose-response curve or vehicle (1mM liq. OA). After 48 h of incubation, cells in dishes were collected, and an MTT assay was performed on the 96-well plate. Proliferation (**A**) and viability (**B**) were assessed by hemocytometer trypan blue dye. The cell metabolic activity (**C**) was assessed by MTT assay. *P-value <0.001 compared to untreated group. Data are presented as fold over the untreated control group. Both data sets are presented as the mean ± SD. The experiment was repeated at least twice with similar results. V, vehicle (methanol + BSA); Liq. OA, liquid oleic acid; and OA/BSA, oleic acid/bovine-serum albumin conjugation

51

**The effects of OA alone or with GPR40 (GW1100), Ca^{2+} (BAPTA AM) or PPARγ**

**(GW9662) on PEDF expression in PCa cells**

Our lab has previously investigated both extracellular and intracellular PEDF

levels in PCa cell lines using an _in vitro_ obesity model simulated by excess OA

treatment. The previous data indicated that secreted PEDF levels were decreased with

1 mM OA treatment in RWPE-1, LNCaP, DU145 and PC-3 cells while cellular PEDF

levels were only suppressed in the two androgen-independent DU145 and PC-3 cells.

However, the molecular mechanisms through which excess OA down-regulates PEDF

in an _in vitro_ obese microenvironment has not been revealed. In the present study, we

investigated if GPR40 was involved in OA-mediated PEDF suppression in PCa cells. In

addition, we asked if OA-suppressed PEDF expression was dependent on two potential

intracellular signaling pathways, Ca^{2+} and PPARγ. To test these mechanisms, LNCaP,

DU145, and PC-3 cells were treated with OA with or without GPR40, Ca^{2+} or PPARγ

inhibitors. Then, extracellular and intracellular PEDF levels were determined by ELISA.

Consistent with previous studies in the Doll Lab, ELISA showed that secreted

PEDF levels were significantly decreased in LNCaP cells treated with OA alone or in the

presence of GPR40 inhibitor while no differences in cellular PEDF levels were found

(**Figure 13A** and **13B**). Similarly, a significant reduction in secreted PEDF levels was

identified in PC-3 cells treated with OA with or without the GPR40 inhibitor (**Figure

14A**). However, no effects on cellular PEDF were detected in PC-3 and DU145 cells

treated with OA alone or with the GPR40 inhibitor (**Figure 14B** and **15**).
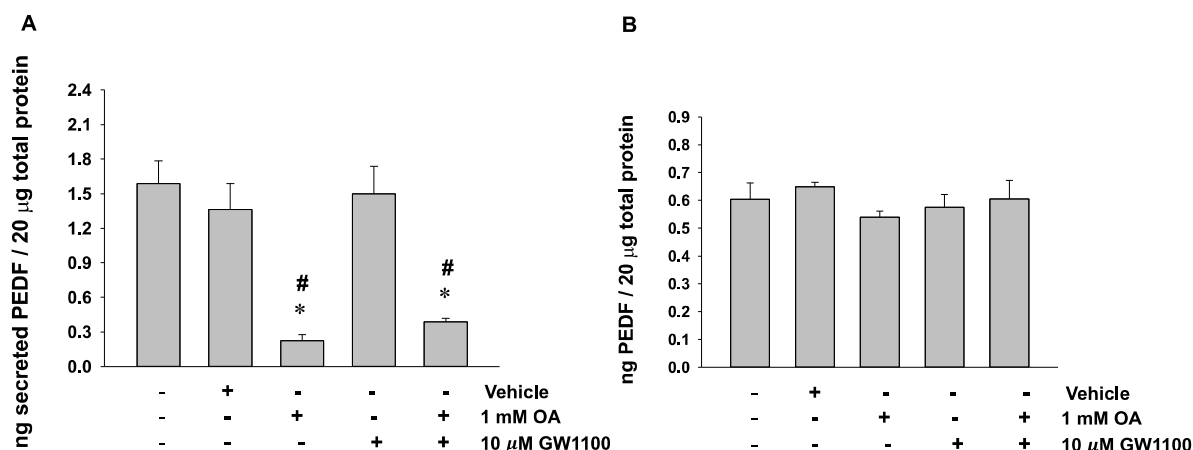
Figure 13. Secreted PEDF levels are decreased in LNCaP cells treated with 1 mM oleic acid (OA) alone or with GPR40 inhibitor. LNCaP cells were seeded at 40,000 cells/cm^2 in tissue culture dishes. The cells were incubated overnight and were then treated with 1 mM OA +/- 10 μM GW110 or vehicle (DMSO; 5.2 μl). After 48 h of incubation, cells were collected, and secreted PEDF levels (**A**) and cellular PEDF levels (**B**) were quantified by ELISA. *P-value <0.029 compared to untreated group. While OA plus GW1100 inhibitor slightly increased secreted PEDF, this increase is not statistically significance (P-value =0.057). #Some data values were below limit of detection and assigned a value of 0.31. Data are presented as fold over the untreated control group. Both data sets are presented as the mean ± SD. The experiment was repeated at least twice with similar results.

Figure 14. Secreted PEDF levels are decreased in PC-3 cells treated with 1 mM oleic acid (OA) alone or with GPR40 inhibitor. PC-3 cells were seeded at 20,000 cells/cm^2 in tissue culture dishes. The cells were incubated overnight and were then treated with 1 mM OA +/- 10 μM GW110 or vehicle (DMSO; 5.2 μl). After 48 h of incubation, cells were collected, and secreted PEDF levels (**A**) and cellular PEDF levels (**B**) were quantified by ELISA. *P-value <0.001 compared to untreated group. #Some data values were below limit of detection and assigned a value of 0.004. Data are presented as fold over the untreated control group. Both data sets are presented as the mean ± SD. The experiment was repeated at least twice with similar results.

Figure 15. Cellular PEDF levels are not changed in DU145 cells treated with 1 mM oleic acid (OA) +/- GPR40 inhibitor. DU145 cells were seeded at 20,000 cells/cm^2 in tissue culture dishes. The cells were incubated overnight and were then treated with 1 mM OA +/- 10 μM GW110 or vehicle (DMSO; 5.2 μl). After 48 h of incubation, cells were collected, and intracellular PEDF levels were measured by ELISA. No significant changes were observed among groups compared to untreated group. Data are presented as fold over the untreated control group. Both data sets are presented as the mean ± SD. The experiment was repeated at least twice with similar results.

No significant changes were observed in the levels of cellular PEDF protein in PC-3 cells cultured with OA alone or with the Ca^{2+} chelator (**Figure 16**). As shown in **Figure 17A**, OA treatment alone decreased secreted PEDF and PPARγ inhibitor did not rescue this effect. Neither OA treatment alone nor PPARγ inhibitor altered intracellular PEDF levels in DU145 cells (**Figure 17B**). Collectively, our *in vitro* data indicated that OA treatment reduced secreted PEDF levels in LNCaP, DU145, and PC-3 cells. This observation is similar to our lab preliminary data. However, OA treatment with the blocking agents of GPR40 or PPARγ did not rescue secreted PEDF in LNCaP, DU145, and PC-3 cells. OA treatment alone did not affect cellular PEDF levels in DU145 and PC-3 cells. These results contrasted with our lab preliminary data showing that cellular PEDF levels decreased in OA-treated DU145 and PC-3 cells. Since OA did not

suppress cellular PEDF levels, we would not expect these inhibitor molecules to have

an effect. While we did not find a decrease in PEDF levels in our current study

compared to our lab's preliminary findings, several possible reasons for these

divergencies are discussed in-depth in the discussion section.
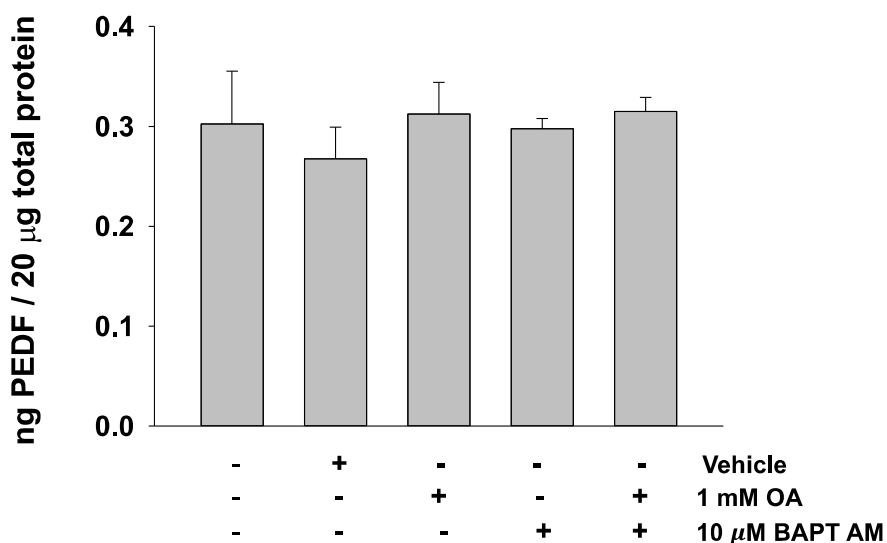
Figure 16. Cellular PEDF levels are not affected in PC-3 cells treated with 1 mM oleic acid (OA) alone or with Ca^{2+} chelator. PC-3 cells were seeded at 20,000 cells/cm^2 in tissue culture dishes. The cells were incubated overnight and were then treated with 1 mM OA +/- 10 µM BAPT AM or vehicle (DMSO; 1.9 µl). After 48 h of incubation, cells were collected, and intracellular PEDF levels were measured by ELISA. No significant changes were observed among groups compared to untreated group. Data are presented as fold over the untreated control group. Both data sets are presented as the mean ± SD. The experiment was repeated at least twice with similar results.
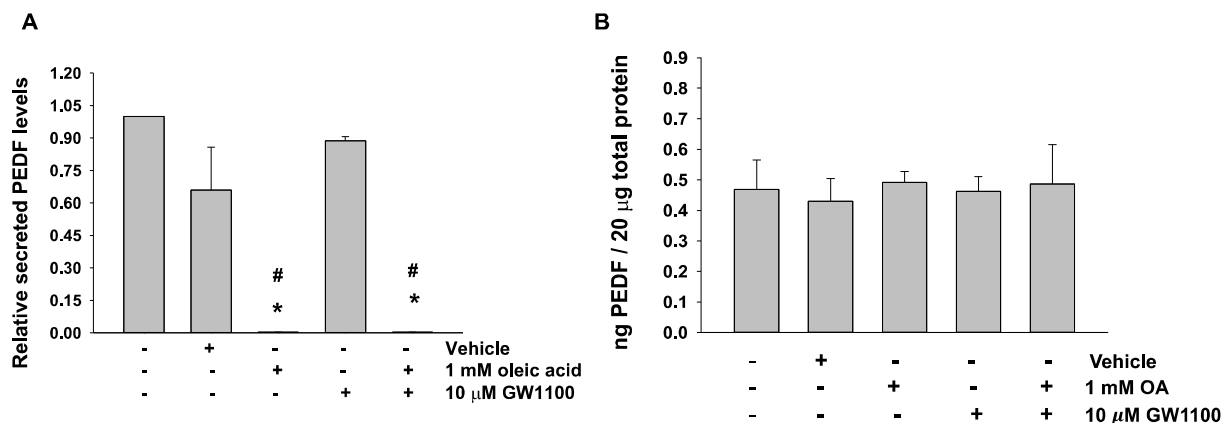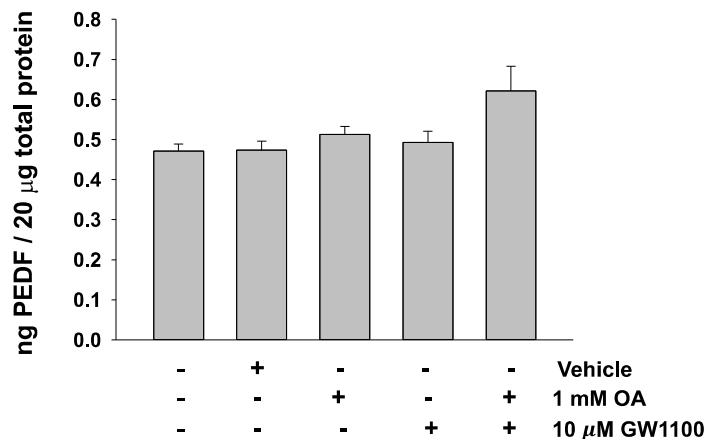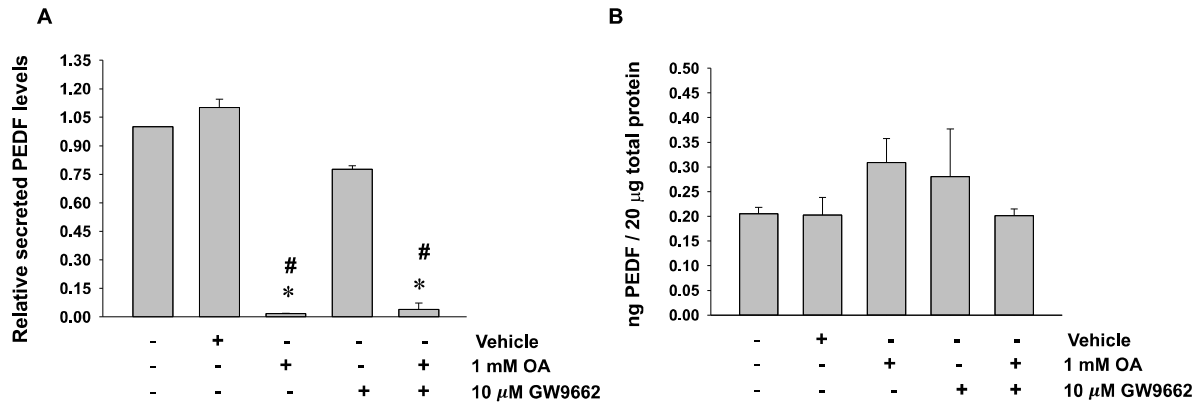
Figure 17. Secreted PEDF levels are decreased in DU145 cells treated with 1 mM oleic acid (OA) alone or with PPARγ inhibitor. DU145 cells were seeded at 20,000 cells/cm^2 in tissue culture dishes. The cells were incubated overnight and were then treated with 1 mM OA +/- 10 μM GW9662 or vehicle (ethanol; 6.9 μl). After 48 h of incubation, cells were collected, and secreted PEDF levels (**A**) and intracellular PEDF levels (**B**) were quantified by ELISA. *P-value <0.001 compared to untreated group. #Some data values were below limit of detection and assigned a value of 0.028. Data are presented as fold over the untreated control group. Both data sets are presented as the mean ± SD. The experiment was repeated at least twice with similar results.

IN VIVO AND *EX VIVO* MOUSE PROSTATE CANCER STUDIES

The weight and volume of TRAMPC2 xenograft tumor tissues increase in ob/ob mice

Obesity and HFD have been associated with increased risk of progression and death from PCa [11], [12]. In addition, PEDF expression levels are decreased in PCa patient tissues [49]. However, in the published study, PEDF levels were not stratified by patient weight or BMI. PEDF is a multifunctional protein that acts as a potent tumor suppressor and a regulator of lipolytic activity [42], [46]. In our lab's previous studies, the 1 mM OA treatment reduced secreted PEDF in all PCa cell lines, LNCaP, PC-3, and DU145, and in normal prostate epithelial cells, RWPE-1, (Doll *et al*. unpublished data). In addition, 1 mM OA treatment also suppressed intracellular PEDF levels in DU145 and PC-3 while no effect on intracellular levels of PEDF was observed in RWPE-1 and LNCaP (Doll *et al*. unpublished observation). Consistent with the OA treatment being used as an obesity model, treated cells demonstrate a dose-dependent increase in lipid accumulation (Doll *et al.* unpublished data). Conversely, rPEDF treatment (10 and 50 nM) reduced intracellular TG levels in basal and in OA-treated conditions, with a concomitant increase in lipolysis (TG breakdown) in PC-3 cells (Doll *et al.* unpublished data). Here, to investigate the impact of obesity on PEDF and pro-tumorigenic protein expression in PCa, we used *in vivo* and *ex vivo* studies using a genetically obese model (ob/ob mice) and a HFD model.

In the genetically obese (ob/ob) model, TRAMPC2 (5.0×10^6) cells were subcutaneously inoculated into the right flank of male WT and obese (ob/ob) mice. When a subset of tumors reached the maximum growth limit, all mice were euthanized. Then, tumor tissues and blood samples were collected. Ob/ob mice and WT mice were fed a standard laboratory diet, and as expected, ob/ob mice gained more weight compared to WT mice during the study. The average end body weight was significantly higher in ob/ob mice (n= 20; 68.71 g ± 0.85) than WT mice (n= 10; 33.80 g ± 0.88; **Figure 18**; P-value <0.001). As there was variability in tumor take rate and time to tumor initiation, a subset of tumor xenograft harvested from ob/ob mice and WT mice was used in the analysis (**Figure 19A**). We observed a significant increase in TRAMPC2 tumor weight in tumors growing in ob/ob mice (n= 20) compared to tumors growing in WT mice (n= 10; P-value =0.018; **Figure 19B**). In addition, the TRAMPC2 tumor volume was significantly higher in ob/ob mice, 4088.84 mm^3, than WT mice, 1335.77 mm^3 (P-value =0.018; **Figure 19C**). These results demonstrate that obesity promotes the growth of TRAMPC2 xenograft in ob/ob mice.
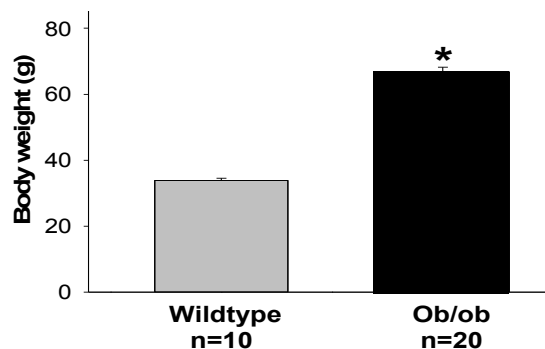
Figure 18. Body weights of wildtype (WT) and obese (ob/ob) mice on a standard laboratory diet. Obese (ob/ob) mice (n= 20) and wildtype (WT) mice (n= 10) were fed a standard chow diet for 4 months. TRAMPC2 cells were subcutaneously injected into mice, and all tumors were collected when a subset reached the maximum growth. Mouse weight was measured using a digital scale. As expected, ob/ob mice showed a significant increase in body weight as compared to WT mice (*P-value <0.001 compared to WT mice). Data are presented as the mean ± SEM at 6 months of age.
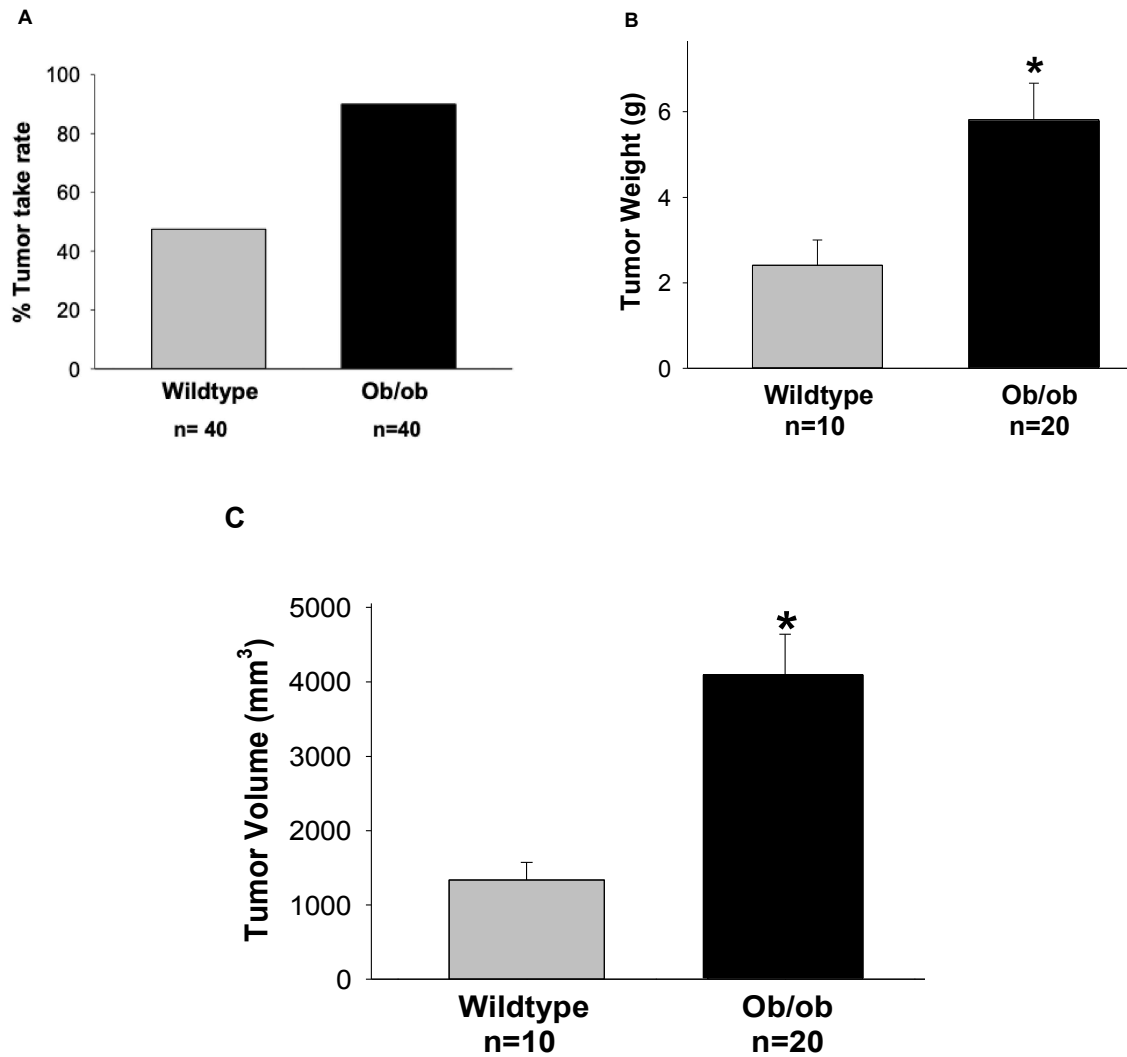
Figure 19. The weight of TRAMPC2 xenograft tumor growing in wildtype (WT) and obese (ob/ob) mice. Ob/ob mice (n= 40) and WT (n= 40) were injected with TRAMPC2 PCa cells in the right flank, and all tumors were collected when a subset reached the maximum growth. The collected tumors were weighed using a digital scale. (**A**) Calculated tumor take rate. (**B**) TRAMPC2 tumor weight from ob/ob mice compared to tumor weight from WT. (**C**) Tumor volumes were measured using digital calipers for length and width measures, then calculated with the following formula: volume = length x width^2 x 0.5. *P-value <0.018 compared to TRAMPC2 tumor grown in WT mice. Data are presented as the mean value ± SEM.

HFD-fed Pbsn-Cre$^+$PTEN$^{fl/fl}$ mice gain more weight than CD-fed Pbsn-Cre$^+$PTEN$^{fl/fl}$ mice

In addition to the genetically obese model, we also used the Pbsn-Cre$^+$PTEN$^{fl/fl}$ PCa mouse model fed either a HFD or a CD for 16 weeks, beginning at 8 weeks of age. The mouse body weight and food consumption were recorded weekly. We observed that Pbsn-Cre$^+$PTEN$^{fl/fl}$ mice on a HFD gained significantly more weight over the 16 week diet as compared to a CD-fed mice (P-value <0.001; **Figure 20A**). As expected, at the end of the study, the average mouse body weight was significantly increased in HFD-fed Pbsn-Cre$^+$PTEN$^{fl/fl}$ mice (52 ±1.8) versus CD-fed mice (37 ±1.8 g; P-value <0.001; **Figure 20B**). Based on a published literature observation [95], we expected that the epididymal fat pad weight would be increased in mice on a HFD; however, unexpectedly, we observed no difference in epididymal fat pad weight from Pbsn-Cre$^+$PTEN$^{fl/fl}$ mice fed a HFD as compared to a CD (**Figure 20C**). Next, we measured whether a HFD increased the weight of the mouse prostate. The mouse prostate lobes (ventral, dorsolateral, and interior) were harvested and weighed. Interestingly, the prostate lobes from HFD-fed Pbsn-Cre$^+$PTEN$^{fl/fl}$ mice were significantly heavier as compared to the prostate lobes harvested from CD-fed mice (0.107 vs. 0.074 g; P-value <0.042; **Figure 21**). Increased prostate weight is associated with an increase tumor burden. Collectively, our data indicated that HFD increased the body weight and stimulated tumor growth in Pbsn-Cre$^+$PTEN$^{fl/fl}$ mice.
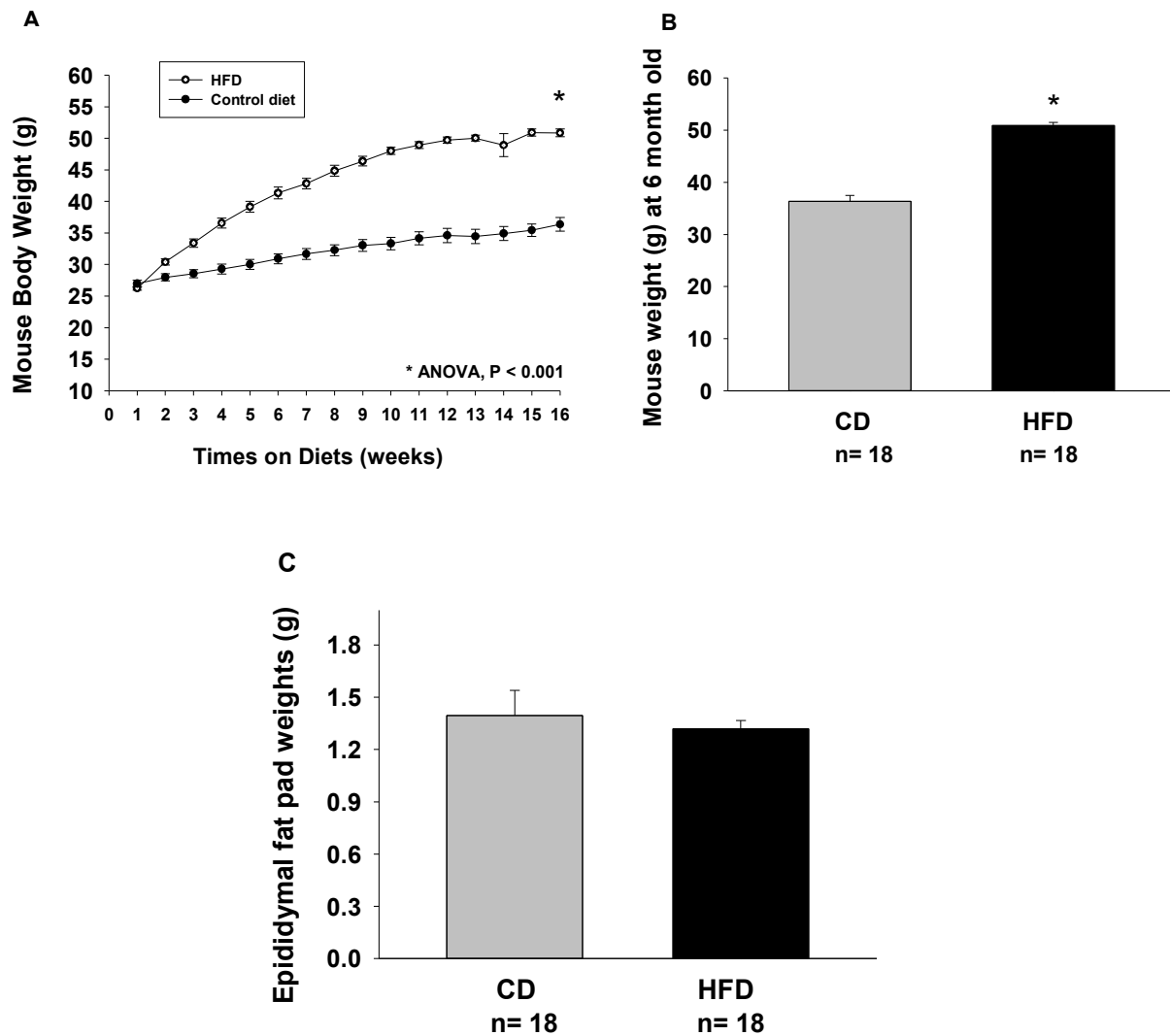
Figure 20. The body weight and epididymal fat pad weight of Pbsn-Cre+PTEN^{fl/fl} mice on control diet (CD) and a high-fat diet (HFD). Pbsn-Cre+PTEN^{fl/fl} in C57BL/6 background mice, n=18 per group, were fed either a CD (16.8% kcal from fat) or a HFD (60.3% kcal from fat) for 16 weeks, starting at 8 weeks of age. Mouse weight was measured weekly using a digital scale. (**A**) Mouse body weight graphed over time. (**B**) Average weight at the end point of the experiment, 6 months of age. (**C**) Epididymal fat pad weights (P-value =0.361). *P-value <0.001 compared to PCa mice fed a CD. Data are presented as the mean value ± SEM.
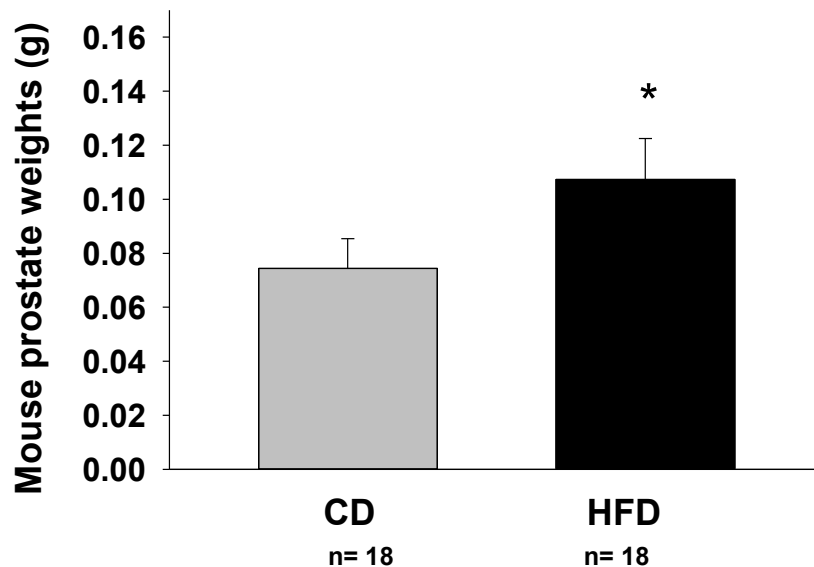
Figure 21. Prostate weight is increased in Pbsn-Cre⁺PTEN^{fl/fl} mice on a high-fat diet HFD vs a control diet (CD). Pbsn-Cre⁺PTEN^{fl/fl} mice were fed either a CD (n=18) or a HFD (n=18) for 16 weeks, starting at 8 weeks of age. The prostate lobes of mice were harvested when the mice are at 6 months of age. *P-value <0.042 compared to Pbsn-Cre⁺PTEN^{fl/fl} mice fed a CD. Data are presented as the mean value ± SEM.

Circulating PEDF levels are not increased in ob/ob mice and they are decreased in HFD-PCa mice

Obese individuals have increased circulating PEDF levels [36], [38]. Our obese mouse models gained significantly more weight than WT control mice (**Figures 18** and **20**). Therefore, we wanted to analyze PEDF expression because to date, circulating PEDF levels have not been quantified in an obese PCa model. Herein, we measured the serum PEDF levels in TRAMPC2 xenograft grown in ob/ob and WT mice. We observed no significant differences in serum levels of PEDF in ob/ob mice versus WT mice (**Figure 22**). This observation could indicate that some secretion of TRAMPC2

tumors grown in ob/ob mice downregulates circulating PEDF since the regulation of

PEDF expression is not well understood. We further asked whether an obese

microenvironment in a HFD would show a similar result in circulating PEDF.
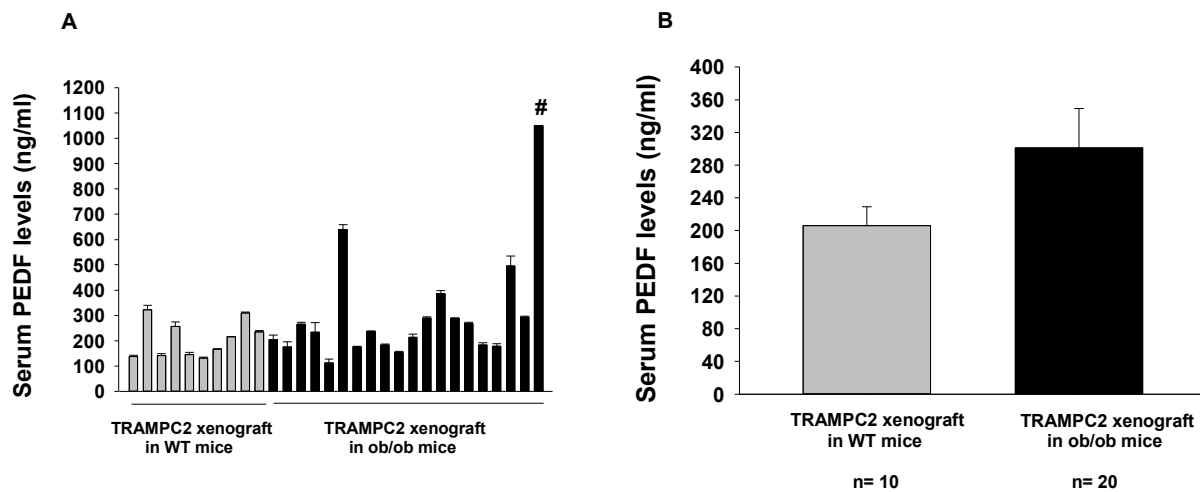
Figure 22. Circulating PEDF concentrations are not increased in ob/ob mice versus wild-type (WT).
Mouse blood samples were collected using a retro-orbital bleeding technique from WT C57Bl/6 mice (n= 10) or ob/ob C57Bl/6 mice (n= 20) on a standard laboratory diet. Blood samples were incubated at RT at least 30 min to allow clot to form. Then, the cellular components were removed by centrifugation, and serum was collected. ELISA was performed to quantify PEDF protein. (**A**) PEDF levels in each serum sample. (**B**) Average concentrations of PEDF levels. No significant differences in PEDF levels were observed (P-value =0.224). #Data value for this sample was above the detection limit of the assay and was assigned a value of 1050 ng/ml. Data are presented as the mean ± SEM.

We examined the circulating levels of PEDF in the Pbsn-Cre[+]PTEN^{fl/fl} mice were

fed either a HFD and or a CD for 16 weeks, beginning at 8 weeks of age. Mouse serum

was collected, and serum PEDF levels were measured. Data from ELISA revealed that

serum PEDF levels were significantly decreased in HFD-fed Pbsn-Cre[+]PTEN^{fl/fl} mice

(74.7 ng/ml ± 13.6) compared to CD-fed mice (133.4 ng/ml ± 12.4) (P-value <0.001;

Figure 23). To the best of our knowledge, this is the first study reporting a decrease in

circulating PEDF levels in HFD-fed PCa mice. In addition, this is the first report to

63

indicate no significant increase in circulating PEDF levels in ob/ob mice bearing PCa

xenografts as compared to WT mice.
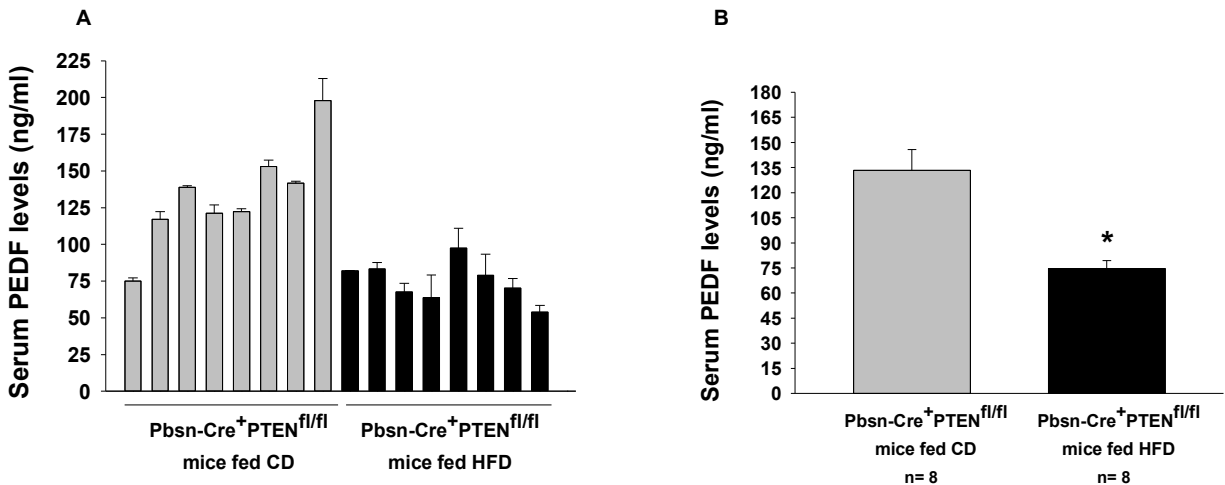
Figure 23. HFD decreases circulating PEDF levels in PCa mice. Pbsn-Cre[+] PTEN^{fl/fl} mice were fed either a HFD (n= 8) or a CD (n= 8) for 16 weeks, beginning at 8 weeks of age. Mouse blood samples were collected using a retro-orbital bleeding technique. Blood samples were incubated at RT at least 30 min to allow clot to form. Then, the cellular components were removed by centrifugation, and serum was collected. An ELISA was performed to quantify PEDF protein. (**A**) PEDF levels in each serum sample collected from mice. (**B**) The mean PEDF levels were a significantly decreased in HFD-fed Pbsn-Cre[+] PTEN^{fl/fl} mice as compared to CD-fed Pbsn-Cre[+] PTEN^{fl/fl} mice. *(P-value <0.001). Data are presented as the mean ± SEM.

Serum leptin levels increase in HFD-fed Pbsn-Cre+PTEN^{fl/fl} mice

Increase in adipose tissue mass is known to increase secretion levels of

adipokines, such as leptin, into the blood [92]. Leptin is a hormone that regulates

appetite, energy expenditure, and body mass composition [92]. Doll *et al.* found that

obese patients with PCa displayed an increased in leptin levels, as expected; however,

there were no differences in PEDF levels in obese PCa patients as compared to lean

patients (Doll *et al.* unpublished study). Based on our mouse observation and these

64

human data, we wanted to confirm that our HFD-fed Pbsn-Cre$^+$PTEN$^{fl/fl}$ mice had more

leptin. Therefore, we examined the serum levels of leptin since elevated leptin levels are

an indicator of adiposity. As shown in **Figure 24**, Pbsn-Cre$^+$PTEN$^{fl/fl}$ mice fed a HFD

had higher serum leptin levels (174.5 ng/ml ± 15.03) than mice fed a CD (30.56 ng/ml ±

7.2). This finding is consistent with our lab data showing that leptin levels are increased

in obese patients with PCa (Doll *et al.* unpublished study). This data is also consistent

with an increased adipose tissue mass in Pbsn-Cre$^+$PTEN$^{fl/fl}$ fed a HFD.
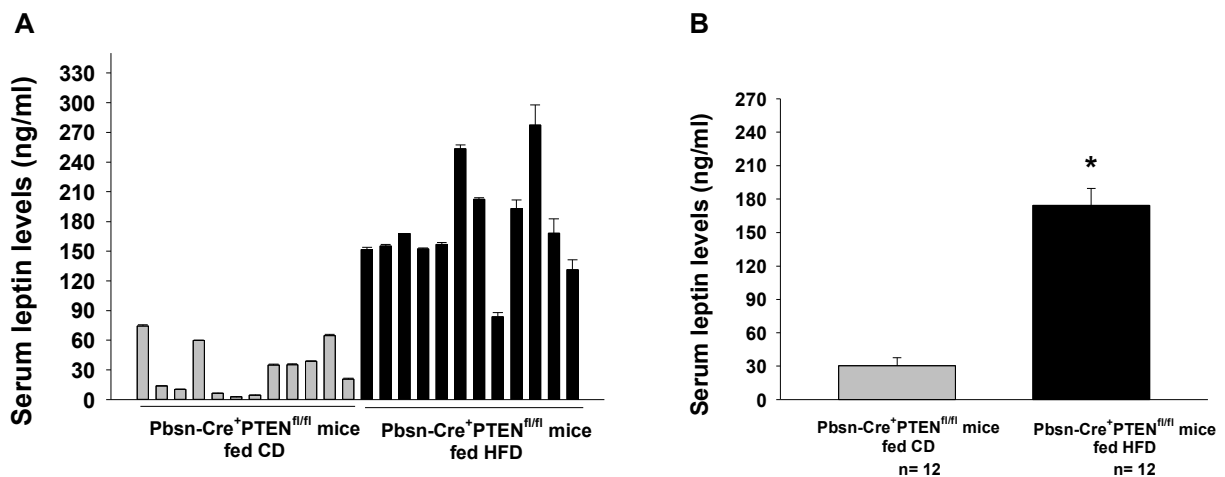
Figure 24. HFD increases serum leptin levels in PCa mice. Pbsn-Cre$^+$ PTEN$^{fl/fl}$ mice were fed either a HFD (n= 12) or a CD (n= 12) for 16 weeks, beginning at 8 weeks of age. Mouse blood samples were collected using a retro-orbital bleeding technique. Blood samples were incubated at RT at least 30 min to allow clot to form. Then, the cellular components were removed by centrifugation, and serum was collected. A leptin ELISA was performed to quantify leptin levels. (**A**) Leptin levels in each serum sample collected from mice. (**B**) The mean leptin levels between groups. *P-value <0.001 compared to Pbsn-Cre$^+$ PTEN$^{fl/fl}$ mice fed CD. Data are presented as the mean ± SEM.

Tissue PEDF levels decrease in TRAMPC2 tumor growth in ob/ob mice

The effects of dietary HFD-induced obesity in PCa models on circulating PEDF were largely unknown. Our preliminary studies suggest that in an *in vitro* obesity model, simulated by using an OA lipid overload model, further suppresses secreted PEDF expression in RWEP-1, LNCaP, PC-3, and DU145, (Doll *et al.* unpublished study). We further explored this observation by examining the tissue PEDF levels in TRAMPC2 tumors grown in ob/ob mice. We found that tumor PEDF levels were significantly decreased in TRAMPC2 tumors grown in ob/ob mice (9793 ± 1235.7) compared to TRAMPC2 tumors grown in WT mice (13308 ± 1754; P-value =0.015; **Figure 25**). These data suggested that PEDF suppression may be one mechanism of obesity-induced PCa progression.
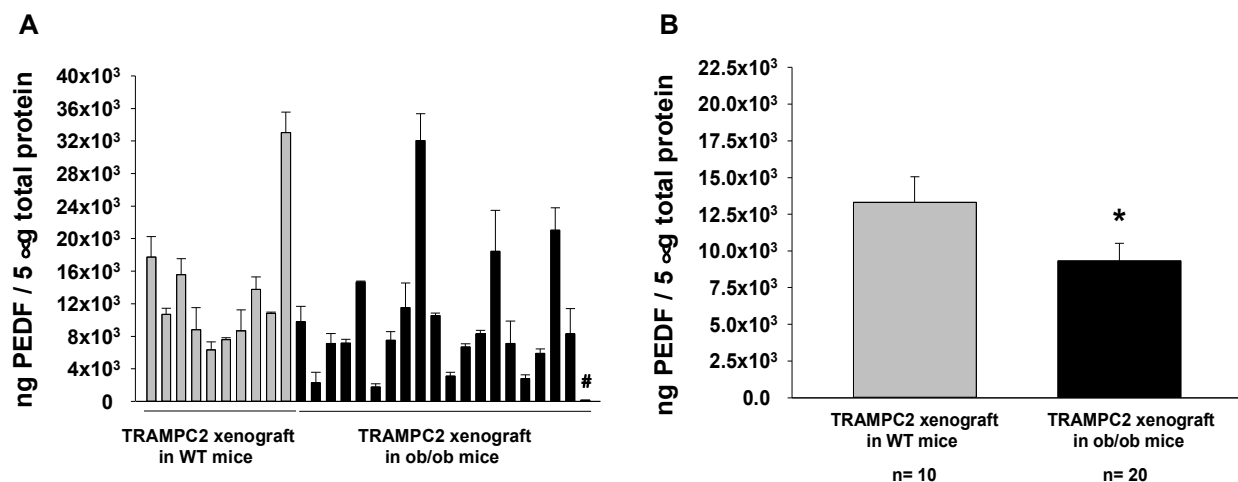
Figure 25. Tissue PEDF levels are decreased in TRAMPC2 tumor tissues grown in ob/ob mice. TRAMPC2 tumors were harvested from WT (n= 10) and ob/ob (n= 20) mice at 4 months post-injection. Tumor tissues were homogenized, and protein levels were quantified with a Coomassie protein assay. PEDF levels were measured by ELISA. (**A**) PEDF levels in each TRAMPC2 tumor tissues harvested from mice. (**B**) The average PEDF levels between groups. *P-value =0.015 compared to TRAMPC2 tumor tissue grown in WT mice. #Data value for this sample was below the detection limit of the assay and was assigned a value of 156.8 ng PEDF / 5 µg. Data are presented as the mean ± SEM.

Excess lipids do not increase the levels of PPARγ in TRAMPC2 tumor growth in ob/ob mice

Although several mechanisms have been most intensively studied to understand the association between obesity and PCa progression, the link between obesity and PCa is still unclear. The insulin/insulin like growth factor-1 axis, sex hormones, adipokine signaling, and pro-inflammatory cytokines have been well examined in PCa [6], [96]. Our study was aimed to further examine several signaling pathways related to PCa progression. PPARγ protein was detected in the nucleus and cytoplasm of PCa cells and prostatic intraepithelial neoplasia, but no detection was observed in normal prostate tissue samples [65], [66]. However, the levels of cytoplasmic PPARγ have not been tested in obese patients with PCa. Here, we examined whether excess lipids in an obese microenvironment increased the cytoplasmic levels of PPARγ in PCa tumor tissue. Therefore, cytoplasmic PPARγ levels were evaluated in TRAMPC2 xenograft tumors grown in obese ob/ob mice (n= 8) versus WT mice (n= 8). Western blot revealed that cytoplasmic PPARγ was expressed in both TRAMPC2 tumor tissues grown in ob/ob mice and WT mice, but no significant differences were observed (P-value =0.713; **Figure 26**).
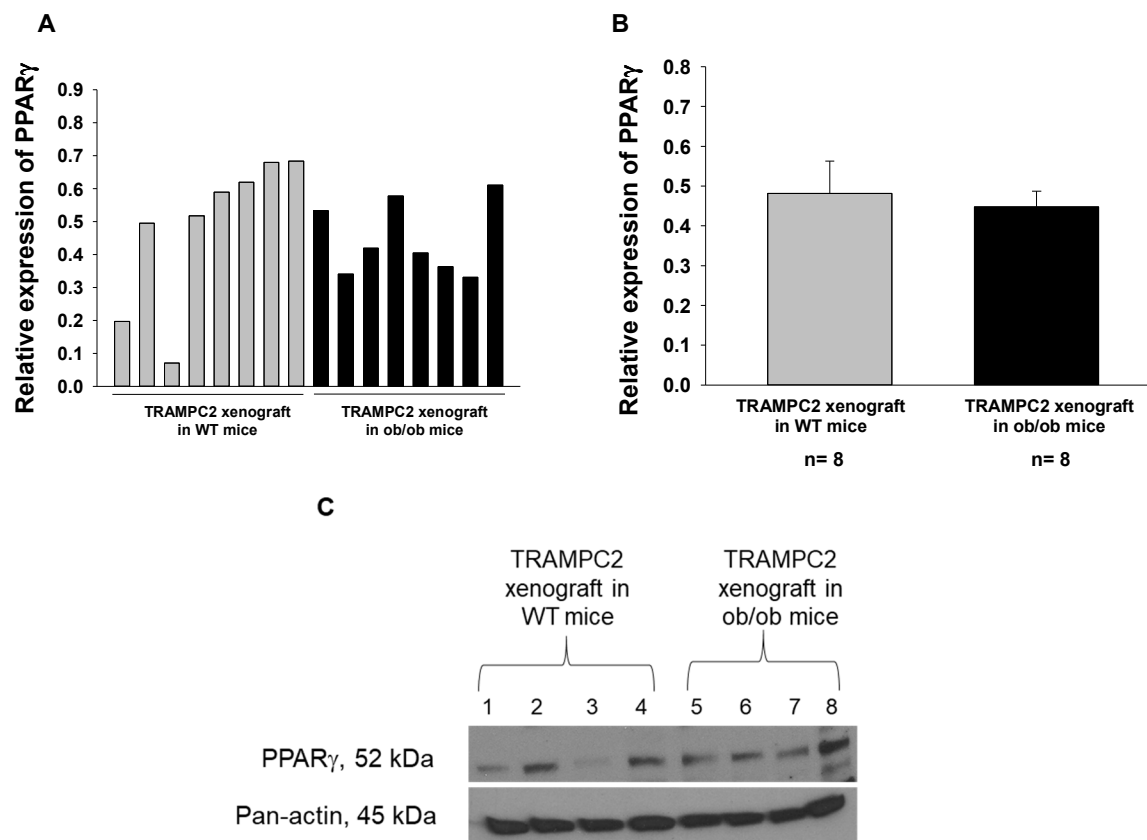
Figure 26. An obese microenvironment did not alter the levels of PPARγ. Tumor tissues were homogenized, and protein levels were quantified with a Coomassie protein assay. Samples (30 µg) were resolved on SDS-PAGE gels. The separated proteins were transferred to PVDF membrane by electroblotting. Membranes were probed with anti- PPARγ antibody, stripped and reprobed with anti-pan-actin antibody, which served as a control for protein loading. (**A**) PPARγ and pan-actin levels were analyzed for each sample by densitometry. (**B**) The relative means of PPARγ to pan-actin expression in all samples were combined and analyzed by densitometry. (**C**) A representative Western blot analysis of PPARγ and pan-actin. Data are presented as the mean value ± SEM (P-value =0.713).

Excess lipids do not alter the activity of Wnt signaling in TRAMPC2 tumor growth in ob/ob mice

We next examined the activity involvement of Wnt signaling in regulation of PCa progression in an obese microenvironment. Thus, we investigated the activity of p-β-catenin Thr41/Ser45 in TRAMPC2 tumor xenograft tissues grown in ob/ob mice (n= 15) versus WT mice (n= 10). In addition, we examined the possible effects of obesity on co-

receptor, LRP6, of Wnt signaling. Western blot analysis was performed on both

phosphorylation and non-phosphorylation status of both β-catenin and LRP6 in

TRAMPC2 tumor tissues in ob/ob mice and WT mice. Densitometry analysis of Western

blot showed that phosphorylated β-catenin Thr41/Ser45 were not changed in TRAMPC2

tumor tissues grown in ob/ob mice (n= 15) versus WT mice (n= 10; P-value =0.265;

Figure 27). Likewise, no significant changes were observed in the levels of pLRP6

ser1490 in TRAMPC2 tumor tissues from ob/ob mice (n= 8) compared to WT mice (n=

8; P-value =0.174; **Figure 28**).
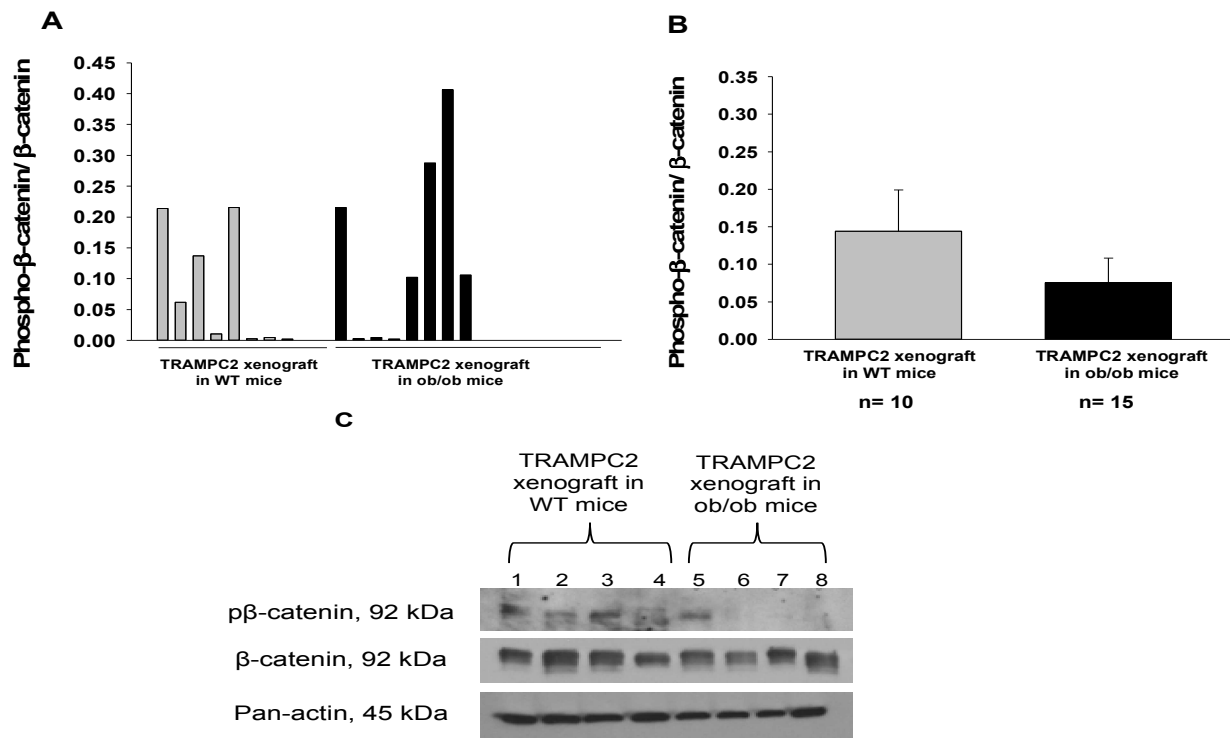
Figure 27. An obese microenvironment did not alter the levels of phosphorylated of β-catenin (pβ-catenin). Tumor tissues were homogenized, and protein levels were quantified with a Coomassie protein assay. Samples (30 µg) were resolved on SDS-PAGE gels. The separated proteins were transferred to PVDF membrane by electroblotting. Membranes were probed with anti-pβ-catenin antibody, stripped and reprobed with anti-β-catenin and pan-actin antibody. (**A**) p-β-catenin, β-catenin, and pan-actin levels were analyzed for each sample by densitometry. (**B**) The relative means of p-β-catenin to β-catenin expression in all samples were combined and analyzed by densitometry. (**C**) A representative Western blot analysis of p-β-catenin, β-catenin, and pan-actin. Data are presented as the mean value ± SEM (P-value =0.265).

Figure 28. An obese microenvironment did not alter the levels of phosphorylated of LRP6 (p-LRP6). Tumor tissues were homogenized, and protein levels were quantified with a Coomassie protein assay. Samples (30 µg) were resolved on SDS-PAGE gels. The separated proteins were transferred to PVDF membrane by electroblotting. Membranes were probed with anti-pLRP6 antibody, stripped and reprobed with anti-LRP6 and pan-actin antibody. (**A**) PLRP6, LRP6, and pan-actin levels were analyzed for each sample by densitometry. (**B**) The relative means of pLRP6 to LRP6 expression in all samples were combined and analyzed by densitometry. (**C**) A representative Western blot analysis of p-LRP6, LRP6, and pan-actin. Data are presented as the mean value ± SEM (P-value =0.174).

The expression levels of cyclin D1 and the phosphorylation of Erk1/2 signaling are not affected in TRAMPC2 tumors grown in obese versus WT mice

Since we did not observe a change in PPARγ and Wnt signaling pathways, we sought to examine whether cyclin D1 and pErk1/2 expression levels were increased with TRAMPC2 tumors grown in ob/ob mice (n= 8) compared to WT mice (n= 8). A published study found increased cyclin D1 expression in the ventral prostate of TRAMP mice fed a Western diet [34]. Cyclin D1 levels were evaluated using Western blot in TRAMPC2 tumor tissues grown in ob/ob mice. Cyclin D1 levels were not further increased in TRAMPC2 tumor tissues harvested from ob/ob mice compared to tumor tissues from WT mice (P-value =0.474; **Figure 29**).

We next examined extracellular signal-regulated protein kinases 1 and 2 (Erk1/2), which are members of the mitogen-activated protein kinase super family. The activity of Erk1/2 is involved in proliferation, survival, invasion, and angiogenesis in PCa [97]. We examined whether the levels of pErk1/2 in TRAMPC2 tumor xenograft tissues harvested from ob/ob mice (n= 15) and WT mice (n= 10) were increased. Western blot analysis revealed that pErk1/2 was expressed in TRAMPC2 tumor tissues grown in ob/ob mice and in WT mice but no significant changes were observed in our model (P-value =0.635; **Figure 30)**. A reason for not finding an increase in p-Erk1/2 might be that TRAMPC2 xenograft was grown in an obese microenvironment that lacked leptin. Leptin has mitogenic effects on PCa cells through leptin stimulated increases p-Erk1/2 levels in DU145 and PC-3 cells [98]. Therefore, this could be the reason for not finding

an increase in the activity of pERK1/2 in TRAMPC2 tumor tissue grown in ob/ob mice.

Other obese models should be tested.
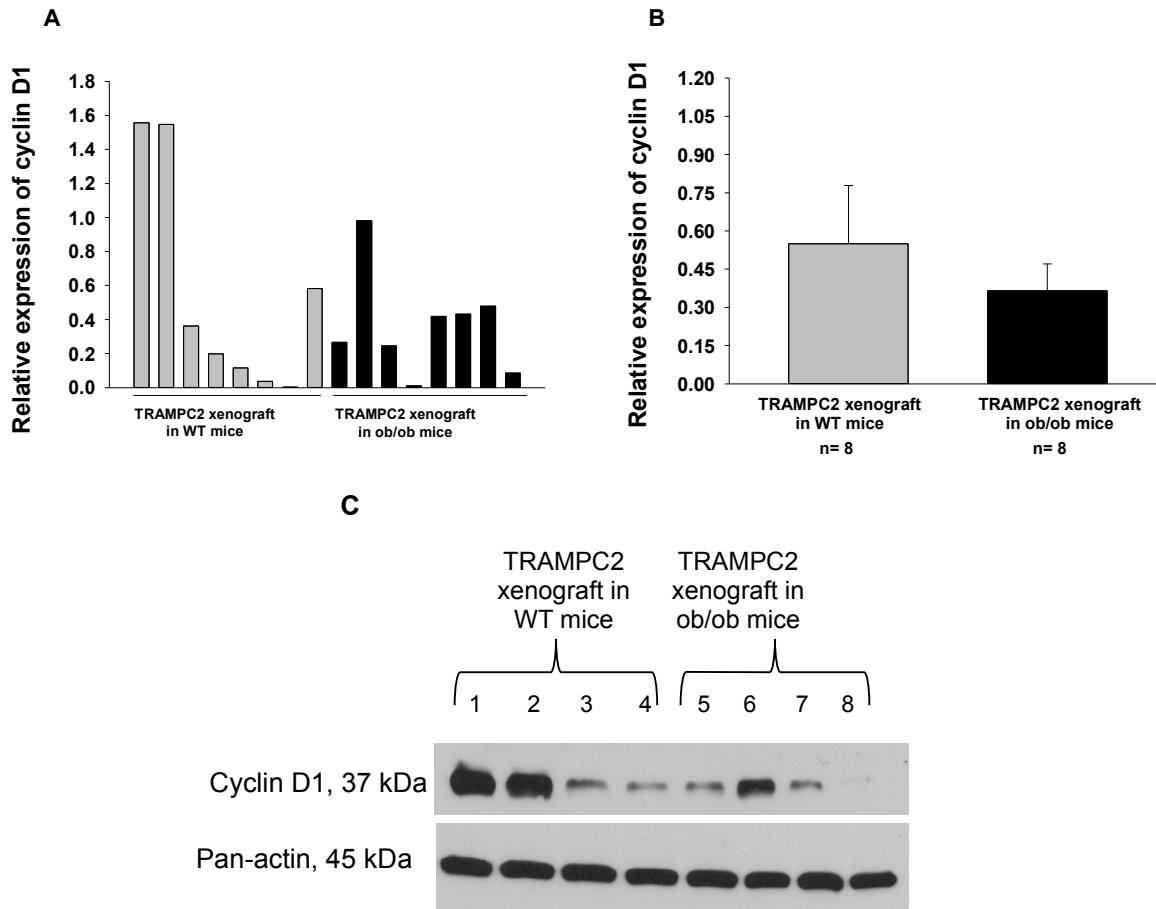
Figure 29. An obese microenvironment did not alter the levels of cyclin D1. Tumor tissues were homogenized, and protein levels were quantified with a Coomassie protein assay. Samples (30 µg) were resolved on SDS-PAGE gels. The separated proteins were transferred to PVDF membrane by electroblotting. Membranes were probed with anti-cyclin D1 antibody, stripped and reprobed with anti-pan-actin antibody, which served as a control for protein loading. (**A**) Cyclin D1 and pan-actin levels were analyzed for each sample by densitometry. (**B**) The relative means of cyclin D1 to pan-actin expression in all samples were combined and analyzed by densitometry. (**C**) A representative Western blot analysis of cyclin D1 and pan-actin. Data are presented as the mean value ± SEM (P-value =0.474).
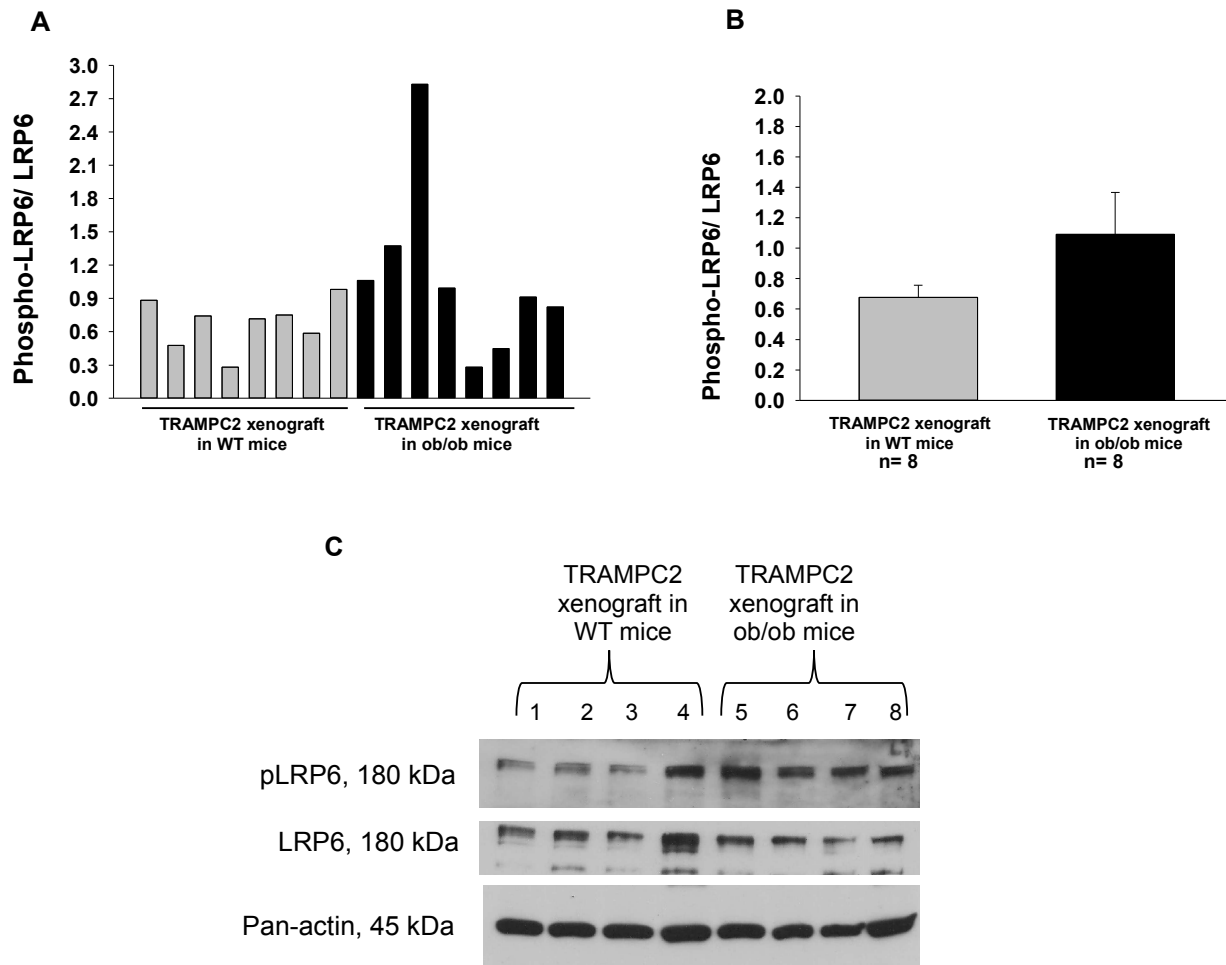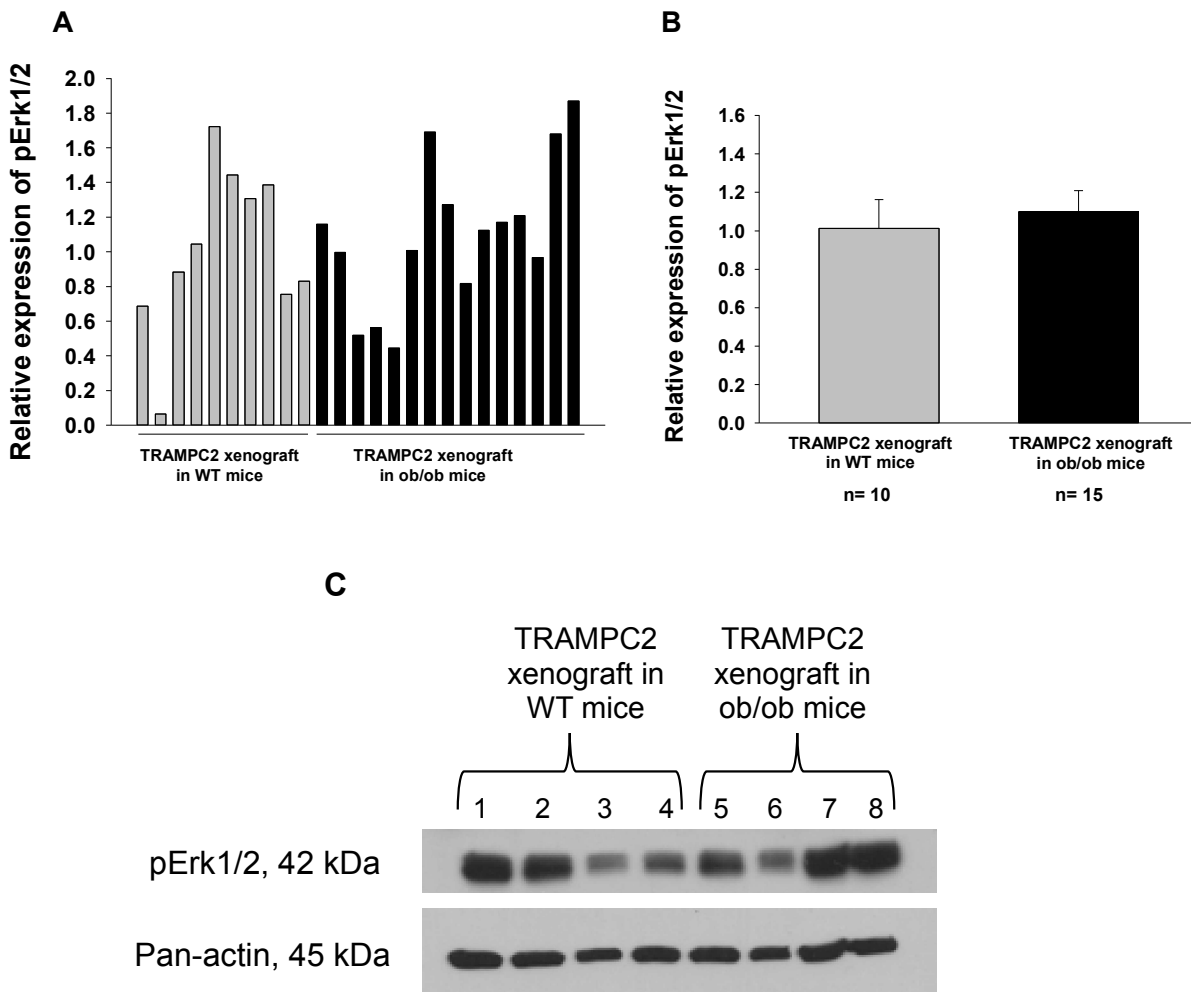
Figure 30. An obese microenvironment did not alter the expression levels of phosphorylated Erk1/2 (pErk1/2). Tumor tissues were homogenized, and protein levels were quantified with a Coomassie protein assay. Samples (30 µg) were resolved on SDS-PAGE gels. The separated proteins were transferred to PVDF membrane by electroblotting. Membranes were probed with anti-pErk1/2 antibody, stripped and reprobed with anti-pan-actin antibody, which served as a control for protein loading. (A) p-Erk1/2 and pan-actin levels were analyzed for each sample by densitometry. (**B**) The relative means of p-Erk1/2 to pan-actin expression in all samples were combined and analyzed by densitometry. (C) A representative Western blot analysis of p-Erk1/2 and pan-actin. Data are presented as the mean value ± SEM (p-value =0.635).

AMPK signaling is activated in TRAMPC2 tumor growth in both WT and ob/ob mice

As our data from signaling experiments did not reveal significant changes in protein levels in TRAMPC2 tumor tissues growing in ob/ob mice versus WT mice, we next studied the involvement of AMPK signaling. Even though AMPKα activity has been found to be increased in human PCa tissues and in human PCa cell lines (LNCaP, CWR22Rv1, DU-145 and PC-3) [99], the phosphorylation of AMPKα and total AMPKα expression have not been investigated in obese patients with PCa. Here, we tested if obesity increased the activity of AMPK signaling. The phosphorylation status of AMPKα was examined in TRAMPC2 xenograft tumors grown in obese mice (n= 4) versus WT mice (n= 4). Western blot analyses indicated that p-AMPKα was expressed in TRAMPC2 tumor tissues grown in ob/ob mice. However, no differences in the ratio of p-AMPKα to total AMPKα were observed in TRAMPC2 tumor tissues grown in ob/ob mice versus WT mice (P-value =0.699; **Figure 31**). Therefore, an obese microenvironment did not affect AMPK Thr172 phosphorylation status in TRAMPC2 tumor xenograft tissues.

Several phosphothreonine and phosphoserine sites have been identified to modulate AMPKα activity [100]. In addition, several isoforms of AMPK have been identified [100]. In our study, we only examined p-AMPKα Thr172 and did not find a difference between TRAMPC2 tumor grown in ob/ob mice versus WT mice. Future studies should examine other phosphorylation sites or isoforms of AMPK that could

reveal an additional link between obesity and PCa progression because the activity of

AMPKα Ser-486/491 was most recently reported to be associated with high advanced

of PCa [101].
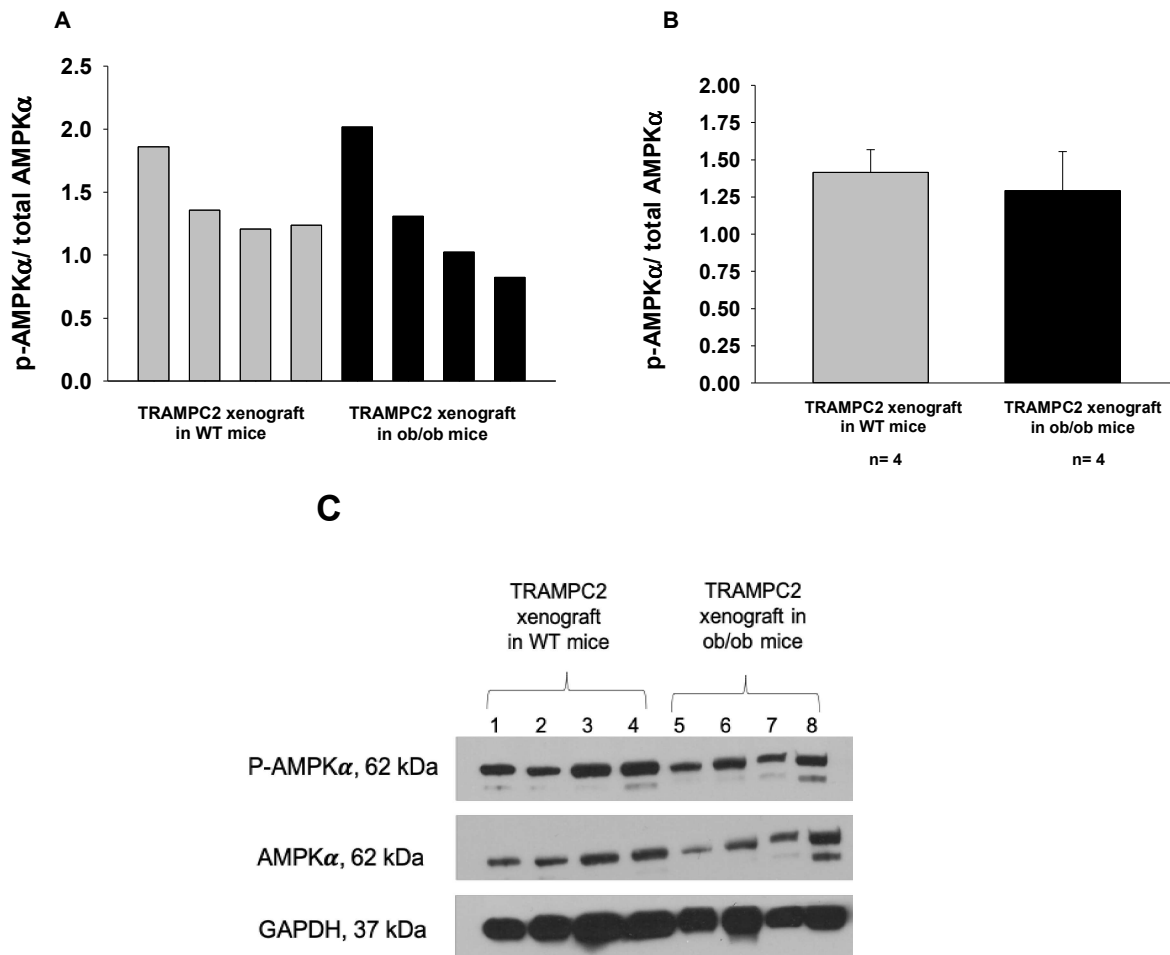
Figure 31. An obese microenvironment did not alter the ratio of phosphorylated AMPKα (p-AMPKα) to total AMPKα. TRAMPC2 tumors were harvested from WT (n=4) and ob/ob (n=4) mice. Tumor tissues were homogenized, and protein levels were quantified with a Coomassie protein assay. Samples (30 μg) were resolved by SDS-PAGE. (**A**) p-AMPKα, total AMPKα, and GAPDH levels were analyzed by densitometry. (**B**) The relative means of p-AMPKα to total AMPKα expression in all samples were combined and analyzed by densitometry. (**C**) A representative Western blot analysis of p-AMPKα and total AMPKα was performed. GAPDH was included as a loading control. Data are presented as the mean value ± SEM (P-value =0.699).

The expression levels of SOD2 are decreased in TRAMPC2 tumor growth in ob/ob mice

We next examined superoxide dismutase 2 (SOD2), a mitochondrial matrix enzyme that is highly expressed in advanced PCa [102]. In PCa cells, the basal expression levels of SOD2 were varied: SOD2 was 10-fold higher in PNT1A normal human prostate cells than LNCaP cells and was also increased in PC-3 and DU145 [102]. The roles of SOD2 in obese patients with PCa has not been yet elucidated. Herein, we examined whether excess lipids in an obese microenvironment induced SOD2 expression. SOD2 levels were evaluated using Western blot in TRAMPC2 tumor tissues grown in obese mice (n= 15) versus WT mice (n= 10). SOD2 levels were significantly decreased in TRAMPC2 tumor tissues harvested from ob/ob mice compared to tumor tissues from WT mice (P-value =0.018; **Figure 32**). Future studies should focus on understanding how obese microenvironment reduced SOD2 levels in PCa.
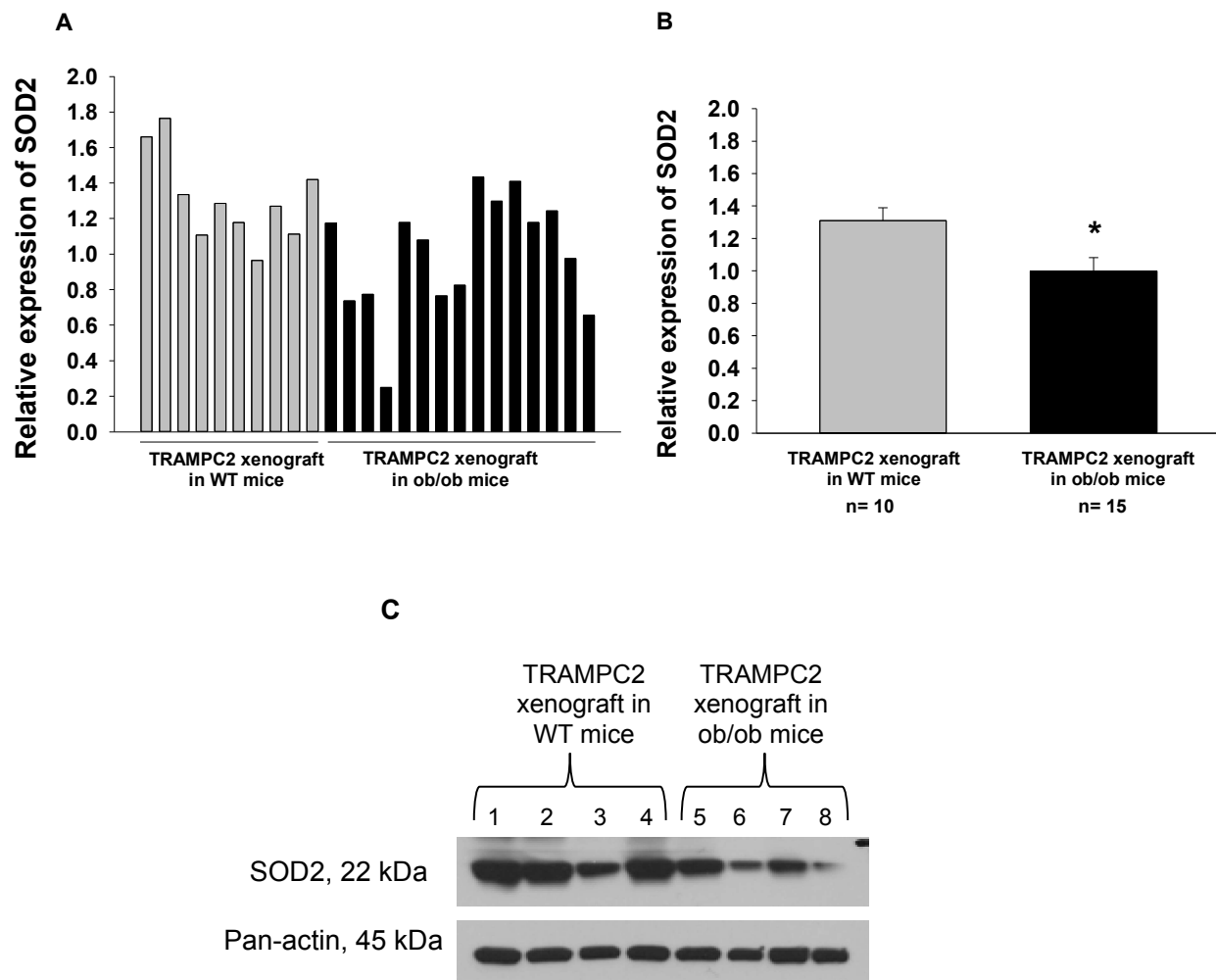
Figure 32. An obese microenvironment decreased the expression levels of SOD2. Tumor tissues were homogenized, and protein levels were quantified with a Coomassie protein assay. Samples (30 μg) were resolved on SDS-PAGE gels. The separated proteins were transferred to PVDF membrane by electroblotting. Membranes were probed with anti-SOD2 antibody, stripped and reprobed with anti-pan-actin antibody, which served as a control for protein loading. (**A**) SOD2 and pan-actin levels were analyzed for each sample by densitometry. (**B**) The relative means of SOD2 to pan-actin expression in all samples were combined and analyzed by densitometry. (**C**) A representative Western blot analysis of SOD2 and pan-actin. *P-value =0.018 compared to TRAMPC2 tumor grown in WT mice. Data are presented as the mean value ± SEM.

The expression levels of SPT are decreased in TRAMPC2 tumor growth in ob/ob mice.

The final molecule that we investigated in our study was serine palmitoyltransferase (SPT), which is the rate limiting enzyme in sphingolipid synthesis. SPT expression has been identified in normal human prostate tissue [103], but its expression has not been reported in PCa patient tissues. To our knowledge, this is the first study to report the expression levels of SPT in TRAMPC2 xenograft tumor grown in ob/ob mice (n= 8) versus WT mice (n= 8). Western blot analysis revealed that SPT levels were significantly decreased in TRAMPC2 tumor tissues grown in ob/ob mice as compared to WT mice (P-value =0.050; **Figure 33**). Thus, obesity due to a genetic alternation decreased SPT levels in TRAMPC2 xenograft tumor.
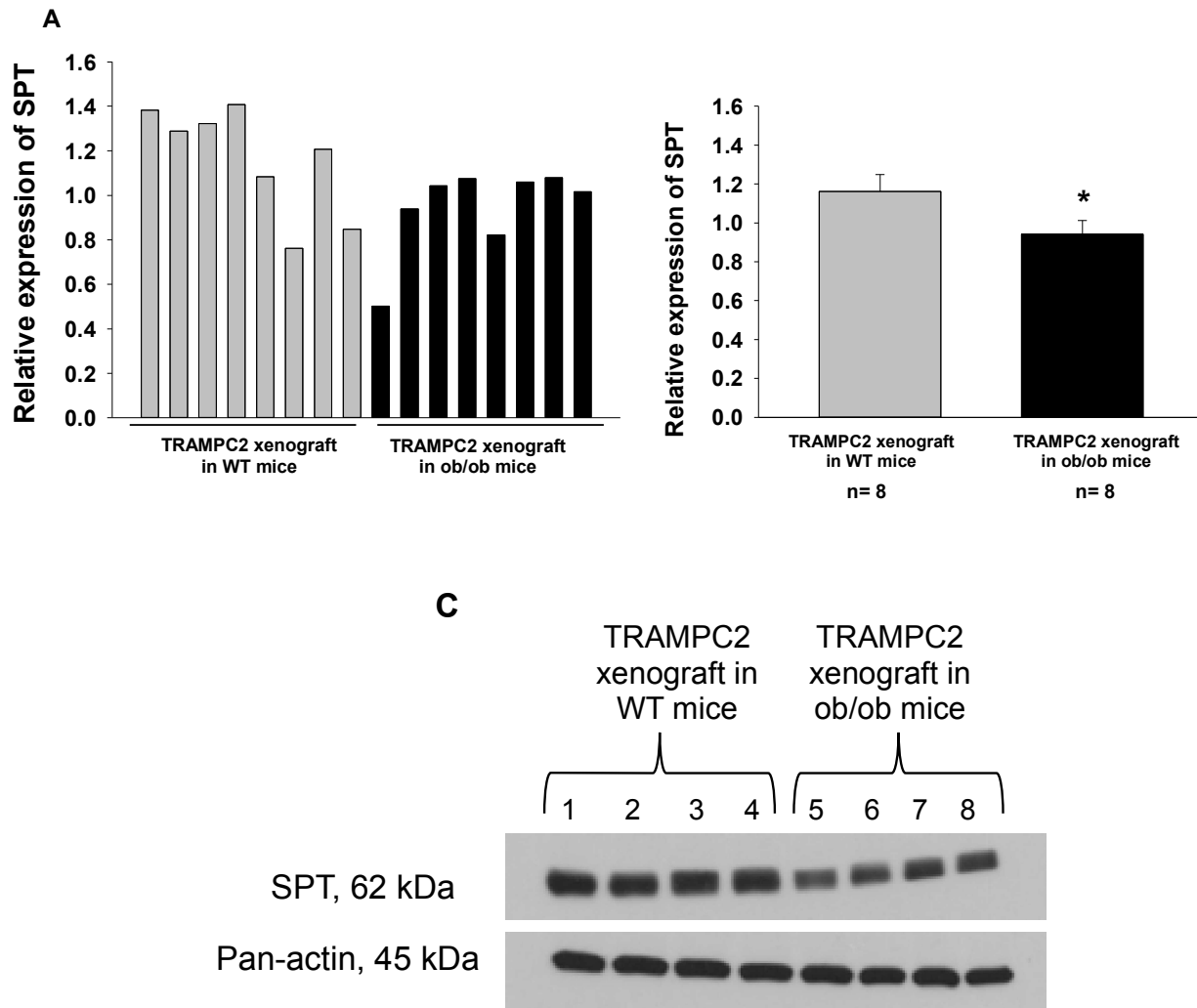
Figure 33. An obese microenvironment decreased the levels of SPT. Tumor tissues were homogenized, and protein levels were quantified with a Coomassie protein assay. Samples (30 μg) were resolved on SDS-PAGE gels. The separated proteins were transferred to PVDF membrane by electroblotting. Membranes were probed with anti-SPT antibody, stripped and reprobed with anti-pan-actin antibody, which served as a control for protein loading. (**A**) SPT and pan-actin levels were analyzed for each sample by densitometry. (**B**) The relative means of SPT to pan-actin expression in all samples were combined and analyzed by densitometry. (**C**) A representative Western blot analysis of SPT and pan-actin. *P-value =0.050 compared to TRAMPC2 tumor grown in WT mice. Data are presented as the mean value ± SEM.

DISCUSSION

Obesity and cancer are both global public health concerns, with obesity incidence drastically increasing over the past three decades [104]. If a PCa patient is obese, he is at a higher risk of aggressive disease and more likely to die from the disease as compared to a lean PCa patient [11], [12]. However, the molecular mechanisms underlying obesity-fueled PCa progression is unclear. Our studies were aimed to reveal a mechanistic insight into this association. Previously, our lab was able to simulate an *in vitro* obese model by treating PCa cells with excess OA to evaluate the underlying mechanisms. In this model, the proliferation and metabolic activity of PCa cells was increased as determined by direct cell counts and MTT assay (Doll *et al*. unpublished observation). In addition, PEDF levels were suppressed in PCa cells treated with excess OA. PEDF is a multifunctional protein that acts as a potent tumor suppressor via its anti-angiogenic and anti-proliferative inhibitory activities [42]. PEDF has been identified as a novel regulator of lipid metabolism through binding and activating ATGL [46], [47]. However, circulating and tissue PEDF levels have not been previously examined *in vivo* under obese conditions in PCa.

In our *in vivo* study, we observed a significant increase in TRAMPC2 tumor volume and in tumor weight, in tumors grown in ob/ob mice as compared to tumors grown in WT mice (**Figure 20**). Consistent with our observation, Ribeiro *et al.* found a significant increase in the tumor weight of RM1 PCa xenografts grown in ob/ob mice

compared to RM1 tumors grown in WT mice [35]. These results suggested that a genetically obese microenvironment accelerates tumor growth of these PCa xenografts. In our *in vivo* dietary study, we expected that the epididymal fat pad weight would be increased in mice placed on a HFD compared to CD-fed mice since the increase of the epididymal fat pad weight is previously reported in HFD-fed mice [32], [95]; however, as compared to the CD-fed mice, in our study, there were no differences in the epididymal fat pad weight, and this is an opposite to what we expected. This observation suggests that HFD-fed mice could promote PCa growth through a mechanism independent of epididymal fat tissues. In addition, it could be that mice did not deposit excess fats from HFD in epididymal fat pad. Therefore, a comprehensive fat depot evaluation should be performed in a HFD mouse model of PCa. In addition, the start age point and duration of time that mice are fed a HFD should be evaluated since there is no standardized protocol for the start age point and length of time that mice stay on a HFD. Chen *et al.* fed Pbsn-Cre+PTEN^{fl/fl} mice a HFD, starting at the age of 12 months for 3 months although they did not report epididymal fat pad weight [33]. In contrast, we fed our Pbsn-Cre+PTEN^{fl/fl} mice a HFD, beginning at the age of 2 months for 4 months.

Our lab previously demonstrated that PEDF-KO mice developed prostatic hyperplasia that evolves to cancer when these mice were fed a HFD (Doll *et al.* unpublished observation). However, it is unknown how the loss of PEDF expression under an obese microenvironment promotes progression of the prostatic hyperplasia to cancer. Interestingly, in other studies, an obese microenvironment increased circulating

PEDF levels in ob/ob mice and HFD-mice [36], [38]. To our knowledge, the circulating

and tissue levels of PEDF in obese mice with PCa has not been previously evaluated.

Additionally, the functional role of PEDF as an anti-tumor has not been examined in

obese individuals with PCa. Herein, we examined if an obese microenvironment alters

circulating PEDF levels and decreases PEDF levels in TRAMPC2 tumor tissue. In the

TRAMPC2 xenograft study, we did not identify an increase in serum PEDF levels in

obese (ob/ob) mice as compared to WT mice (**Figure 22**). A possible explanation for

not finding increased circulating PEDF in our ob/ob mice is that secretions from

TRAMPC2 xenograft tumors led to lower PEDF levels in ob/ob mice since the increased

serum PEDF levels are well-documented in mouse obesity models [36], [38]. In

addition, the major source of circulating PEDF is the liver that could be affected in the

presence of TRAMPC2 tumor xenografts [41]. Li *et al.* injected mice with squamous cell

carcinoma (SCC) and evaluated the liver functions [105]. They found that mice with

SCC xenograft tumors showed hepatomegaly and liver injury. In addition, they identified

reduced albumin/globulin ratios, elevated serum TG, increased hepatic mRNA levels of

inflammatory cytokines, and decreased fatty acid oxidation in the liver of mice with SCC

xenografts [105].

Interestingly, when we induced obesity by using a HFD in Pbsn-Cre[+]PTEN^{fl/fl}

mice, we found that the serum levels of PEDF were significantly reduced in HFD-fed

PCa mice compared to CD-fed mice (**Figure 23**). Our findings contrasted with other

published studies regarding increased circulating PEDF levels in HFD-fed mouse model

[36], [38]. In non-tumor bearing mice, a HFD increased circulating PEDF levels that contributed to insulin resistance [36], [38]. Specifically, the plasma PEDF levels were significantly increased (15 ng/ml) in non-tumor mice fed a HFD compared to mice fed a low chow fat (4.9 ng/ml) [38]. Conversely, in our study, HFD-fed PCa mice showed high levels of serum PEDF levels (74.7 ng/ml ± 13.6) versus CD-fed mice (133.4 ng/ml ± 12.4). It has been proposed that the elevated circulating PEDF is a compensatory mechanism in response to the increased body weight since its expression is decreased with the body weight loss [36]. To confirm that increased PEDF is a compensatory mechanism, a recent report showed that HFD-fed mice treated with PEDF showed decreased body weight, increased lipolytic activity, and improved insulin sensitivity [106]. Another reason may be due to the variation of PEDF isoforms. There are two identified isoforms, PEDF-1 and PEDF-2, with different functional roles. PEDF-2 has more a potent anti-tumor activity than PEDF-1 [43]. Also, they have different charge and molecular mass: PEDF-1 is 46,063 ± 13 Da and PEDF-2 is 47,176 ± 87 Da [43]. Further studies are needed to distinguish which isoform is affected by obesity.

We also examined tumor PEDF levels in TRAMPC2 tumor tissues grown in ob/ob mice versus WT mice. A significant reduction in PEDF levels was found in TRAMPC2 tissues grown in ob/ob mice compared to tumor tissues harvested from WT mice (**Figure 25**). The reduction of PEDF suggests that PEDF could have an anti-tumor effects in obese conditions since a significant increase in TRAMPC2 tumor volume and weight was observed in tumors growing in ob/ob mice compared to tumors growing in

WT mice. However, the mechanisms through which an obese microenvironment decreases tissue PEDF are still unknown.

Of note, while we found a significant reduction in the serum levels of PEDF in HFD-fed Pbsn-Cre+PTEN^{fl/fl} mice, we did observe a significant increase in serum leptin levels in HFD-fed Pbsn-Cre+PTEN^{fl/fl} mice as expected (**Figure 24**). In a pilot study in our lab, it was observed that obese patients with PCa showed an increased in leptin levels, but not in PEDF levels (Doll *et al,* unpublished study). An association between these two molecule's expression was published in the context of angiogenic regulation [107], [108]. Leptin treatment increased secreted vascular endothelial growth factor, transforming growth factor-β1, and basic fibroblast growth factor in DU145 and PC-3 cells [109]. Additionally, leptin can stimulate angiogenesis in endothelial cells [110]; however, PEDF is a potent anti-angiogenic protein, and rPEDF treatment of PC-3 tumor xenografts in nude mice decreased stromal vasculature and induced apoptosis [49]. Importantly, Yamagishi *et al.* found that PEDF inhibited leptin-induced angiogenesis of microvascular endothelial cells [107]. Likewise, a recent published study showed that HFD-fed mice treated with PEDF showed a decrease in the serum leptin levels [106].

In our studies, we examined other pathways related to PCa progression. We did not find changes in the activity and/or expression levels of PPARγ, p-β-catenin, pLRP6, pErk1/2, cyclin D1, and p-AMPKα in TRAMPC2 tumor tissues grown in ob/ob mice versus WT mice. However, we did find a significant decrease in SOD2 and SPT

signaling pathways in TRAMPC2 tumor tissues grown in ob/ob mice versus WT mice (**Figure 32** and **33**).

SOD2 is an enzyme localized in the mitochondrial matrix to catalyze the conversion of superoxide anion ($O_2^{\bullet-}$) to hydrogen peroxide (H_2O_2) that is further metabolized to water by other antioxidants such as catalase and glutathione peroxidase [111]. Thus, SOD2 controls the concentration of reactive oxygen species (ROS), which is associated with increased oxidative DNA damage in PCa cells [112]. Interestingly, PEDF and its 44 mer peptide have demonstrated antioxidant activity via increasing the activity of total SOD and decreasing ROS in cardiomyocytes, H9c2 cells [113]. Gong *et al.* showed in pancreatic intraepithelial neoplasia (PanIN) cells that PEDF specifically induced SOD2 expression [114]. Thus, if PEDF regulates SOD2 activity in PanIN cells, then it is possible that decreased PEDF in PCa tissues could lead to decreased SOD2 activity.

SOD2 expression levels, evaluated by immunohistochemistry, are decreased in PIN and PCa patient tissues compared to benign epithelium tissues [115]; however, others reported that the protein levels of SOD2, analyzed by Western blotting and by immunocytochemistry, are highly expressed in PCa tumor tissues in advanced and middle stage of disease [102], [116]. However, none of these studies stratified PCa patients by BMI. A possible explanation of these conflicting findings was stated in Miar *et al.*'s study [116]. They explained that as different mutations occur in low-grade versus

85

high-grade PCa, this could be reason for different levels of SOD2 in PCa tissues [116].

It could be also that increased SOD2 expression in advanced PCa cancer is a

compensatory mechanism against the increased oxidative stress [117].

Previous studies showed that obesity reduced SOD2 levels in the liver and

kidney and increased oxidative stress in the form of ROS in mouse plasma and adipose

tissues [118], [119]. In a tumor setting, the decreased SOD2 levels could result in

increased ROS generation that could promote tumor progression. In addition, obesity

increases ROS production in PCa cells [112], [120], but a mechanism was not

described. If SOD2 levels are decreased, then the resulting increases in ROS would

lead to increased pro-inflammatory cytokines [95], [96], [121]. It could be that obesity

mediates suppression of SOD2 expression results in increased ROS which in turn

increased pro-inflammatory cytokines. A recent study showed that overexpression of

SOD2 reduced inflammation [122] while increased chronic inflammation impaired SOD2

function [123]. Together, downstream pathways altered by decreased SOD2

expression, including inflammatory responses and ROS homeostasis, should be further

investigated.

To our knowledge, this is the first study to report the expression levels of SPT in

PCa TRAMPC2 tumor xenograft. We demonstrated that SPT expression was

significantly reduced in TRAMPC2 xenograft tissues grown in ob/ob mice as compared

to WT mice. Reduced SPT levels could be one mechanism of obesity to protect cancer

cells against lipotoxicity since SPT is involved in the process of ceramide production that acts as a lipid mediator of apoptotic signaling cascade [124], [125]. Lipotoxicity is a pathway through which an excess lipid accumulation in non-adipose tissues leads to cellular dysfunction and death through lipoapoptosis [126]. Ceramide can be generated via the hydrolysis of sphingomyelin by sphingomyelinases and via condensation of serine and palmitoyl-CoA, which is catalyzed by SPT and ceramide synthase enzymes, respectively [127]. The activity of these enzymes has not been examined in obese individuals with PCa.

Ceramide has been identified as an anti-tumor lipid, stimulating apoptotic signaling in various cancer cell types, including PCa [124], [125], [128]. The pathways activated by ceramide include the stress-activated protein kinase (SAPK/JNK) pathway, apoptotic caspases pathway, and Fas cell surface death receptor pathway [124], [125], [128]. Wang *et al.* showed that the anticancer agent, fenretinide N-(4-hydroxyphenyl)retinamide;4-HPR), stimulated the formation of ceramide in LNCaP and PC-3 cells via increasing the activity of SPT resulting in enhancing apoptosis in these cells [125]. Another study by Fillet *et al.* displayed that the exogenous treatment of ceramide induced apoptosis in both human colon cancer (HCT116) and human ovarian carcinoma (OVCAR-3) cell lines [129]. They specifically showed that C2- and C6-ceramides increased the activity of caspase-3 and mitochondrial cytochrome c in HCT116 and OVCAR-3 cells [129]. In human promyelocytic leukemia cells (HL-60) treated with ceramide, Kim *et al.* showed an induction of cell death through the

mitochondrial pathway [130]. Specifically, ceramide induced cytochrome c release and increased activity of Bax, a pro-apoptotic factor, in HL-60 cells [130].

These results indicate that elevation of ceramide levels in tumor cells can result in cell death; however, reduced SPT could reduce ceramide production in TRAMPC2 tumor tissues grown in ob/ob mice which suggests that TRAMPC2 tumors in an obese microenvironment are protected from lipotoxicity and lipoapoptosis. Moreover, the loss and/or reduction of SPT expression has been found to increase the formation of lipid droplet and to alter lipid metabolism. In hereditary sensory neuropathy type 1 (HSN-1), which is an autosomal dominant neurodegenerative disease, caused by a mutation in SPT gene, Marshall *et al.* showed increases in the number of lipid droplets and changes in lipid metabolism in HSN-1 patient-derived lymphoblasts [131].

Our lab's previous data showed that in an *in vitro* obesity model of PCa, excess OA suppressed both secreted and cellular PEDF levels in DU145 and PC-3 cells. Herein, we investigated whether excess OA activated GPR40-induced Ca^{2+} signaling and/or PPARγ signaling to decrease PEDF expression in normal prostate cell and PCa cell lines. In addition, we explored whether excess lipids, due to obesity and HFD microenvironments, increased pro-tumorigenic signaling activity and reduced PEDF expression.

In the present study, the proliferation and viability of PCa cells treated with OA alone or plus chemical inhibitors were assessed as these features are an indicator of tumor progression. RWPE-1 and DU145 proliferation were not affected with OA treatment at 1 mM alone while the proliferation of TRAMPC2 was reduced with OA treatment alone. All cells exposed to GPR40 or PPARγ chemical inhibitor alone or in the presence of OA showed no effects on proliferation. Published studies in OA treated PCa cells vary. Inconsistent with our observation, Hughes-Fulford et al. found a reduction in proliferation of PC-3 cells treated with OA treatment at 0.1 mM using used CyQUANT cell proliferation assays [132]; other studies reported that an increase in PC-3 proliferation using MTT assay with OA treatment at 0.1-0.4 mM [94], [133]. Hagen et al. demonstrated no changes on DU145 proliferation using the MTT assay when the cells were cultured with OA [133], while Liotti et al. found increased DU145 proliferation with OA [94]. These inconsistent findings in PCa cell proliferation could be due to use of different OA doses, different incubation times, and different OA preparations.

Viability of RWPE-1, LNCaP, DU145, and PC-3 cells was not affected with 1 mM OA treatment alone or in the presence of GPR40, Ca^{2+}, or PPARγ chemical inhibitors compared to untreated group. Similar to our observation, Gasmi et al. treated RWPE-1, LNCaP, and PC-3 cells with two different forms of OA, which were cis- and trans-vaccenic acids, at 0.1 mM and found no changes on cell viability in any of the cell lines [134]. Hagen et al. treated LNCaP, DU145, and PC-3 cells with 0.1 mM OA, and viability of these cells was evaluated. They found no effects on LNCaP and PC-3 cell viability

while a reduction in DU145 cell viability was observed [133]. These results are consistent with our observation in LNCaP and PC-3 cell viability, but not in DU145 cell viability. Together, our data demonstrated that no effects on viability were produced from OA treatment alone or with chemical inhibitors of GPR40 or PPARγ on PCa cells.

The potential explanations for the variability associated with FA treatment within our study and other published studies are that this variability could be associated to human-, device-, dosage-, assays- or sample preparation-differences. In our study, we starved PCa cells for 4 h before adding FA treatment while Liotti *et al.* starved PCa cells for 16 h [94]. In addition, PCa cells are able to grow in different culture medium conditions. DU145 and PC-3 cells have the ability to grow in DMEM or RPMI media, and this is a factor added to these discrepancies. Hughes-Fulford *et al.* and we grew PCa cells in RPMI media [132] while Liotti *et al.* grew PCa cells in DMEM media [94]. Another important factor is that various FA preparations and concentrations used in PCa studies significantly contribute to divergent results. In our study, we used different lots of OA that produced inconsistent effects on PCa growth response since we were unable to find similar results in LNCaP and PC-3 cell proliferation. Previously, our lab found a decrease in viability of LNCaP and PC-3 cells treated with OA treatment [135] while we did not find a change in LNCaP and PC-3 cell viability treated with the same OA treatment but the lot numbers of OA are not the same.

Our lab's previous data suggested that after 48 h of OA treatment, a suppression in cellular PEDF expression was identified in two androgen-independent PCa cells, DU145 and PC-3 cells; conversely, no changes were found in RWPE-1 and LNCaP cells. Secreted PEDF were decreased in RWPE-1, LNCaP, DU145, and PC-3 cells treated with excess OA (Doll *et al.* unpublished observation). In our studies, we sought to determine the molecular mechanisms through which excess OA suppresses PEDF expression in PCa cells. However, we did not find that OA bound to GPR40 that activates Ca^{2+} and/or PPARγ to exert its effects on PEDF suppression.

Of significant note, we observed no changes in cellular PEDF levels in our current study, which contrasts to our lab's preliminary studies in DU145 and PC-3 cells treated with OA alone. One of the important reasons for these discrepancies is that the type of growth media for DU145 and PC-3 cells was changed from DMEM to RPMI due to growth issues. In breast cancer cell Lines (MCF7, MDA-MB-436, and SkBr3), using different types of growth media (DMEM and RPMI-1640) were found to have differences in phenotypic markers and growth rates [136]. Thus, it could happen that the metabolic responses to OA are altered in PCa cells with changing the media from DMEM to RPMI. In addition, we purchased a prepared OA from Sigma that is ready to use. We noticed that OA treatment has different effects on PCa viability as determined in the current and previous studies conducted in our lab [135]. There could be issues with differences in the quality of OA batch-to-batch. Future study should evaluate batch-to-batch quality consistency of OA.

CONCLUSION AND FUTURE DIRECTIONS

Conclusion

The aim of this study was to investigate whether excess lipids, in obesity and HFD microenvironments, alter lipid metabolism, which in turn, decreases PEDF expression and increases pro-tumorigenic activity in PCa. We included two *in vivo* models of obesity: the genetically obese model (ob/ob) and a HFD-induced obese model. We also used an excess OA model to simulate obesity *in vitro.* These models were used to evaluate how excess lipids in an obese microenvironment promoted PCa progression and decreased anti-tumor PEDF protein. We examined GPR40, Ca^{2+}, and PPARγ as potential molecular mechanisms for OA to suppress PEDF. However, our data indicated that inhibition of GPR40 and PPARγ did not abolish OA-induced suppression of secreted PEDF expression in PCa cells (LNCaP, PC-3, and DU145) compared to untreated group. These results did not support that OA exerts its effects on secreted PEDF suppression through activation of GPR40 and PPARγ.

In the *in vivo* obese (ob/ob) mouse study, our data indicated that serum PEDF levels were not increased in ob/ob mice compared to WT mice; whereas, tissue PEDF levels were significantly decreased in TRAMPC2 tumor tissues grown in ob/ob mice versus WT mice. In HFD-fed Pbsn-Cre^{+}PTEN$^{fl/fl}$ PCa mice, the serum levels of leptin and PEDF were quantified. We found that leptin was increased while PEDF was

decreased. Leptin displays a pro-tumorigenic activity; whereas, PEDF exhibits anti-tumorigenic activity. No changes were observed in PPARγ, β-catenin, pErk1/2, cyclin D1, and AMPKα signaling pathways. However, a significant decrease was observed in SOD2 and SPT signaling pathways in TRAMPC2 tumor tissues grown in ob/ob mice versus WT mice.

Future direction

Future studies are required to fully understand how an obese microenvironment decreases PEDF, SOD2, and SPT expression in PCa. One of the future directions is to explore the effects of PEDF treatment on inhibition of PCa progression in an obese microenvironment. For this set of studies, we will use PEDF-KO mice and WT mice fed a CD or a HFD, and ob/ob mice fed a CD. All mice will be then injected with mouse PCa xenografts and treated with exogenous PEDF or vehicle. Tumor tissue growth, metastasis, and the underlying molecular mechanisms through which PEDF treatment inhibits PCa progression should be investigated. Specifically, we will evaluate if PEDF functions as an activator of the intrinsic apoptotic signaling through upregulated BAX and BCL-2 proteins and as an anti-inflammatory activator via reduced interleukin-6 and tumor-necrosis factor-α levels. In addition, we will examine if PEDF as an antioxidative stress protein through decreased ROS and increased SOD2 levels. These experiments will identify a novel relationship between PEDF and obese PCa suppression and

determine if PEDF has anti-obesity properties. Therefore, this study could identify PEDF as a new and effective therapy for obese PCa patients.

Our study is the first study to report SOD2 in obese model of PCa. Evaluating the expression levels of SOD2 in obese patients with PCa is an important future step. While there are a few studies that reported the levels of SOD2 in PCa patients [102], [116], further investigation of the effects of antioxidant SOD2 treatment such as manganese (to activate SOD2) or overexpression of SOD2 in preventing obesity-driven PCa progression should be conducted.

To our knowledge, this is the first preliminary study to identify the decreased levels of SPT in obese model of PCa. Future studies should further investigate the regulation of ceramide pathway in an obese microenvironment. For this set of experiments, we will include human PCa xenografts in nude mice that will be placed on a CD or a HFD. In addition, we will include Pbsn-Cre$^+$-PTEN$^{fl/fl}$ PCa model fed either a CD or HFD as well as TRAMPC2 xenografts in WT mice and ob/ob mice. Then, all mice will be treated with nanoliposomal C6-ceramide or liposomal-C8 ceramide treatment as described previously [137]. Tumor tissues will be collected and analyzed for markers of apoptotic signaling cascades and for ceramide signaling pathways such as SPT and ceramide synthase enzymes. If this experiment shows a significant reduction in tumor growth in obese models, this could be used as an effective therapy for obese PCa patients.

REFERENCES

[1] S. W. Fine and V. E. Reuter, "Anatomy of the prostate revisited: implications for prostate biopsy and zonal origins of prostate cancer.," *Histopathology*, vol. 60, no. 1, pp. 142–52, Jan. 2012.

[2] P. H. Gann, "Risk factors for prostate cancer.," *Rev. Urol.*, vol. 4 Suppl 5, no. Suppl 5, pp. S3–S10, 2002.

[3] American Cancer Society, "Key Statistics for Prostate Cancer | Prostate Cancer Facts," 2019. [Online]. Available: https://www.cancer.org/cancer/prostate-cancer/about/key-statistics.html. [Accessed: 09-Jun-2019].

[4] J. E. McNeal, "Origin and evolution of benign prostatic enlargement," *Invest Urol*, vol. 15, no. 4, pp. 340–345, 1978.

[5] M. S. Litwin and H.-J. Tan, "The Diagnosis and Treatment of Prostate Cancer," *JAMA*, vol. 317, no. 24, p. 2532, Jun. 2017.

[6] E. H. Allott, E. M. Masko, and S. J. Freedland, "Obesity and Prostate Cancer: Weighing the Evidence," *Eur. Urol.*, vol. 63, no. 5, pp. 800–809, May 2013.

[7] L. Cheng, R. Montironi, D. G. Bostwick, A. Lopez-Beltran, and D. M. Berney, "Staging of prostate cancer," *Histopathology*, vol. 60, no. 1, pp. 87–117, Jan. 2012.

[8] J. Ramos, E. Uchio, M. Aslan, and J. Concato, "Changes in Gleason scores for prostate cancer: what should we expect from a measurement?," *J. Investig. Med.*, vol. 58, no. 4, pp. 625–8, Apr. 2010.

[9] W. A. Sakr, D. J. Grignon, G. P. Haas, L. K. Heilbrun, J. E. Pontes, and J. D. Crissman, "Age and racial distribution of prostatic intraepithelial neoplasia.," *Eur. Urol.*, vol. 30, no. 2, pp. 138–44, 1996.

[10] M. N. Bashir, "Epidemiology of prostate cancer," *Asian Pacific Journal of Cancer Prevention*, vol. 16, no. 13. pp. 5137–5141, 2015.

[11] S. J. Freedland and W. J. Aronson, "Examining the Relationship Between Obesity

and Prostate Cancer," *Rev. Urol.*, vol. 6, no. 2, pp. 73–81, 2004.

[12] T. Golabek, J. Bukowczan, P. Chlosta, J. Powroznik, J. Dobruch, and A. Borowka, "Obesity and prostate cancer incidence and mortality: a systematic review of prospective cohort studies.," *Urol. Int.*, vol. 92, no. 1, pp. 7–14, 2014.

[13] F. Q. Nuttall, "Body Mass Index: Obesity, BMI, and Health: A Critical Review.," *Nutr. Today*, vol. 50, no. 3, pp. 117–128, May 2015.

[14] A. C. Vidal, L. E. Howard, D. M. Moreira, R. Castro-Santamaria, G. L. Andriole, and S. J. Freedland, "Obesity Increases the Risk for High-Grade Prostate Cancer: Results from the REDUCE Study," *Cancer Epidemiol. Biomarkers Prev.*, vol. 23, no. 12, pp. 2936–2942, Dec. 2014.

[15] D. Mandair, R. Rossi, M. Pericleous, T. Whyand, and M. Caplin, "Prostate cancer and the influence of dietary factors and supplements: a systematic review," *Nutr. Metab. (Lond).*, vol. 11, no. 1, p. 30, 2014.

[16] C. Agostoni and M. G. Bruzzese, "Fatty acids: their biochemical and functional classification," *Pediatr. Med. Chir.*, vol. 14, no. 5, pp. 473–9, 1992.

[17] R. J. de Souza *et al.*, "Intake of saturated and trans unsaturated fatty acids and risk of all cause mortality, cardiovascular disease, and type 2 diabetes: systematic review and meta-analysis of observational studies," *BMJ*, vol. 351, p. h3978, 2015.

[18] M. G. Kokatnur, M. C. Oalmann, W. D. Johnson, G. T. Malcom, and J. P. Strong, "Fatty acid composition of human adipose tissue from two anatomical sites in a biracial community," *Am. J. Clin. Nutr.*, vol. 32, no. 11, pp. 2198–2205, 1979.

[19] U. Gogus and C. Smith, "n☐3 Omega fatty acids: a review of current knowledge," *Int. J. Food Sci. Technol.*, vol. 45, no. 3, pp. 417–436, 2010.

[20] Z. Gu, J. Suburu, H. Chen, and Y. Q. Chen, "Mechanisms of omega-3 polyunsaturated fatty acids in prostate cancer prevention," *Biomed Res Int*, vol. 2013, p. 824563, 2013.

[21] J. Baillargeon and D. P. Rose, "Obesity, adipokines, and prostate cancer (review)," *Int. J. Oncol.*, vol. 28, no. 3, pp. 737–745, 2006.

[22] M. F. Leitzmann *et al.*, "Dietary intake of n-3 and n-6 fatty acids and the risk of prostate cancer," *Am J Clin Nutr*, vol. 80, no. 1, pp. 204–216, 2004.

[23] P. A. Godley, M. K. Campbell, P. Gallagher, F. E. A. Martinson, J. L. Mohler, and R. S. Sandier, "Biomarkers of essential fatty acid consumption and risk of prostatic carcinoma," *Cancer Epidemiol. Biomarkers Prev.*, vol. 5, no. 11, pp. 889–895, 1996.

[24] L. M. Newcomer, I. B. King, K. G. Wicklund, and J. L. Stanford, "The association of fatty acids with prostate cancer risk.," *Prostate*, vol. 47, no. 4, pp. 262–8, 2001.

[25] H. Moussa *et al.*, "Omega-3 Fatty Acids Survey in Men under Active Surveillance for Prostate Cancer: from Intake to Prostate Tissue Level," *Nutrients*, vol. 11, no. 7, p. 1616, Jul. 2019.

[26] Y. J. Yang, S. H. Lee, S. J. Hong, and B. C. Chung, "Comparison of fatty acid profiles in the serum of patients with prostate cancer and benign prostatic hyperplasia," *Clin. Biochem.*, vol. 32, no. 6, pp. 405–409, 1999.

[27] F. L. Crowe *et al.*, "Fatty acid composition of plasma phospholipids and risk of prostate cancer in a case-control analysis nested within the European Prospective Investigation into Cancer and Nutrition.," *Am. J. Clin. Nutr.*, vol. 88, no. 5, pp. 1353–63, 2008.

[28] S. J. Pocock *et al.*, "Issues in the reporting of epidemiological studies: a survey of recent practice," *BMJ*, vol. 329, no. 7471, p. 883, Oct. 2004.

[29] T. Petan, E. Jarc, and M. Jusović, "Lipid Droplets in Cancer: Guardians of Fat in a Stressful World.," *Molecules*, vol. 23, no. 8, p. 1941, Aug. 2018.

[30] M. M. Grabowska *et al.*, "Mouse models of prostate cancer: picking the best model for the question.," *Cancer Metastasis Rev.*, vol. 33, no. 2–3, pp. 377–97, Sep. 2014.

[31] S. Wang *et al.*, "Prostate-specific deletion of the murine Pten tumor suppressor gene leads to metastatic prostate cancer.," *Cancer Cell*, vol. 4, no. 3, pp. 209–21, Sep. 2003.

[32] J. Liu *et al.*, "High-calorie diet exacerbates prostate neoplasia in mice with haploinsufficiency of Pten tumor suppressor gene.," *Mol. Metab.*, vol. 4, no. 3, pp. 186–98, Mar. 2015.

[33] M. Chen *et al.*, "An aberrant SREBP-dependent lipogenic program promotes metastatic prostate cancer," *Nat. Genet.*, vol. 50, no. 2, pp. 206–218, Feb. 2018.

[34] G. Llaverias *et al.*, "A Western-type diet accelerates tumor progression in an autochthonous mouse model of prostate cancer.," *Am. J. Pathol.*, vol. 177, no. 6, pp. 3180–91, Dec. 2010.

[35] A. M. Ribeiro *et al.*, "Prostate cancer cell proliferation and angiogenesis in different obese mice models.," *Int. J. Exp. Pathol.*, vol. 91, no. 4, pp. 374–86, Aug. 2010.

[36] M. Sabater *et al.*, "Circulating Pigment Epithelium-Derived Factor Levels Are Associated with Insulin Resistance and Decrease after Weight Loss," *J. Clin. Endocrinol. Metab.*, vol. 95, no. 10, pp. 4720–4728, Oct. 2010.

[37] A. Jenkins *et al.*, "Increased serum pigment epithelium derived factor levels in Type 2 diabetes patients.," *Diabetes Res. Clin. Pract.*, vol. 82, no. 1, pp. e5-7, Oct. 2008.

[38] S. Crowe *et al.*, "Pigment Epithelium-Derived Factor Contributes to Insulin Resistance in Obesity," *Cell Metab.*, vol. 10, no. 1, pp. 40–47, Jul. 2009.

[39] J. M. Moreno-Navarrete *et al.*, "Liver, but not adipose tissue PEDF gene expression is associated with insulin resistance," *Int. J. Obes.*, vol. 37, no. 9, pp. 1230–1237, Sep. 2013.

[40] A. K. Gattu *et al.*, "Insulin resistance is associated with elevated serum pigment epithelium-derived factor (PEDF) levels in morbidly obese patients.," *Acta Diabetol.*, vol. 49 Suppl 1, no. S1, pp. S161-9, Dec. 2012.

[41] S. Filleur, T. Nelius, W. De Riese, and R. C. Kennedy, "Characterization of pedf: A multi-functional serpin family protein," *Journal of Cellular Biochemistry*, vol. 106, no. 5. pp. 769–775, 2009.

[42] E. T. H. Ek, C. R. Dass, and P. F. M. Choong, "Pigment epithelium-derived factor: a multimodal tumor inhibitor.," *Mol. Cancer Ther.*, vol. 5, no. 7, pp. 1641–1646.

[43] P. Subramanian *et al.*, "Identification of pigment epithelium-derived factor protein forms with distinct activities on tumor cell lines.," *J. Biomed. Biotechnol.*, vol. 2012, p. 425907, 2012.

[44] S. Filleur *et al.*, "Two functional epitopes of pigment epithelial-derived factor block angiogenesis and induce differentiation in prostate cancer," *Cancer Res*, vol. 65, no. 12, pp. 5144–5152, 2005.

[45] H. Zhang *et al.*, "PEDF and 34-mer inhibit angiogenesis in the heart by inducing tip cells apoptosis via up-regulating PPAR-γ to increase surface FasL," *Apoptosis*, vol. 21, no. 1, pp. 60–68, 2016.

[46] C. Chung *et al.*, "Anti-angiogenic pigment epithelium-derived factor regulates hepatocyte triglyceride content through adipose triglyceride lipase (ATGL)," *J. Hepatol.*, vol. 48, pp. 471–478, 2008.

[47] M. L. Borg, Z. B. Andrews, E. J. Duh, R. Zechner, P. J. Meikle, and M. J. Watt, "Pigment epithelium-derived factor regulates lipid metabolism via adipose triglyceride lipase," *Diabetes*, vol. 60, no. 5, pp. 1458–1466, 2011.

[48] H. Zhang *et al.*, "PEDF and PEDF-derived peptide 44mer stimulate cardiac triglyceride degradation via ATGL.," *J. Transl. Med.*, vol. 13, no. 1, p. 68, Feb. 2015.

[49] J. A. Doll *et al.*, "Pigment epithelium-derived factor regulates the vasculature and mass of the prostate and pancreas.," *Nat. Med.*, vol. 9, pp. 774–780, 2003.

[50] S. Halin *et al.*, "Decreased pigment epithelium-derived factor is associated with metastatic phenotype in human and rat prostate tumors.," *Cancer Res.*, vol. 64, pp. 5664–5671, 2004.

[51] J. C. Byrne *et al.*, "2D-DIGE as a strategy to identify serum markers for the progression of prostate cancer," *J Proteome Res*, vol. 8, no. 2, pp. 942–957, 2009.

[52] H. Ide *et al.*, "Circulating pigment epithelium-derived factor (PEDF) is associated with pathological grade of prostate cancer.," *Anticancer Res.*, vol. 35, no. 3, pp. 1703–8, Mar. 2015.

[53] M. Guan, H. Jiang, C. Xu, R. Xu, Z. Chen, and Y. Lu, "Adenovirus-mediated PEDF expression inhibits prostate cancer cell growth and results in augmented expression of PAI-2," *Cancer Biol Ther*, vol. 6, no. 3, pp. 419–425, 2007.

[54] Z. Dai *et al.*, "Intracellular pigment epithelium-derived factor contributes to triglyceride degradation," *Int J Biochem Cell Biol*, vol. 45, no. 9, pp. 2076–2086, 2013.

[55] Z. Liu *et al.*, "Omega-3 fatty acids and other FFA4 agonists inhibit growth factor signaling in human prostate cancer cells.," *J. Pharmacol. Exp. Ther.*, vol. 352, no. 2, pp. 380–94, 2015.

[56] C. P. Briscoe *et al.*, "The orphan G protein-coupled receptor GPR40 is activated by medium and long chain fatty acids," *J. Biol. Chem.*, vol. 278, no. 13, pp. 11303–11311, 2003.

[57] K. Fujiwara, F. Maekawa, and T. Yada, "Oleic acid interacts with GPR40 to induce Ca2+ signaling in rat islet beta-cells: mediation by PLC and L-type Ca2+ channel and link to insulin release.," *Am. J. Physiol. Endocrinol. Metab.*, vol. 289, no. 4, pp. E670-7, 2005.

[58] A. Matoba *et al.*, "The free fatty acid receptor 1 promotes airway smooth muscle cell proliferation through MEK/ERK and PI3K/Akt signaling pathways.," *Am. J. Physiol. Lung Cell. Mol. Physiol.*, vol. 314, no. 3, pp. L333–L348, 2018.

[59] Y. Koyama *et al.*, "Induction of amyloid β accumulation by ER calcium disruption and resultant upregulation of angiogenic factors in ARPE19 cells," *Investig. Ophthalmol. Vis. Sci.*, vol. 49, no. 6, pp. 2376–2383, 2008.

[60] T. Taniwaki, N. Hirashima, S. P. Becerra, G. J. Chader, R. Etcheberrigaray, and J. P. Schwartz, "Pigment epithelium-derived factor protects cultured cerebellar granule cells against glutamate-induced neurotoxicity.," *J. Neurochem.*, vol. 68, no. 1, pp. 26–32, 1997.

[61] P. Lu *et al.*, "Pigment Epithelium☐Derived Factor (PEDF) Improves Ischemic Cardiac Functional Reserve Through Decreasing Hypoxic Cardiomyocyte Contractility Through PEDF Receptor (PEDF☐R)," *J Am Hear. Assoc*, vol. 5, no. 7, p. e003179, 2016.

[62] K. Mizuta *et al.*, "Novel identification of the free fatty acid receptor FFAR1 that promotes contraction in airway smooth muscle," *Am. J. Physiol. - Lung Cell. Mol. Physiol.*, vol. 309, no. 9, pp. L970–L982, 2015.

[63] M. A. Hidalgo *et al.*, "Oleic acid induces intracellular calcium mobilization, MAPK phosphorylation, superoxide production and granule release in bovine neutrophils," *Biochem. Biophys. Res. Commun.*, vol. 409, no. 2, pp. 280–286, 2011.

[64] J. M. Ntambi and K. Young-Cheul, "Adipocyte differentiation and gene expression.," *J. Nutr.*, vol. 130, no. 12, pp. 3122S-3126S, 2000.

[65] Y. Nakamura, T. Suzuki, A. Sugawara, Y. Arai, and H. Sasano, "Peroxisome proliferator-activated receptor gamma in human prostate carcinoma," *Pathol. Int.*, vol. 59, no. 5, pp. 288–293, 2009.

[66] Y. Segawa *et al.*, "Expression of peroxisome proliferator-activated receptor (PPAR) in human prostate cancer," *Prostate*, vol. 51, no. 2, pp. 108–116, 2002.

[67] T. Kubota *et al.*, "Ligand for peroxisome proliferator-activated receptor γ (Troglitazone) has potent antitumor effect against human prostate cancer both in vitro and in vivo," *Cancer Res.*, vol. 58, no. 15, pp. 3344–3352, 1998.

[68] B. Grygiel-Górniak, "Peroxisome proliferator-activated receptors and their ligands: nutritional and clinical implications--a review.," *Nutr. J.*, vol. 13, p. 17, 2014.

[69] J. Hirsch, C. L. Johnson, T. Nelius, R. Kennedy, W. de Riese, and S. Filleur,

"PEDF inhibits IL8 production in prostate cancer cells through PEDF receptor/phospholipase A2 and regulation of NFκB and PPARγ," *Cytokine*, vol. 55, no. 2, pp. 202–210, Aug. 2011.

[70] W. Luo, J. Lin, Y. Zhang, J. Ouyang, and L. Mao, "[Effects of oleic acid on expression of adiponectin and its PPARgamma mechanism in 3T3-L1 adipocytes]," *Wei Sheng Yan Jiu*, vol. 42, no. 2, pp. 245–249, 2013.

[71] M. Ricchi *et al.*, "Differential effect of oleic and palmitic acid on lipid accumulation and apoptosis in cultured hepatocytes," *J. Gastroenterol. Hepatol.*, vol. 24, no. 5, pp. 830–840, 2009.

[72] M. Wang *et al.*, "Pigment epithelium-derived factor suppresses adipogenesis via inhibition of the MAPK/ERK pathway in 3T3-L1 preadipocytes.," *Am. J. Physiol. Endocrinol. Metab.*, vol. 297, no. 6, pp. E1378-87, 2009.

[73] J. Hirsch, C. L. Johnson, T. Nelius, R. Kennedy, W. Riese, and S. Filleur, "PEDF inhibits IL8 production in prostate cancer cells through PEDF receptor/phospholipase A2 and regulation of NFkappaB and PPARgamma," *Cytokine*, vol. 55, no. 2, pp. 202–210, 2011.

[74] G. Chen *et al.*, "Up-regulation of Wnt-1 and beta-catenin production in patients with advanced metastatic prostate carcinoma: potential pathogenetic and prognostic implications.," *Cancer*, vol. 101, no. 6, pp. 1345–56, 2004.

[75] J. K. Sethi and A. Vidal-Puig, "Wnt signalling and the control of cellular metabolism," *Biochem. J.*, vol. 427, no. 1, pp. 1–17, Apr. 2010.

[76] K. Park *et al.*, "Identification of a novel inhibitor of the canonical Wnt pathway.," *Mol. Cell. Biol.*, vol. 31, no. 14, pp. 3038–3051, 2011.

[77] P. Protiva *et al.*, "Pigment Epithelium-Derived Factor (PEDF) Inhibits Wnt/β-catenin Signaling in the Liver," *CMGH*, vol. 1, no. 5, pp. 535–549, 2015.

[78] X. Yu, Y. Wang, D. J. DeGraff, M. L. Wills, and R. J. Matusik, "Wnt/β-Catenin activation promotes prostate tumor progression in a mouse model," *Oncogene*, vol. 30, no. 16, pp. 1868–1879, 2011.

[79]   H. Clevers and R. Nusse, "Wnt/β-catenin signaling and disease," *Cell*, vol. 149, no. 6. pp. 1192–1205, 2012.

[80]   W. Lu, C. Lin, T. D. King, H. Chen, R. C. Reynolds, and Y. Li, "Silibinin inhibits Wnt/β-catenin signaling by suppressing Wnt co-receptor LRP6 expression in human prostate and breast cancer cells," *Cell. Signal.*, vol. 24, no. 12, pp. 2291–2296, 2012.

[81]   W. Lu and Y. Li, "Salinomycin suppresses LRP6 expression and inhibits both Wnt/β-catenin and mTORC1 signaling in breast and prostate cancer cells," *J. Cell. Biochem.*, vol. 115, no. 10, pp. 1799–1807, 2014.

[82]   A. Debebe *et al.*, "Wnt/β-catenin activation and macrophage induction during liver cancer development following steatosis," *Oncogene*, vol. 36, no. 43, pp. 6020–6029, 2017.

[83]   C. C. Scott *et al.*, "Wnt directs the endosomal flux of LDL-derived cholesterol and lipid droplet homeostasis," *EMBO Rep.*, vol. 16, no. 6, pp. 741–752, 2015.

[84]   D. Bello, M. M. Webber, H. K. Kleinman, D. D. Wartinger, and J. S. Rhim, "Androgen responsive adult human prostatic epithelial cell lines immortalized by human papillomavirus 18.," *Carcinogenesis*, vol. 18, no. 6, pp. 1215–1223.

[85]   J. S. Horoszewicz *et al.*, "LNCaP model of human prostatic carcinoma.," *Cancer Res.*, vol. 43, no. 4, pp. 1809–1818.

[86]   M. E. Kaighn, K. S. Narayan, Y. Ohnuki, J. F. Lechner, and L. W. Jones, "Establishment and characterization of a human prostatic carcinoma cell line (PC-3).," *Invest. Urol.*, vol. 17, no. 1, pp. 16–23.

[87]   K. R. Stone, D. D. Mickey, H. Wunderli, G. H. Mickey, and D. F. Paulson, "Isolation of a human prostate carcinoma cell line (DU 145)," *Int J Cancer*, vol. 21, no. 3, pp. 274–281, 1978.

[88]   B. A. Foster, J. R. Gingrich, E. D. Kwon, C. Madias, and N. M. Greenberg, "Characterization of prostatic epithelial cell lines derived from transgenic adenocarcinoma of the mouse prostate (TRAMP) model," *Cancer Res.*, vol. 57,

no. 16, pp. 3325–3330, 1997.

[89] T. Kita *et al.*, "Diverse effects of G-protein-coupled free fatty acid receptors on the regulation of cellular functions in lung cancer cells," *Exp. Cell Res.*, vol. 342, no. 2, pp. 193–199, 2016.

[90] Z. Rekasi *et al.*, "Antagonist of growth hormone-releasing hormone induces apoptosis in LNCaP human prostate cancer cells through a Ca2+-dependent pathway.," *Proc. Natl. Acad. Sci. U. S. A.*, vol. 102, no. 9, pp. 3435–40, 2005.

[91] C. L. Chaffer, D. M. Thomas, E. W. Thompson, and E. D. Williams, "PPARgamma-independent induction of growth arrest and apoptosis in prostate and bladder carcinoma.," *BMC Cancer*, vol. 6, no. 1, p. 53, Mar. 2006.

[92] R. S. Ahima, "Revisiting leptin's role in obesity and weight loss.," *J. Clin. Invest.*, vol. 118, no. 7, pp. 2380–3, Jul. 2008.

[93] A. Faustino-Rocha *et al.*, "Estimation of rat mammary tumor volume using caliper and ultrasonography measurements.," *Lab Anim. (NY).*, vol. 42, no. 6, pp. 217–24, Jun. 2013.

[94] A. Liotti *et al.*, "Oleic acid promotes prostate cancer malignant phenotype via the G protein-coupled receptor FFA1/GPR40.," *J. Cell. Physiol.*, vol. 233, no. 9, pp. 7367–7378, Sep. 2018.

[95] M.-B. Hu *et al.*, "High-fat diet-induced adipokine and cytokine alterations promote the progression of prostate cancer in vivo and in vitro.," *Oncol. Lett.*, vol. 15, no. 2, pp. 1607–1615, Feb. 2018.

[96] K. Fujita, T. Hayashi, M. Matsushita, M. Uemura, and N. Nonomura, "Obesity, Inflammation, and Prostate Cancer," *J. Clin. Med.*, vol. 8, no. 2, p. 201, Feb. 2019.

[97] N. Torrealba *et al.*, "Expression of ERK1 and ERK2 in prostate cancer," *MAP Kinase*, vol. 4, no. 1, Dec. 2015.

[98] M. R. Hoda, G. Theil, N. Mohammed, K. Fischer, and P. Fornara, "The adipocyte-derived hormone leptin has proliferative actions on androgen-resistant prostate

cancer cells linking obesity to advanced stages of prostate cancer.," *J. Oncol.*, vol. 2012, p. 280386, 2012.

[99] H. U. Park *et al.*, "AMP-activated protein kinase promotes human prostate cancer cell growth and survival," *Mol. Cancer Ther.*, vol. 8, no. 4, pp. 733–741, Apr. 2009.

[100] M. M. Mihaylova and R. J. Shaw, "The AMPK signalling pathway coordinates cell growth, autophagy and metabolism," *Nat. Cell Biol.*, vol. 13, no. 9, pp. 1016–1023, Sep. 2011.

[101] M. A. Babcook *et al.*, "Ser-486/491 phosphorylation and inhibition of AMPKα activity is positively associated with Gleason score, metastasis, and castration-resistance in prostate cancer: A retrospective clinical study.," *Prostate*, vol. 78, no. 10, pp. 714–723, Jul. 2018.

[102] I. Quirós *et al.*, "Upregulation of manganese superoxide dismutase (SOD2) is a common pathway for neuroendocrine differentiation in prostate cancer cells.," *Int. J. cancer*, vol. 125, no. 7, pp. 1497–504, Oct. 2009.

[103] A. D. Batheja, D. J. Uhlinger, J. M. Carton, G. Ho, and M. R. D'Andrea, "Characterization of Serine Palmitoyltransferase in Normal Human Tissues," *J. Histochem. Cytochem.*, vol. 51, no. 5, pp. 687–696, May 2003.

[104] I. Vucenik and J. P. Stains, "Obesity and cancer risk: evidence, mechanisms, and recommendations," *Ann. N. Y. Acad. Sci.*, vol. 1271, no. 1, pp. 37–43, Oct. 2012.

[105] F. Li *et al.*, "Metabolomics reveals that tumor xenografts induce liver dysfunction.," *Mol. Cell. Proteomics*, vol. 12, no. 8, pp. 2126–35, Aug. 2013.

[106] C.-C. Chen, T.-Y. Lee, Y.-L. Leu, and S.-H. Wang, "Pigment epithelium-derived factor inhibits adipogenesis in 3T3-L1 adipocytes and protects against high-fat diet-induced obesity and metabolic disorders in mice," *Transl. Res.*, vol. 210, pp. 26–42, Aug. 2019.

[107] S. Yamagishi, S. Amano, Y. Inagaki, T. Okamoto, M. Takeuchi, and H. Inoue, "Pigment epithelium-derived factor inhibits leptin-induced angiogenesis by suppressing vascular endothelial growth factor gene expression through anti-

oxidative properties.," *Microvasc. Res.*, vol. 65, no. 3, pp. 186–90, May 2003.

[108] S. Yamagishi, Y. Inagaki, S. Amano, T. Okamoto, and M. Takeuchi, "Up-regulation of vascular endothelial growth factor and down-regulation of pigment epithelium-derived factor messenger ribonucleic acid levels in leptin-exposed cultured retinal pericytes.," *Int. J. Tissue React.*, vol. 24, no. 4, pp. 137–42, 2002.

[109] K. A. Frankenberry, P. Somasundar, D. W. McFadden, and L. C. Vona-Davis, "Leptin induces cell migration and the expression of growth factors in human prostate cancer cells," *Am. J. Surg.*, 2004.

[110] M. R. Sierra-Honigmann *et al.*, "Biological Action of Leptin as an Angiogenic Factor," *Science (80-.).*, vol. 281, no. 5383, pp. 1683–1686, Sep. 1998.

[111] Y. S. Kim, P. Gupta Vallur, R. Phaëton, K. Mythreye, and N. Hempel, "Insights into the Dichotomous Regulation of SOD2 in Cancer.," *Antioxidants (Basel, Switzerland)*, vol. 6, no. 4, p. 86, Nov. 2017.

[112] D. A. Cavazos, M. J. deGraffenried, S. A. Apte, L. W. Bowers, K. A. Whelan, and L. A. deGraffenried, "Obesity promotes aerobic glycolysis in prostate cancer cells.," *Nutr. Cancer*, vol. 66, no. 7, pp. 1179–86, Oct. 2014.

[113] X. Gao *et al.*, "PEDF and PEDF-derived peptide 44mer protect cardiomyocytes against hypoxia-induced apoptosis and necroptosis via anti-oxidative effect.," *Sci. Rep.*, vol. 4, no. 1, p. 5637, Jul. 2014.

[114] J. Gong, G. Belinsky, U. Sagheer, X. Zhang, P. J. Grippo, and C. Chung, "Pigment Epithelium-derived Factor (PEDF) Blocks Wnt3a Protein-induced Autophagy in Pancreatic Intraepithelial Neoplasms.," *J. Biol. Chem.*, vol. 291, no. 42, pp. 22074–22085, Oct. 2016.

[115] D. G. Bostwick *et al.*, "Antioxidant enzyme expression and reactive oxygen species damage in prostatic intraepithelial neoplasia and cancer.," *Cancer*, vol. 89, no. 1, pp. 123–34, Jul. 2000.

[116] A. Miar *et al.*, "Manganese superoxide dismutase (SOD2/MnSOD)/catalase and SOD2/GPx1 ratios as biomarkers for tumor progression and metastasis in

prostate, colon, and lung cancer.," *Free Radic. Biol. Med.*, vol. 85, pp. 45–55, Aug. 2015.

[117] J. M. Flynn and S. Melov, "SOD2 in mitochondrial dysfunction and neurodegeneration," *Free Radic. Biol. Med.*, vol. 62, pp. 4–12, Sep. 2013.

[118] S. Furukawa *et al.*, "Increased oxidative stress in obesity and its impact on metabolic syndrome," *J. Clin. Invest.*, vol. 114, no. 12, pp. 1752–1761, Dec. 2004.

[119] J. R. Prohaska, L. E. Wittmers, and E. W. Haller, "Influence of genetic obesity, food intake and adrenalectomy in mice on selected trace element-dependent protective enzymes.," *J. Nutr.*, vol. 118, no. 6, pp. 739–46, Jun. 1988.

[120] V. Laurent *et al.*, "Periprostatic Adipose Tissue Favors Prostate Cancer Cell Invasion in an Obesity-Dependent Manner: Role of Oxidative Stress," *Mol. Cancer Res.*, vol. 17, no. 3, pp. 821–835, Mar. 2019.

[121] H. Xu *et al.*, "Proinflammatory cytokines in prostate cancer development and progression promoted by high-fat diet," *Biomed Res. Int.*, vol. 2015, p. 249741, 2015.

[122] Y. Yoon, T.-J. Kim, J.-M. Lee, and D.-Y. Kim, "SOD2 is upregulated in periodontitis to reduce further inflammation progression.," *Oral Dis.*, vol. 24, no. 8, pp. 1572–1580, Nov. 2018.

[123] Y. Baumer *et al.*, "Chronic skin inflammation accelerates macrophage cholesterol crystal formation and atherosclerosis.," *JCI insight*, vol. 3, no. 1, Jan. 2018.

[124] L. Samsel *et al.*, "The ceramide analog, B13, induces apoptosis in prostate cancer cell lines and inhibits tumor growth in prostate cancer xenografts.," *Prostate*, vol. 58, no. 4, pp. 382–93, Mar. 2004.

[125] H. Wang, A. G. Charles, A. J. Frankel, and M. C. Cabot, "Increasing intracellular ceramide: an approach that enhances the cytotoxic response in prostate cancer cells.," *Urology*, vol. 61, no. 5, pp. 1047–52, May 2003.

[126] R. H. Unger and L. Orci, "Lipoapoptosis: its mechanism and its diseases.,"

Biochim. Biophys. Acta, vol. 1585, no. 2–3, pp. 202–12, Dec. 2002.

[127] C. R. Gault, L. M. Obeid, and Y. A. Hannun, "An Overview of Sphingolipid Metabolism: From Synthesis to Breakdown," in *Advances in experimental medicine and biology*, vol. 688, 2010, pp. 1–23.

[128] W. C. Huang, C. L. Chen, Y. S. Lin, and C. F. Lin, "Apoptotic sphingolipid ceramide in cancer therapy," *J Lipids*, vol. 2011, p. 565316, 2011.

[129] M. Fillet *et al.*, "Mechanisms involved in exogenous C2- and C6-ceramide-induced cancer cell toxicity.," *Biochem. Pharmacol.*, vol. 65, no. 10, pp. 1633–42, May 2003.

[130] H. J. Kim, J. Y. Mun, Y. J. Chun, K. H. Choi, and M. Y. Kim, "Bax-dependent apoptosis induced by ceramide in HL-60 cells.," *FEBS Lett.*, vol. 505, no. 2, pp. 264–8, Sep. 2001.

[131] L. L. Marshall, S. E. Stimpson, R. Hyland, J. R. Coorssen, and S. J. Myers, "Increased lipid droplet accumulation associated with a peripheral sensory neuropathy.," *J. Chem. Biol.*, vol. 7, no. 2, pp. 67–76, Apr. 2014.

[132] M. Hughes-Fulford, Y. Chen, and R. R. Tjandrawinata, "Fatty acid regulates gene expression and growth of human prostate cancer PC-3 cells," *Carcinogenesis*, vol. 22, no. 5, pp. 701–707, 2001.

[133] R. M. Hagen, A. Rhodes, and M. R. Ladomery, "Conjugated linoleate reduces prostate cancer viability whereas the effects of oleate and stearate are cell line-dependent.," *Anticancer Res.*, vol. 33, no. 10, pp. 4395–400, Oct. 2013.

[134] J. Gasmi and J. Thomas Sanderson, "Jacaric acid and its octadecatrienoic acid geoisomers induce apoptosis selectively in cancerous human prostate cells: a mechanistic and 3-D structure-activity study.," *Phytomedicine*, vol. 20, no. 8–9, pp. 734–42, Jun. 2013.

[135] L. Crump, "Antioxidant Function of Pigment Epithelium Derived Factor in Adipose Tissue, the Prostate, and Prostate Cancer," *Thesis Dissertation*, Aug. 2015.

[136] V. Pirsko *et al.*, "An Effect of Culture Media on Epithelial Differentiation Markers in Breast Cancer Cell Lines MCF7, MDA-MB-436 and SkBr3," *Medicina (B. Aires).*, vol. 54, no. 2, Mar. 2018.

[137] L. K. Ryland *et al.*, "C6-ceramide nanoliposomes target the Warburg effect in chronic lymphocytic leukemia.," *PLoS One*, vol. 8, no. 12, p. e84648, 2013.

<div align="center">

CURRICULUM VITAE

Nizar Ahmed Khamjan

</div>

Permanent and mailing address:

Al Swiss Street

P. O. Box 3246

Jizan, Jazan, Saudi Arabia 45142

Email:

nkhamjan@jazanu.edu.sa /

nkhamjan@yahoo.com

Cell phone: +1 414-324-2741

Permanent phone: +966 54 572 1172

Date of birth: September 23, 1986

Nationality: Saudi

Social status: Married

Education:

- **MS Biomedical Sciences**, August 2014, University of Wisconsin-Milwaukee, College of Health Sciences, Milwaukee, WI, United States

  Cum GPA: 3.084 out of 4

  Thesis title: Thrombospondin-1 Signaling Mechanisms Regulating Pigment Epithelium-Derived Factor Expression and Lipolytic Activity in Prostate Cancer

  Supervisor: Jennifer A. Doll, PhD

- **BS Medical Laboratory Sciences**, July 2007

  King Khalid University, College of Applied Medical Sciences, Abha, Saudi Arabia.

  Cum GPA: 4.02 out of 5

Research interests:

- Cancer biology

- Prostate cancer
- Obesity and dietary fats in prostate cancer

Professional Positions:

- Teaching Assistant at Faculty of Applied Medical Sciences, Jazan University, Saudi Arabia in September 2008 till January 2010 and from May 2011 to August 2012
- Responsibilities: Responsible for the lab part of Histotechnology courses
  A committee member of providing medical equipments and supplies for all departments

Specific Training Programs:

Practical applied training year in King Fahd Central Hospital, Jazan, Saudi Arabia from August 1, 2007 to August 1, 2008 in the following laboratories:

- Hematology Laboratory (12 weeks).
- Biochemistry Laboratory (10 weeks).
- Histopathology Laboratory (4 weeks).
- Microbiology Laboratory (12 weeks).
- Blood bank (6 weeks).
- Reception of Laboratory (2 week).
- Quality Assurance unit (2 weeks).

Conference attending and presentation:

- Attending 4th Annual Conference of Al-Noor Specialist Hospital in Laboratory Medicine and Family Health, 10-14 May 2008, Makah, KSA.
- Attending Symposium of new trends in clinical laboratories held in King Fahd central hospital, April 2008, Jazan, KSA.

- Khamjan N. *et al*, 2014 "TSP-1 signaling mechanisms regulating PEDF expression and lipolytic activity in prostate cancer" UWM Health Research Symposium, Milwaukee, WI, USA

- Khamjan N. *et al*, 2017 "Molecular pathways of Pigment Epithelium-Derived Factor Suppression by Obesity in Prostate Cancer Cells" UWM Health Research Symposium, Milwaukee, WI, USA

- Attending 2nd International Conference on Tumor & Cancer Immunology and Immunotherapy, July 17-18, 2017, Chicago, Illinois, USA

- Khamjan N. *et al*, 2018 "Mechanisms of fatty acid-mediated PEDF suppression and effects on downstream lipid regulatory pathways in prostate cancer" UWM Health Research Symposium, Milwaukee, WI, USA

- Khamjan N. *et al*, 2019 "Signaling Mechanisms in Obesity-Fueled Prostate Cancer Progression" UWM Health Research Symposium, Milwaukee, WI, USA

Scholarship and Award

- Receiving a fully scholarship to study English as a second language at University of Pittsburgh, Pittsburgh, United States from January 2010 to May 2011

- Receiving a fully scholarship to study a Master of Science degree at University of Wisconsin-Milwaukee, Milwaukee, WI, United States

- Receiving a fully scholarship to study a PhD degree at University of Wisconsin-Milwaukee, Milwaukee, WI, United States

- Receiving a Fall 2013 College of Health Science Student Research Grant Award, University of Wisconsin-Milwaukee

- Receiving a Fall 2018 College of Health Science Student Research Grant Award, University of Wisconsin-Milwaukee

Publications

- **Competitive, peer-reviewed poster presentation:** S Wcislak, A Chawla, **N Khamjan**, BA Plunkett, and JA Doll. Thrombospondin-1 regulates lipolytic activity

in prostate cancer cells. Society of Basic Urologic Research Annual Fall meeting, Tampa, FL, November 9-12, 2017. (Proceedings of meeting).

- **Competitive, peer-reviewed poster presentation:** S Wcislak, A Chawla, **N Khamjan**, BA Plunkett, CB Brendler and JA Doll. Novel Lipid-regulatory Function for Thrombospondin-1 in Prostate Cancer. Society of Basic Urologic Research Annual Fall meeting, Dallas, TX, November, 2014. (Proceedings of meeting).

- **Competitive, peer-reviewed poster presentation:** S Wcislak, A Chawla, **N Khamjan**, BA Plunkett, CB Brendler and JA Doll. Novel Lipid-regulatory Function for Thrombospondin-1 in Prostate Cancer. Urology Research Symposium, Wisconsin Urologic Research Institute, University of Wisconsin, Madisen, WI. June 1-July 2, 2014. (Proceedings of meeting).

Personal Skills:

I can describe myself as ambitious, and insist on success and ready to hard work, self-confidence, and academic ability to achieve goals.

Teaching and Computer Skills:

- I'm familiar using teaching tools and equipment's:
- Skills using PowerPoint for presentations
- Very professional in computer applications Microsoft word and Internet

Language Skills:

- Fluent in Arabic
- Excellent in English